Epigenetic consequences of *in utero* exposure to rosuvastatin include altered histone methylation patterns in newborn rat brains

Karolina Fábián-Dulka

Theoretical Medicine Doctoral School

PhD Thesis

Department of Cell Biology and Molecular Medicine

Albert Szent-Györgyi Medical School – Faculty of Science and Informatics

University of Szeged, Hungary

Thesis advisor: Professor Karoly Gulya, PhD, DSc

Szeged, 2021

LIST OF PUBLICATIONS

PUBLICATION DIRECTLY RELATED TO THE THESIS

I) **Dulka K**, Szabo M, Lajkó N, Belecz I, Hoyk Z, Gulya K (2021) Epigenetic consequences of *in utero* exposure to rosuvastatin: Alteration of histone methylation patterns in newborn rat brains. **Int J Mol Sci**. 22(7):3412. doi: 10.3390/ijms22073412. (**IF: 5.923**) (Q1)

PUBLICATIONS NOT DIRECTLY RELATED TO THE THESIS

I) **Dulka K**, Nacsa K, Lajkó N, Gulya K (2021) Quantitative morphometric and cell-type-specific population analysis of microglia-enriched cultures subcloned to high purity from newborn rat brains. **IBRO Neurosci Rep**. 10:119-129. doi: 10.1016/j.ibneur.2021.01.007.

II) Legradi A, **Dulka K**, Jancsó G, Gulya K (2020) Orofacial skin inflammation increases the number of macrophages in the maxillary subregion of the rat trigeminal ganglion in a corticosteroid-reversible manner. **Cell Tissue Res**. 382(3):551-561. doi: 10.1007/s00441-020-03244-3. (**IF: 5.249**) (Q1)

III) Lajkó N, Kata D, Szabó M, Mátyás A, **Dulka K**, Földesi I, Fülöp F, Gulya K, Vécsei L, Mihály A (2020) Sensitivity of rodent microglia to kynurenines in models of epilepsy and inflammation *in vivo* and *in vitro*: Microglia activation is inhibited by kynurenic acid and the synthetic analogue SZR104. **Int J Mol Sci**. 21(23):9333. doi: 10.3390/ijms21239333. (**IF: 5.923**) (Q1)

IV) Szabo M, **Dulka K**, Gulya K (2016) Calmodulin inhibition regulates morphological and functional changes related to the actin cytoskeleton in pure microglial cells. **Brain Res Bull**. 120:41-57. doi: 10.1016/j.brainresbull.2015.11.003. (**IF: 3.37**) (Q2)

Number of full publications: 5 (2 first author, 1 first co-author)
Cumulative impact factor: 20.47 (3 Q1 and 1 Q2 publications)

POSTER DIRECTLY RELATED TO THE THESIS

I) **Dulka K**, Szabo M, Lajko N, Belecz I, Hoyk Z, Gulya K (2020) Prenatal exposure to rosuvastatin changes histone methylation patterns in the newborn rat brain. **12th FENS 2020 Virtual Forum of Neuroscience**, 2020.07.11-15. *(e-poster)*

POSTERS NOT DIRECTLY RELATED TO THE THESIS

I) Szabo M, Lajko N, **Dulka K**, Mihály A, Vécsei L, Gulya K (2020) Kynurenic acid and its analog SZR104 exhibit strong anti-inflammatory effects in microglia-enriched newborn rat cerebral cultures. **12th FENS 2020 Virtual Forum of Neuroscience**, 2020.07.11-15. *(e-poster)*

II) Légrádi Á, Szebeni G J, Yaqub M, **Dulka K**, Lajko N, Szabó M, Monostori É, Gulya K (2020) Galectin-1 expression correlates with the microglial activation state in primary and secondary cultures of newborn rat cortical tissue. **12th FENS 2020 Virtual Forum of Neuroscience**, 2020.07.11-15. *(e-poster)*

III) **Dulka K**, Nacsa K, Lajkó N, Gulya K (2018) Nagy tisztaságú mikroglia kultúra készítése primer és szekunder tenyészetekből. **Magyar Élettani Társaság Vándorgyűlése**, Szeged, Hungary, 2018.06.27-30. *(P1.56)*

IV) **Dulka K**, Szabo M, Gulya K (2015) Calmodulin inhibition affects proliferation and cell viability in unchallenged and LPS-challenged pure microglial cultures. **XII European Meeting on Glial Cell Function in Health and Disease**, Bilbao, Spain, 2015.07.15-18. *(TO2-04B)* **GLIA**: 63 (1) pp. E95-E95

OTHER PUBLICATION NOT RELATED TO THE THESIS

I) Kata D, Nacsa K, Légrádi Á, **Dulka K**, Gulya K (2015) Állati sejtek és szövetek tenyésztése. Egyetemi jegyzet. SZTE, Szeged, pp. 1-233. https://elearning.szte.hu/mod/szte/course.php?id=84 (in Hungarian)

TABLE OF CONTENTS   page

ABBREVIATIONS

ANOVA	analysis of variance
CNS	central nervous system
CNPase	2′,3′-cyclic nucleotide 3′-phosphodiesterase
DAPI	2-[4-(aminoiminomethyl)phenyl]-1H-indole-6-carboximidamide hydrochloride
DNA	deoxyribonucleic acid
EAAT1	excitatory amino acid transporter 1 (also known as glutamate aspartate transporter 1 (GLAST-1))
ERGs	epigenetic regulator genes
GAPDH	glyceraldehyde 3-phosphate dehydrogenase (EC 1.2.1.12)
GFAP	glial fibrillary acidic protein
H	histone
HGM-CoA	3-hydroxy-3-methylglutaryl coenzyme A
H&E	hematoxylin and eosin
Iba1	ionized calcium-binding adaptor molecule 1
IgG	immunoglobulin G
Ki67	proliferation marker antigen identified by the monoclonal antibody Ki67
Lys (K)	Lysine
me	methylation/methyl group
NeuN	anti-neuronal nuclei protein (hexaribonucleotide-binding protein-3)
PBS	phosphate-buffered saline
PTM	posttranslational modification
RNA	ribonucleic acid
RST	rosuvastatin
RT	room temperature
SDS	sodium dodecyl sulfate
SEM	standard error of the mean
TBS	Tris-buffered saline

SUMMARY

Epigenetics, in a broad sense, is a hereditary phenomenon that changes gene expression and thereby alters the cellular phenotype without changing the DNA sequence. Posttranslational covalent modifications of histone tails are associated with epigenetic regulation because histone modification is one of the main mechanisms for epigenetic modifications. It is highly specific in a site- and residue-specific manner, and mostly includes methylation and acetylation. Histone methylation has been linked to transcription initiation and elongation, heterochromatin silencing and other functions. Histone marks are known to be linked with chromatin accessibility thereby impacting the transcriptional status (active or silent) of the underlying DNA sequence. During embryonal development histone methylation landscapes of brain cells are sensitive to a wide range of environmental perturbations. Several studies have been conducted in recent years on the mechanisms involved in epigenetic changes during *in utero* development.

In the drug class known as statins, there is a member called rosuvastatin (RST). It catalyzes the conversion of 3-hydroxy-3-methylglutaryl coenzyme A (HMG-CoA) to mevalonate and it is mainly used for the treatment of patients with high cholesterol levels. Although it has additional beneficial effects (antiinflammatory, anticancer, etc.), it also has some unwanted side effects. For instance, it has potentially harmful but not well-documented effects on embryos, and RST is contraindicated during pregnancy. Since about half of all pregnancies are unplanned, there is a possibility that a pregnant woman may be taking RST at least for a while.

Mammalian embryonic/fetal development involves precise molecular interactions between intrinsic factors such as genetics and epigenetics, and extrinsic maternal factors such as environmental perturbations. The aim of this study was to assess the epigenetic changes in the brains of the newborn rats whose mothers had been treated with RST during pregnancy.

To demonstrate whether RST could induce molecular epigenetic events, measured as histone methylations, pregnant mothers were treated daily with oral RST doses from the 11th day of pregnancy for 10 days (or until delivery). On postnatal day 1, the brains of control and RST-treated rats were removed for western blots and immunohistochemistry. Several antibodies that recognize different methylation sites for

H2A, H2B, H3 and H4 histones were then quantified in these immunoblotting and fluorescent immunohistochemical experiments.

Various analyses of cell-type specific markers in the newborn brain demonstrated that prenatal RST administration did not affect the composition and/or the cell type ratios compared to controls. A histological analysis of brains taken from newborn rats revealed no morphological alterations after exposure to RST. Prenatal RST administration did, however, induce a general, nonsignificant increase in H2AK118me1, H2BK5me1, H3, H3K9me3, H3K27me3, H3K36me2, H4, H4K20me2 and H4K20me3 levels compared to controls. Moreover, significant changes were detected in the number of H3K4me1 and H3K4me3 sites ($134.3\% \pm 19.2\%$ and $127.8\% \pm 8.5\%$ of the controls, respectively), which are generally recognized as transcriptional activators. The newborn rat brain is a tissue populated mostly by neurons that are gradually complemented with glial and other cells. Multicolor fluorescent/confocal imaging of immunohistochemically stained cell-type-specific markers and histone methylation marks on tissue sections indicated that most of the increase in methylation marks at these sites were localized to nuclei of the most abundant cell type, the neurons.

Hence, prenatal RST treatment induces epigenetic changes that could affect neuronal differentiation and development. The epigenetic changes elicited by RST need to be taken into account. Although there are no such data available yet on humans, our results could be telling us that the drug should be applied with caution.

1. INTRODUCTION

1.1. Epigenetics and histone methylation

The genetic information in eukaryotic cells is encoded in the nuclear DNA. In the nucleus, DNA is packed in a chromatin structure which determines its accessibility for functions such as transcription, replication, and DNA repair. Chromatin composed of a specialized set of proteins, the so-called histones (H), that organize DNA into the nucleosome (**Figure 1**). The nucleosome is the fundamental unit of chromatin and it is composed of four core histones (H2A, H2B, H3, and H4), around which 146 base pairs of DNA is coiled (Kornberg and Lorch, 1999). A fifth histone protein, the linker histone H1, seals the nucleosome by binding to the entry and exit sites of DNA (Henn et al., 2020); histone H1 however does not form a part of the nucleosome itself and it plays a pivotal role in shaping chromatin architecture.
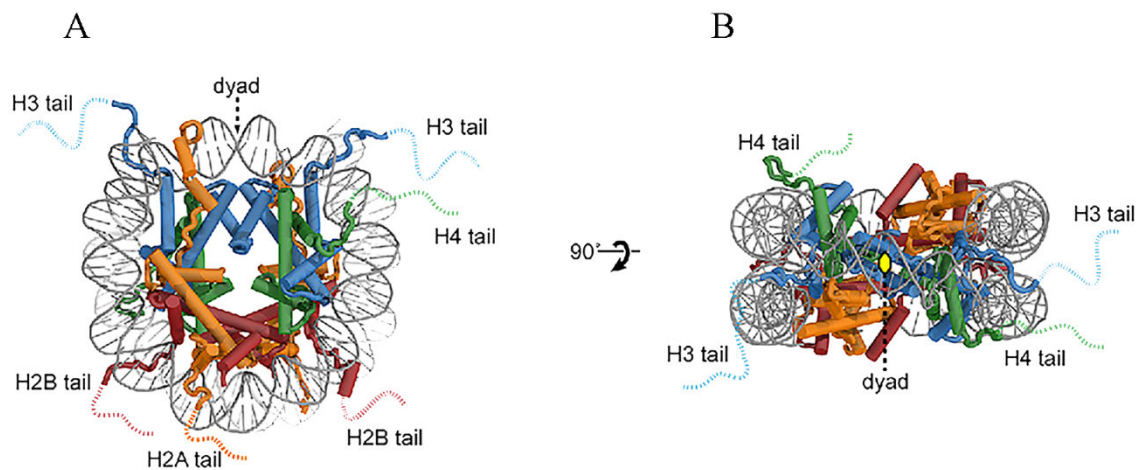

Figure 1. Overview of nucleosome architecture. (**A**) Face and (**B**) top view of the nucleosome structure (adapted from Bowman and Poirier, 2015).

Chromatin exists in two forms, which provide a useful qualitative indication of the chromatin compaction state. Transcription is largely confined to euchromatin, while the heterochromatin defines genome regions where transcription is inactive. Originally, these two types of chromatin were distinguished cytologically by staining intensity during interphase; euchromatin stains lightly, whereas heterochromatin stains darkly (Passarge, 1979; Shahbazian and Grunstein, 2007). Darker stained heterochromatin consist of tightly packaged protein and nucleic acid complexes mainly found at the

nuclear periphery and it frequently forms blocks around the nucleolus. Nowadays, the term heterochromatin is more loosely applied, as constitutive heterochromatin is always compact, and it tends to be enriched in repetitive, gene-poor DNA sequences, whereas facultative heterochromatin can undergo reversible transitions from a transcriptionally inactive state to become transcriptionally competent (Woodcock and Ghosh, 2010).

The term "epigenetics" was initially coined by C.H. Waddington in the 1940's and it has been modified over the years by various researchers (see Tronick and Hunter, 2016, for further references). It now denotes the heritable changes in gene expression without affecting the core DNA sequence (Biswas and Rao, 2018). In molecular epigenetics, the term "epi" is interpreted as meaning "over," as in the molecular process sitting over and operating on the genes (Tronick and Hunter, 2016). Epigenetic regulation bridges genotype and phenotype by changing the function of the chromatin (Goldberg et al., 2007). While mutations directly affect the genetic material by altering the genetic code, epigenetic modifications change the chromatin structure or modify the nucleic acid without changing the genetic code. This makes epigenetic modifications flexible, reversible, and quickly responsive to changes in the environment and other factors (Schäfer and Baric, 2017). The study of epigenetic modifications involves the interplay between the environment and the genome (Goldberg et al., 2007). Epigenetic modifications play a significant role in regulating cellular mechanisms and signaling pathways, during embryonic development, in memory function, in immunity and in disease (Goldberg et al., 2007; Gupta et al., 2010; Schäfer and Baric, 2017).

Epigenetic modifications (**Figure 2**) that affect gene expression are: 1) DNA methylation, the enzymatic addition of a methyl group (-CH3) at 5'-carbon of the pyrimidine ring of cytosine nucleotide (methylated cytosine (5-mC)); 2) enzymatic modifications of histones, primarily acetylation and methylation, and 3) synthesis of 19-30 nucleotide-long non-coding RNAs, including microRNAs, Piwi-interacting RNAs and long non-coding RNAs that can target messenger RNAs and interfere with transcription or translation (Vaiserman, 2013; Kumar et al., 2018). In general, DNA methylation that (typically occurs at cytosine guanine dinucleotide (CpG) sites; Relton and Smith, 2010)) has a role in silencing gene expression and heterochromatin remodeling, histone methylation either activates or represses transcription, although the effect of the methylation depending on the location where the histone modification has been made. The histone acetylation is typically linked to transcriptional activation. Acetylated

histones are associated with unmethylated DNA and they are almost absent in methylated DNA regions (Vaiserman, 2013). RNA-mediated silencing occurs when RNAs of 19 to 24 nucleotides bind target messenger RNAs and induce their translational repression, cleavage, or accelerated decay (Gómez-Díaz et al., 2012). Specific combinations of epigenetic modifications determine the functional and structural features of each genomic region.
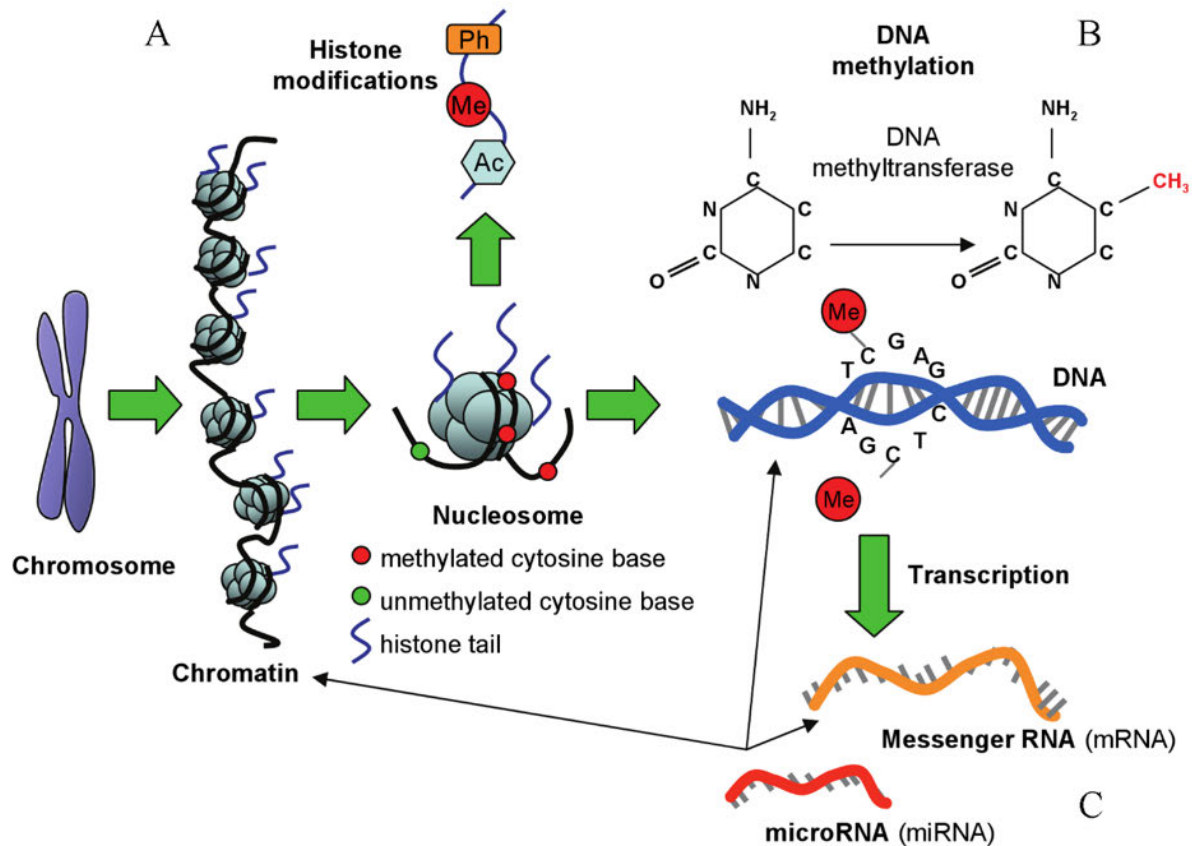

Figure 2. The major epigenetic mechanisms that affect gene expression. (**A**) enzymatic modifications of histones; (**B**) DNA methylation; (**C**) synthesis of small non-coding RNAs (miRNAs) (adapted from Relton and Smith, 2010).

Epigenetic mechanisms act in a highly flexible and coordinated manner to regulate gene expression, replication, repair, etc. Genes encoding proteins that directly regulate the epigenome are the epigenetic regulator genes (ERGs). ERGs are a group of over 400 coding genes, most of which encode enzymes that add ("writers"), modify/revert ("editors/erasers"), or recognize ("readers") epigenetic modifications, and they control a range of critical cellular processes (Plass et al., 2013; Halaburkova et al, 2020). The products of ERGs are involved in processes such as DNA methylation, histone

modification and other chromatin-based modifications. ERGs also play a crucial role in the establishment and maintenance of cell identity and genome integrity (Halaburkova et al., 2020).
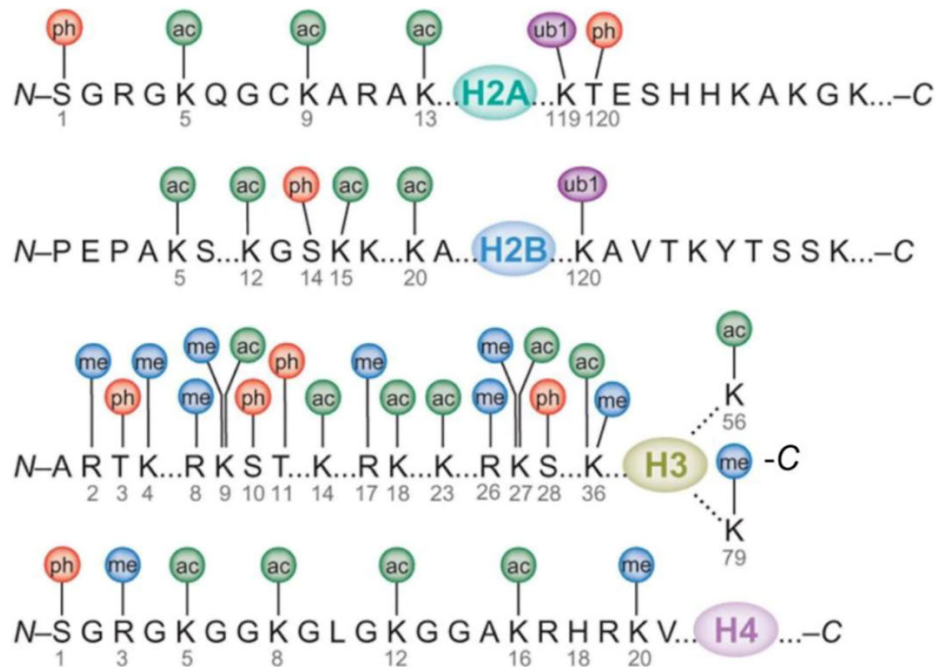

Figure 3. Schematic representation of nucleosomal histone PTMs. Most of the known histone modifications occur on the N-terminal tails of histones. The modifications include acetylation (ac), methylation (me), phosphorylation (ph) and ubiquitination (ub1). N: N-terminal tails; C: C-terminal tails; globular domains of each core histone are represented as colored ovals (adapted from Bhaumik et al., 2007).

Chromatin architecture, nucleosomal positioning, and ultimately access to DNA for gene expression, is strongly controlled by histone proteins. In addition to playing a vital role in chromatin structure and dynamics, histones undergo posttranslational modifications (PTMs), which provide mechanisms for mediating diverse cellular processes (Klein et al., 2018). The N-terminal tails of histones contain many amino acids that can be modified posttranslationally (Bhaumik et al., 2007).

Epigenetic marks are constituted by the set of PTMs on histones, which consist in the covalent additions of different chemical groups to particular residues and affects their interactions with DNA (**Figure 3**; also see Bhaumik et al., 2007). On the one hand some modifications impair histone-DNA interactions, causing open chromatin conformation, when DNA is accessible to binding of transcription factors and resulting gene

expression. On the other hand, some modifications strengthen histone-DNA interactions and create a tightly packed chromatin structure when transcriptional machinery cannot access DNA, and this results in gene silencing. The N-terminal tails of histones are subject to a number of highly site- and residue-specific posttranslational modifications, including methylation, acetylation, phosphorylation, ubiquitylation, and SUMOylation, which are implicated in influencing gene expression and genome function, as they coordinate the recruitment of chromatin remodelers and transcriptional machinery for transcriptional regulation (Kouzarides, 2007). The regulation of these epigenetic marks relies on molecular cooperativity by enzymes that have the capacity to recognize a given mark and to tag other histones using the same mark. This epigenetic modification requires several different histone modifying enzymes, including "writers" that attach modifications to histone tails, "erasers" that remove modifications and "readers" that recognize these modifications (Biswas and Rao, 2018; Hyun et al., 2017; Klein et al., 2018; Venkatesh and Workman, 2015). The balance between the writers and erasers generally dictates which marks are present on histones.

Histone modification is one of the main mechanisms of epigenetic modifications that regulate gene expression. Of all the known modifications, histone Lys (K) methylation is regarded as a stable chromatin modification that, together with DNA methylation, defines epigenetic programs (Trojer and Reinberg, 2006). Histone Lys methylation has been linked, among other things, to transcription initiation and elongation and heterochromatin silencing (Hyun et al., 2017). The location and the degree of methylation of the Lys residue on a histone tail are associated with differential gene expression status. Lys methylation marks, such as H3K4 and H3K36, are implicated in the activation of transcription and linked to open chromatin, whereas H3K9, H3K27, and H4K20 Lys methylation sites are associated with transcriptional repression and they are characteristic of condensed chromatin (Trojer and Reinberg, 2006; Vermeulen et al., 2010). Thus, Lys methylation is implicated in both transcriptional activation and repression, and this flexibility may be explained by the fact that methylation does not alter histone charge, so it does not directly affect histone-DNA interactions, unlike other PTMs such as acetylation (Bannister and Kouzarides, 2011).

The complexity of the methylation patterns of histone proteins and the methylation state at any given Lys residue (unmethylated, mono- (me1), di- (me2), or trimethylated (me3)) also influence gene expression. The enzyme performing these

modifications is the histone lysine methyltransferase (KMT) and it can add up to three methyl groups on a single Lys residue. Several protein domains have evolved in mammalian cells that can identify and bind to these modifications and they are known as readers of the epigenome (Biswas and Rao, 2018). Readers of methylated Lys residues were recently systematically categorized and they include various proteins that contain specialized domains that promote the identification of these Lys modifications (Yun et al., 2011). Furthermore, Lys methylation marks can be removed by epigenetic "erasers" that oppose the activity of the "writers". The demethylation of Lys residues on histone proteins is carried out by the histone demethylases. The two known families of histone demethylases are the KDM1 (previously LSD1) and JmjC domain-containing proteins (Zhou and Ma, 2008). Histone methylation was originally thought to be irreversible; however, the discovery of a histone lysine-specific demethylase proved that histone methylation is, in fact, reversible, although methyl groups are still believed to turn over more slowly than many other PTMs (Greer and Shi, 2012).

1.2. The mechanisms of statins and their effects in pregnancy

Statins (3-hydroxy-3-methylglutaryl coenzyme A (HMG-CoA) reductase inhibitors (HMGCRIs)) are a class of lipid-lowering agents used in the treatment of high blood cholesterol levels (Taylor et al., 2013). They were discovered in 1975 as natural products of some molds. These inhibitors can be subdivided into two groups. Namely, natural compounds derived from fungal fermentation (mevastatin, lovastatin, simvastatin and pravastatin), and purely synthetic compounds (fluvastatin, atorvastatin, rosuvastatin and pitavastatin) (Zipp et al., 2007). All statins bind strongly to plasma proteins. Statins act by blocking the cholesterol synthesis through inhibition of the enzyme necessary for the production of L-mevalonate. The inhibition of the first and rate-limiting step of cholesterol synthesis also reduces the pools of intermediate metabolites in the pathway that regulate a wide range of cellular functions including hormonal communication, protein synthesis, cell membrane maintenance and lipid modifications (Zipp et al., 2007). Statins enter the cells through an organic anion transporter to exert their actions on cholesterol synthesis and they may also need to enter subcompartments to be fully active (Wierzbicki et al., 2003).

The main effects of statins are related to lipid metabolism, notably the inhibition of cholesterol synthesis, but their action is not just by lowering lipid levels. Apart from

the inhibition of cholesterol synthesis, reduction of circulating levels of low-density lipoproteins and triglycerides, and stimulation of the expression of high-density lipoproteins, they also strongly modulate inflammatory cells surrounding atherosclerotic plaques (Wierzbicki et al., 2003) and improve vascular endothelial function (Treasure et al., 1995). Furthermore, statins have long been known to induce apoptosis in various cancer cell lines (Jones et al., 1994; Karlic et al., 2017), and they have antitumor properties (Afshari et al., 2020; Gachpazan et al., 2019). The beneficial effects of statins on the expression of inflammasome-related genes in animal models (Luo et al., 2014) or human *in vitro* models (Satoh et al., 2014) have also been noted. Moreover, statins may have beneficial effects in the central nervous system (CNS) (Famer et al., 2010; Van der Most et al., 2009; Zipp et al., 2007). For example, *in vivo* (Kurata et al., 2012) and *in vitro* (Kata et al., 2016) studies have demonstrated that statins can attenuate neuroinflammation. In particular, RST strongly inhibited the expression of certain proinflammatory genes, while concomitantly vigorously stimulating several antiinflammatory genes in microglial cultures (Kata et al., 2016).

Of all the commercially available statins, RST is one of the highest-selling prescription drugs on the market (Crestor; Astra-Zeneca Pharmaceuticals, LP, Wilmington, DE, USA) (see http://www.drugs.com/stats/top100/2013/sales; accessed on August 6, 2021). RST belongs to the third-generation statins, which are synthetic and in the form of pure active enantiomers, and it has the greatest inhibitory effect on cholesterol biosynthesis (McTaggart et al., 2001), and among the statins, it alters the high-density lipoprotein profile most favorably (Asztalos et al., 2007). RST is administered in daily doses of 5–40 mg, and its half-life is approximately 19 hours (Lwin et al., 2018). Theoretically, RST may be the most suitable for use in breastfeeding as it has a relatively large molecular weight (1,001.14 g/mol), a higher degree of protein binding (90%) and a higher volume of distribution compared with other statins (Lwin et al., 2018).

Besides their beneficial properties, statins also have numerous adverse effects that include relatively low rates of severe myopathy, rhabdomyolysis, renal failure and increases in liver enzymes (Kostapanos et al., 2010). During pregnancy, the use of statins also requires caution because of their interference with cholesterol biosynthesis. Proper HMG-CoA reductase activity and cholesterol levels are essential for cell proliferation and early embryonal development (Ohashi et al., 2003). The inhibition of this enzyme by

statins may disrupt membrane synthesis, cellular proliferation and growth, metabolism and protein glycosylation, which are crucial for the normal development of the placenta (Lecarpentier et al., 2012). HMG-CoA reductase mRNA is highly expressed in the post-implantation rat embryos, from the gastrulation through neurulation, and early organogenesis, with strong signal observed in primitive ectoderm and neural tube, which may reflect developmental requirements for products of the mevalonate pathway in these organs (Brewer et al., 1993). The importance of mevalonate-derived intermediates in early embryogenesis was reported earlier in mouse models (Surani et al., 1983) when the inhibition of HMG-CoA reductase interrupted pre-implantation development, although this effect was reversed by mevalonate supplementation. Furthermore, an examination of growth-arrested embryos revealed a predominance of nuclei with highly condensed chromatin, which is a hallmark of apoptosis. A study also showed that the alteration of maternal levels of steroids synthesized from cholesterol could potentially play a role in developmental toxicity arising from prenatal exposure to HMG-CoA reductase inhibitors (Henck et al., 1998). It should be mentioned, however, that there is limited evidence of statin usage in human studies.

During normal pregnancy, there is a physiological increase in serum lipid concentration, with a concomitant increase in blood cholesterol level. While the maternal cholesterol supply is of minimal importance to the developing fetus as 80% of fetal cholesterol is produced endogenously (Smith and Costantine, 2020), the interruption of cholesterol biosynthesis might affect embryonic development (Godfrey et al., 2012). As a result of their potentially harmful, but not well documented effects on the embryo, statin treatments for women should be discontinued 3 months before attempting to become pregnant, and they should not be used during pregnancy or breastfeeding (Thorogood et al., 2009). Lwin et al. (2018) confirmed that statin appears to pass preferentially into breast milk, but the estimated infant exposure is low.

As recent studies have emphasized the importance of maternal effects on chromatin structure and the interrelationship between the genome, epigenome, and environment (Danielewicz et al., 2020; Monk et al., 2019) on one hand, and because we have very limited data on any epigenetic study involving RST on the other, we decided to investigate whether RST elicited molecular epigenetic events such as histone methylation in the brains of the newborn rats whose mothers had been treated over time with the drug.

2. SPECIFIC AIMS

Epigenetic regulation allows the alteration of the phenotype or transcriptional state of a cell or an organism without affecting its genome, and this leads to adaptation to various developmental and/or environmental cues. Histone modification is one of the main mechanisms for epigenetic modifications. Examining histone modifications at a particular genomic region, or across the genome, can reveal the structure of chromatin, thereby permitting DNA accessibility and gene activation states, or even locations of gene regulatory elements (Kimura, 2013). Histone methylation has been linked to transcription initiation and elongation, heterochromatin silencing and other functions. During the embryonal development histone methylation landscapes of brain cells are sensitive to a wide range of environmental perturbations (Shen et al., 2014).

RST, as a member of statins, catalyzes the conversion of HMG-CoA to mevalonate and it is generally used for the treatment of high cholesterol levels (Taylor et al., 2013). While it has beneficial effects on inflammation and may reduce the risk of certain cancers, there are a few known side effects of the drug. Currently, the use of statins is contraindicated during pregnancy. The main clinical concern is the teratogenic effect of statins on the fetus, though there is no evidence to suggest that the use of statins in pregnancy increases the risk of fetal abnormalities.

Since a large percentage of pregnancies are unplanned, there is a good chance that a pregnant woman may be unknowingly taking a statin during the early part of the pregnancy. As regards epigenetics, we have limited data on epigenetic studies involving RST. In an attempt to shed more light on the epigenetic effects of RST, we set out to characterize, partly by applying quantitative techniques, and determining the distributions and levels of selected histone PTMs in newborn rat brains. As far as we know, no similar epigenetic study has been reported to date.

Our specific aims were:
1) To determine whether RST induces molecular epigenetic events in the brains of newborn rats whose mothers were pretreated with the drug during their pregnancy;
2) To determine whether *in utero* RST treatment could be related to cytoarchitectonic alteration and/or influence cell proliferation in newborn brains;

3) To quantitatively analyze the changes in methylation patterns as a consequence of *in utero* RST exposure, and identify the cell types that display these epigenetic changes in newborn brains.

3. MATERIALS AND METHODS

3.1. Animal handling and treatment

Pregnant Sprague–Dawley rats (190–210 g) were kept under standard housing conditions and fed *ad libitum* with regular laboratory chow. Pregnant rats were divided into three groups. Besides the absolute controls (no supplements at all), the vehicle-treated control animals received a small amount (650 mg) of liver pâté in pellet form once a day, whereas treated rats were given daily oral doses of RST (0.25 mg/kg body weight) mixed into pellets of liver pâté. The dose administered to rats was within the human therapeutic dose range (5–40 mg; see https://www.drugs.com/crestor.html; accessed on August 6, 2021). Both groups received this liver pâté supplement (with or without RST) from the 11th day of pregnancy for 10 days (or until delivery). Feeding with the liver pâté was carried out individually, using forceps. Five breeding runs (4–6 pregnant rats each) provided the litters (6–12 pups from each mother) from which independent experiments were performed. On postnatal day 1, the cerebral hemispheres of absolute control, vehicle-treated control, and RST-treated rats were removed and either homogenized for western blot analysis or embedded in paraffin for hematoxylin and eosin (H&E) staining and fluorescent immunohistochemistry/confocal microscopy.

3.2. Antibodies

The antibodies used in this study are listed in **Tables 1** and **2**. Several antibodies specific for Lys methylation sites and states of H2A, H2B, H3, and H4 histone proteins were selected for western blot analyses and fluorescent immunohistochemistry. Antibodies for cell-specific markers were used to detect neurons, astrocytes, oligodendrocytes and microglial cells, as well as to check for possible changes in their ratios. The anti-Ki67 antibody was used to visualize proliferating cells (Szabo et al., 2016; Dulka et al., 2021).

Primary antibody, full/abbrev. name	Final dilution	Company name	Secondary antibody with fluorochrome, full name	Company	Final dilution
Mouse anti-NeuN, monocl. ab. (**NeuN**)	1:100	Chemicon, Temecula, CA, USA	Alexa Fluor 488 goat anti-mouse IgG	Invitrogen, Carlsbad, CA, USA	1:1000
Mouse anti-Iba1, monocl. ab. (**Iba1**)	1:250	Abcam, Cambridge, UK	Alexa Fluor 488 goat anti-mouse IgG	Invitrogen, Carlsbad, CA, USA	1:1000
Rabbit anti-Iba1, polycl. ab. (**Iba1**)	1:300	Abcam, Cambridge, UK	Alexa Fluor 568 goat anti-rabbit IgG	Invitrogen, Carlsbad, CA, USA	1:1000
Rabbit anti Ki-67, polycl. ab. (**Ki-67**)	1:400	Thermo Fisher Scientific, Inc., Waltham, MA, USA	Alexa Fluor 568 goat anti-rabbit IgG	Invitrogen, Carlsbad, CA, USA	1:1000
Mouse anti-GFAP, monocl. ab. (**GFAP**)	1:100	Thermo Fisher Scientific, Inc., Waltham, MA, USA	Alexa Fluor 488 goat anti-mouse IgG	Invitrogen, Carlsbad, CA, USA	1:1000
Rabbit anti-Histone H3 (mono methyl K4) polycl. ab. (**H3K4me1**)	1:500	Biorbyt, Cambridge, UK	Alexa Fluor 568 goat anti-rabbit IgG	Invitrogen, Carlsbad, CA, USA	1:1000
Rabbit anti-Histone H3 (tri methyl K4) polycl. ab. (**H3K4me3**)	1:500	Biorbyt, Cambridge, UK	Alexa Fluor 568 goat anti-rabbit IgG	Invitrogen, Carlsbad, CA, USA	1:1000

Table 1. Primary and secondary antibodies used in immunohistochemistry. Abbreviations are listed on page 5.

Primary antibody, full/abbrev. name	Final dilution	Company name	Secondary antibody with fluorochrome, full name	Company	Final dilution
Rabbit anti-Histone H2A (mono methyl K118) monocl. ab. (EPR17488) (**H2AK118me1**)	1:1000	Abcam, Cambridge, UK	Anti-rabbit IgG, peroxidase conjug.	Sigma, St. Louis, MO, USA	1:2000
Rabbit anti-Histone H2B (mono methyl K5) polycl. ab. (**H2BK5me1**)	1:1000	Abcam, Cambridge, UK	Anti-rabbit IgG, peroxidase conjug.	Sigma, St. Louis, MO, USA	1:2000
Rabbit anti-Histone H3 polycl. ab. (**H3**)	1:1500	Abcam, Cambridge, UK	Anti-rabbit IgG, peroxidase conjug.	Sigma, St. Louis, MO, USA	1:2000

Rabbit anti-Histone H3 (mono methyl K4) polycl. ab. (**H3K4me1**)	1:1000	Biorbyt, Cambridge, UK	Anti-rabbit IgG, peroxidase conjug.	Sigma, St. Louis, MO, USA	1:2000
Rabbit anti-Histone H3 (tri methyl K4) polycl. ab. (**H3K4me3**)	1:1000	Biorbyt, Cambridge, UK	Anti-rabbit IgG, peroxidase conjug.	Sigma, St. Louis, MO, USA	1:2000
Rabbit anti-Histone H3 (tri methyl K9) polycl. ab. (**H3K9me3**)	1:1000	Abcam, Cambridge, UK	Anti-rabbit IgG, peroxidase conjug.	Sigma, St. Louis, MO, USA	1:2000
Rabbit anti-Histone H3 (tri methyl K27) polycl. ab. (**H3K27me3**)	1:1000	Biorbyt, Cambridge, UK	Anti-rabbit IgG, peroxidase conjug.	Sigma, St. Louis, MO, USA	1:2000
Rabbit anti-Histone H3 (di methyl K36) monocl. ab. (EPR16994(2)) (**H3K36me2**)	1:5000	Abcam, Cambridge, UK	Anti-rabbit IgG, peroxidase conjug.	Sigma, St. Louis, MO, USA	1:2000
Rabbit anti-Histone H4 polycl. ab. (**H4**)	1:1500	Abcam, Cambridge, UK	Anti-rabbit IgG, peroxidase conjug.	Sigma, St. Louis, MO, USA	1:2000
Rabbit anti-Histone H4 (di methyl K20) polycl. ab. (**H4K20me2**)	1:2000	Abcam, Cambridge, UK	Anti-rabbit IgG, peroxidase conjug.	Sigma, St. Louis, MO, USA	1:2000
Rabbit anti-Histone H4 (tri methyl K20) polycl. ab. (**H4K20me3**)	1:1000	Abcam, Cambridge, UK	Anti-rabbit IgG, peroxidase conjug.	Sigma, St. Louis, MO, USA	1:2000
Mouse anti-GAPDH, monocl. ab., clone GAPDH-71.1 (**GAPDH**)	1:20000	Sigma, St. Louis, MO, USA	Anti-mouse IgG, peroxidase conjug.	Sigma, St. Louis, MO, USA	1:2000
Rabbit anti-Iba1, polycl. ab. (**Iba1**)	1:500	FUJIFILM Wako, Osaka, Japan	Anti-rabbit IgG, peroxidase conjug.	Sigma, St. Louis, MO, USA	1:2000
Mouse anti-beta III Tubulin, monocl. ab., clone TU-20 (**β-III tubulin**)	1:500	Abcam, Cambridge, UK	Anti-mouse IgG, peroxidase conjug.	Sigma, St. Louis, MO, USA	1:2000
Mouse anti-EAAT1, monocl. ab. (**EAAT1**)	1:1000	Abcam, Cambridge, UK	Anti-mouse IgG, peroxidase conjug.	Sigma, St. Louis, MO, USA	1:2000
Mouse anti-CNPase, monocl. ab. (**CNPase**)	1:250	Abcam, Cambridge, UK	Anti-mouse IgG, peroxidase conjug.	Sigma, St. Louis, MO, USA	1:2000

Table 2. Primary and secondary antibodies used in western blots. Abbreviations are listed on page 5.

3.3. Histology

Newborn rat brains were removed quickly, then fixed in 0.05 M phosphate-buffered saline (PBS) containing 4% formaldehyde, and embedded in paraffin. Sections were cut (6 μm thickness) on a microtome (Leica RM2235; Leica Mikrosysteme Vertrieb GmbH, Wetzlar, Germany), mounted on glass slides coated with (3-aminopropyl)triethoxysilane (Menzel GmbH, Saarbrücken, Germany), and subsequently used for H&E staining and immunohistochemistry (Legradi et al., 2020).

3.4. Fluorescent and confocal immunohistochemistry

Paraffin-embedded tissue sections were deparaffinized, rehydrated, and placed in a jar filled with 0.01 M citrate buffer (pH 6.0) containing 0.05% Tween-20, and then heated at 95°C for 20 min. The sections were washed 3 × 10 min in 0.05 M PBS containing 0.05% Tween-20 and blocked in 0.05 M PBS solution containing 0.05% Tween-20, and 5% normal goat serum (NGS) for 1 h at room temperature (RT). The sections were then incubated with primary antibodies in a 0.05 M PBS solution containing 0.05% Tween 20 and 5% NGS overnight at 4 °C. After washing (4 × 10 min in 0.05 M PBS containing 0.05% Tween-20), primary antibodies were labeled with either Alexa 568–conjugated goat anti-rabbit IgG or Alexa 488–conjugated goat anti-mouse IgG secondary antibodies (final dilution 1:1000; Invitrogen, Carlsbad, CA, USA) in blocking solution for 3 h at RT. After 4 × 10 min washes in 0.05 M PBS containing 0.05% Tween-20, cell nuclei were stained in 2-[4-(aminoiminomethyl)phenyl]-1H-indole-6-carboximidamide hydrochloride (DAPI) solution (Thermo Fisher Scientific, Waltham, MA, USA). Digital images were captured on a Leica DMLB epifluorescence microscope using a Leica DFC7000 T CCD camera (Leica Microsystems CMS GmbH, Wetzlar, Germany) and the LAS X Application Suite X (Leica) (Legradi et al., 2020; Dulka et al., 2021).

Selected immunolabeled sections were also examined with a confocal laser scanning microscope (Olympus Fluoview FV1000, Olympus Life Science Europa GmbH, Hamburg, Germany). Images (512 × 512 pixels) were captured along the Z-axis, with a distance of 0.5 μm between consecutive optical slices using the following microscope configuration: objective lens, UPLSAPO 60x; numerical aperture, 1.35; sampling speed, 4 μs/pixel; optical zoom, 2x; and scanning mode, sequential unidirectional. Excitation wavelengths

were as follows: 405 nm (DAPI), 488 nm (Alexa Fluor 488), and 543 nm (Alexa Fluor 568). Z-stack images were prepared using 10–12 consecutive optical slices.

3.5. Western blot analysis

Brains from newborn rats were dissected, homogenized in 50 mM Tris-HCl (pH 7.5 at 4 °C) containing 150 mM NaCl, 2 μg/ml leupeptin, 1 μg/ml pepstatin, 2 mM phenylmethylsulfonyl fluoride, and 2 mM EDTA, and centrifuged at 14,000 × g for 10 min. The supernatant was aliquoted, and the pellet was rehomogenized in 50 mM Tris-HCl (pH 7.5 at 4 °C) containing 150 mM NaCl, 0.1% Nonidet-P40, 0.1% cholic acid, 2 μg/ml leupeptin, 1 μg/ml pepstatin, 2 mM phenylmethylsulfonyl fluoride, and 2 mM EDTA. The samples were incubated on ice for 30 min and then aliquoted. The protein concentrations of the samples were determined by the method of Lowry et al. (1951).

Western blot analysis was performed as previously described (Szabo et al., 2016; Legradi et al., 2020; Lajkó et al., 2020). For western blot analyses, 15–30 mg of protein was separated on a SDS polyacrylamide gel (4%–12% stacking gel/resolving gel), transferred onto a Hybond-ECL nitrocellulose membrane (Amersham Biosciences, Little Chalfont, Buckinghamshire, England), blocked for 1 h in 5% nonfat dry milk in Tris-buffered saline (TBS) containing 0.1% Tween-20, and incubated overnight with the appropriate primary antibodies as well as with that of the internal control (mouse anti-GAPDH monoclonal antibody). After five rinses in 0.1% TBS–Tween-20, the membranes were incubated for 1 h with the appropriate horseradish peroxidase-conjugated goat anti-rabbit or rat anti-mouse secondary antibodies, and washed three times as above. The enhanced chemiluminescence method (ECL Plus western blotting detection reagents; Amersham Biosciences) was used to identify immunoreactive bands according to the manufacturer's protocol. The exposure time and film development were optimized for each antibody.

3.6. Digital processing and image analysis

Grayscale digital images of the immunoblots were acquired by scanning the autoradiographic films with a desktop scanner (Epson Perfection V750 PRO; Seiko Epson Corp., Suwa, Japan). The images were scanned and processed at identical settings to allow comparisons of western blots obtained from different samples. The bands were analyzed by densitometry via the computer program ImageJ (version 1.47; developed at the U.S.

National Institutes of Health by W. Rasband, available at https://imagej.net/Downloads)
(Schneider et al., 2012) as we published earlier (Lajkó et al., 2020; Legradi et al., 2020).
The immunoreactive densities of equally loaded lanes were quantified, the samples were
normalized to the densities of internal controls (GAPDH), and, for epigenetic studies,
presented as a percentage of controls.

3.7. Statistical analysis

All statistical comparisons were made using SigmaPlot software (v. 12.3, Systat Software,
Inc., Chicago, IL, USA), and data were analyzed with one-way analysis of variance
(ANOVA) or the Mann–Whitney rank sum test. For western blots, values were presented
as mean ± standard errors of mean (SEM) from at least five immunoblots, each
representing an independent newborn from independent breeding runs. A *p*-value of
< 0.05 was considered significant.

4. RESULTS

4.1. Histone methylation patterns of absolute and vehicle-treated controls do not differ significantly in the newborn brain

When investigating epigenetic events in the newborn brain after the *in utero*
administration of RST, we assumed that liver pâté, the vehicle used to deliver RST, did
not elicit changes in histone methylation patterns. To ascertain such possible effects of
the liver pâté, we assayed H2AK118me1, H2BK5me1, H3, H3K4me1, H3K4me3,
H3K9me3, H3K27me3, H3K36me2, H4, H4K20me2, and H4K20me3 levels using western
blots from absolute control and vehicle-treated control newborn rat brain samples.

Our data showed that liver pâté, as a nutritional supplement, had no significant
effect on the methylation patterns of these sites (**Figure 4**). As all vehicle-based controls
had values between 93.2% ± 7.7% and 106.4% ± 10.7% of the absolute controls, with no
significant differences among them from at least five separate experiments, we refer to
vehicle-treated controls henceforth as merely "controls", and further data presentation
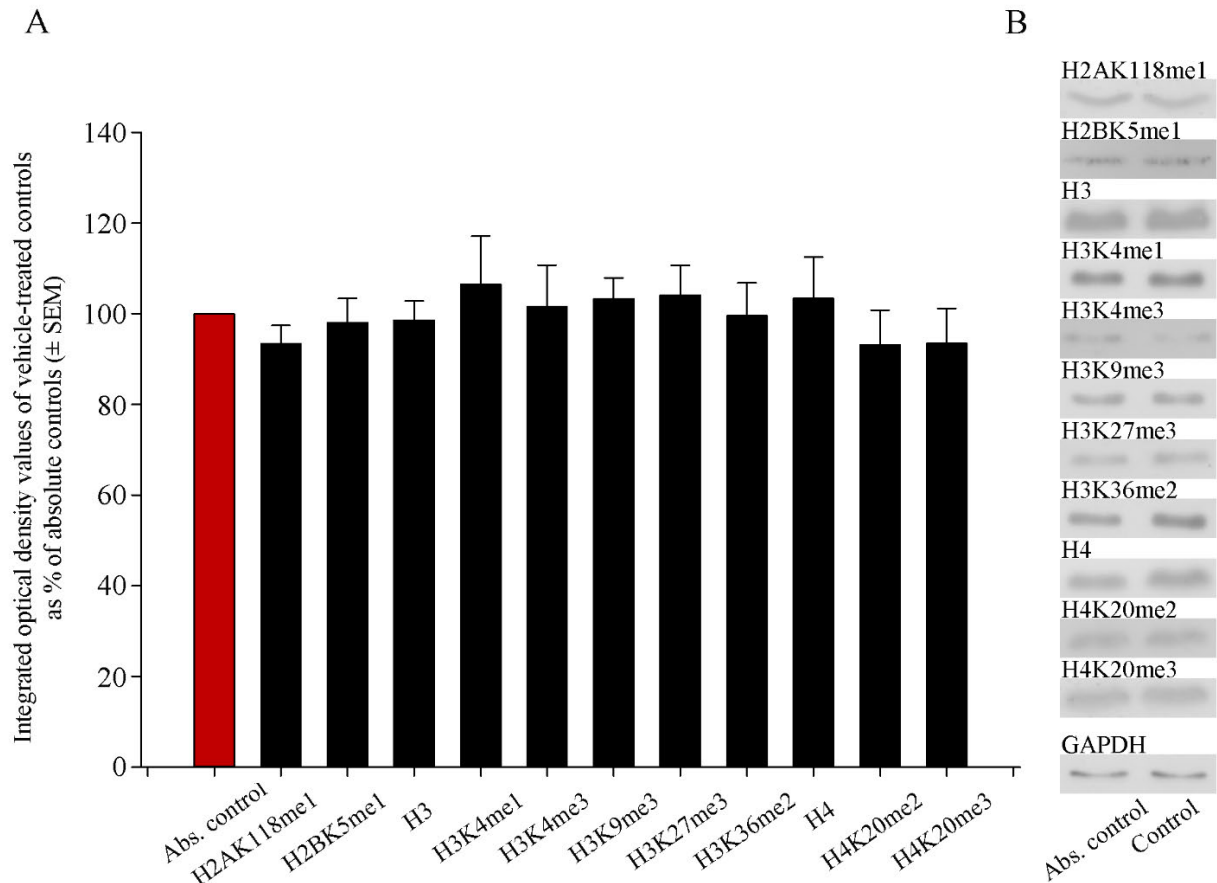uses vehicle-based controls as a reference point.

Figure 4. Quantitative western blot analyses of histone methylation patterns in the brains of absolute control (red column) and vehicle-treated control newborn rats. (**A**) Protein contents from absolute controls and vehicle-treated controls were determined and assayed on western blots. Gel-loaded protein samples were separated by gel electrophoresis, transferred to nitrocellulose membranes, and assayed for immunoreactivity with antibodies that recognize core histones and histone methylations. Grayscale digital images of the immunoblots were scanned and processed under identical settings to allow comparisons to be made between western blots obtained from different samples. Values indicate the mean ± SEM. Integrated optical density data were analyzed with ANOVA using SigmaPlot. No statistically significant differences were observed between the absolute control and vehicle-control samples. (**B**) Representative western blot images of immunoreactivity toward antibodies specific to methylation sites and states, together with the GAPDH immunoreactive bands that served as inner standards.

4.2. *In utero* RST exposure does not affect cell composition in the newborn brain

RST exposure *in utero* did not bring about structural abnormalities in the newborn brain at the level of light microscopy, as evidenced by H&E staining (**Figure 5**).
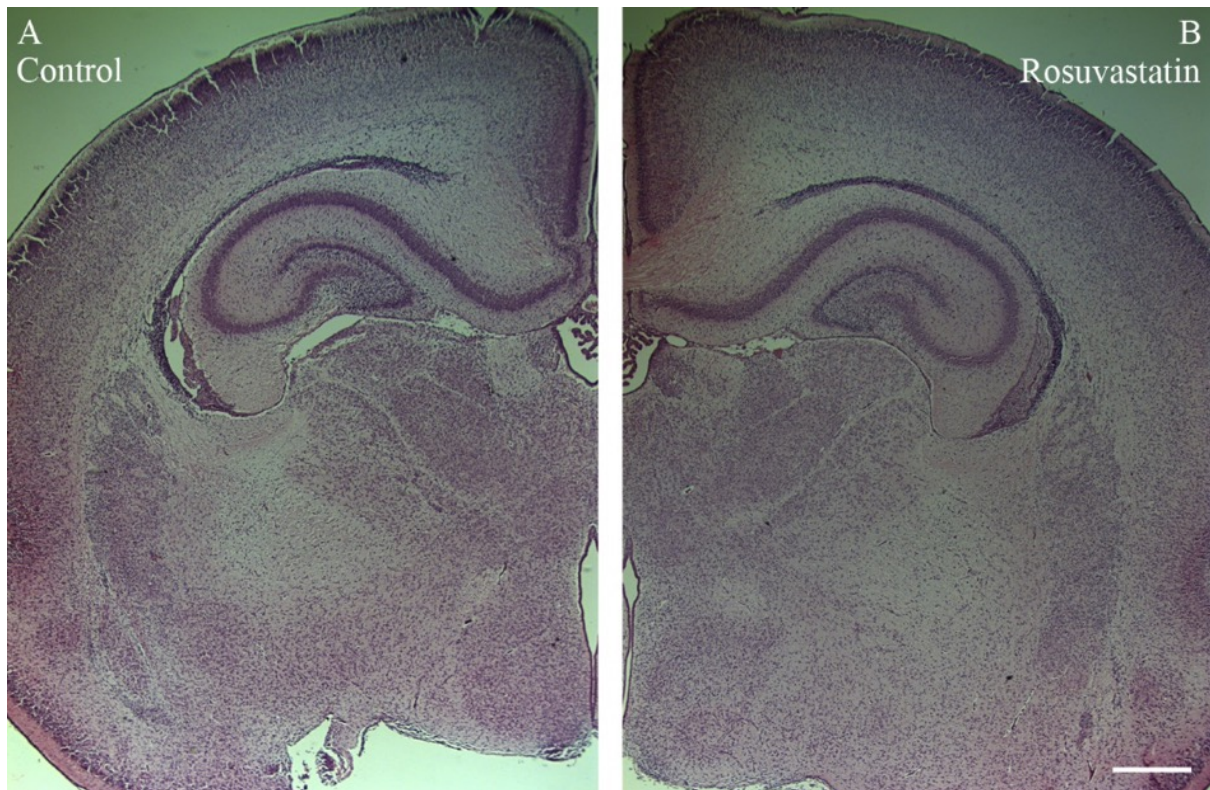
Figure 5. Representative pictures on the cytoarchitecture of the newborn rat brain. No differences were observed in paraffin-embedded, H&E-stained tissue sections between (**A**) control and (**B**) RST-treated newborn brains by light microscopy. Scale bar in (**B**): 1 mm.

Double immunofluorescent staining for microglial and neuronal cell markers revealed that the ratios of these cells did not change between the control and RST-treated group (**Figure 6**).

A quantitative western blot analysis of cell-specific markers showed that prenatal exposure to RST did not cause abnormalities in cell composition in the newborn brains, as the ratios of these cells did not change significantly between control and treated groups (**Figure 7**).
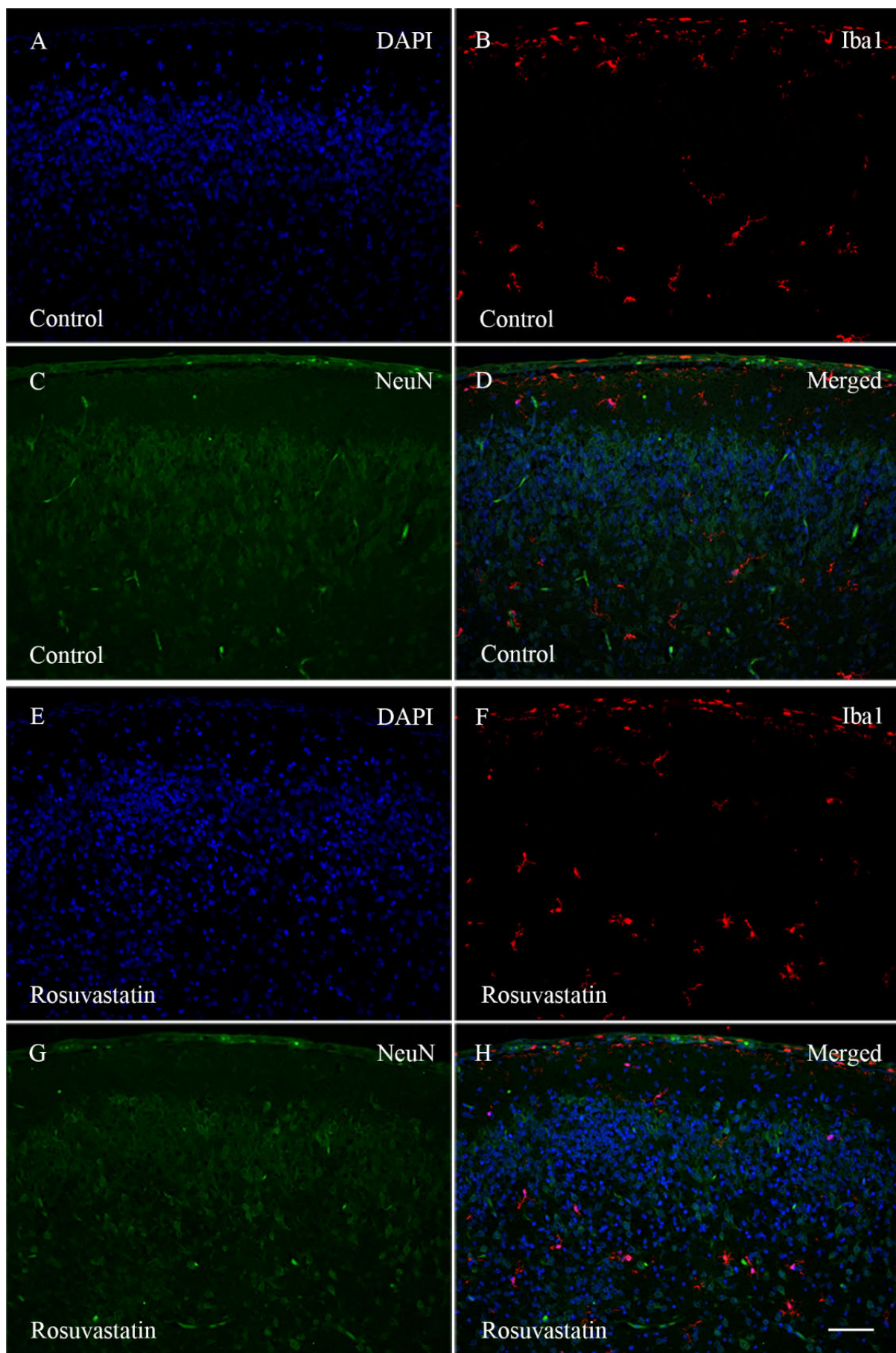
Figure 6. Representative double immunofluorescent pictures with specific stainings for microglia and neurons in the cortex of the newborn rat brain. Microglia were labeled with the anti-Iba1 antibody/Alexa Fluor 568 goat anti-rabbit IgG complex (red), whereas neurons were detected with the anti-NeuN antibody/Alexa Fluor 488 goat anti-mouse IgG complex (green). Cell nuclei were labeled with DAPI (blue). The pictures indicate that prenatal exposure to RST did not cause cytoarchitectural abnormalities that could be detected by light microscopy at this magnification. The ratio of microglia (**B**, **F**) to neurons (**C**, **G**) is similar between the control (**A**–**D**) and RST-treated (**E**–**H**) newborn brains. Scale bar for all in (**H**): 100 μm.
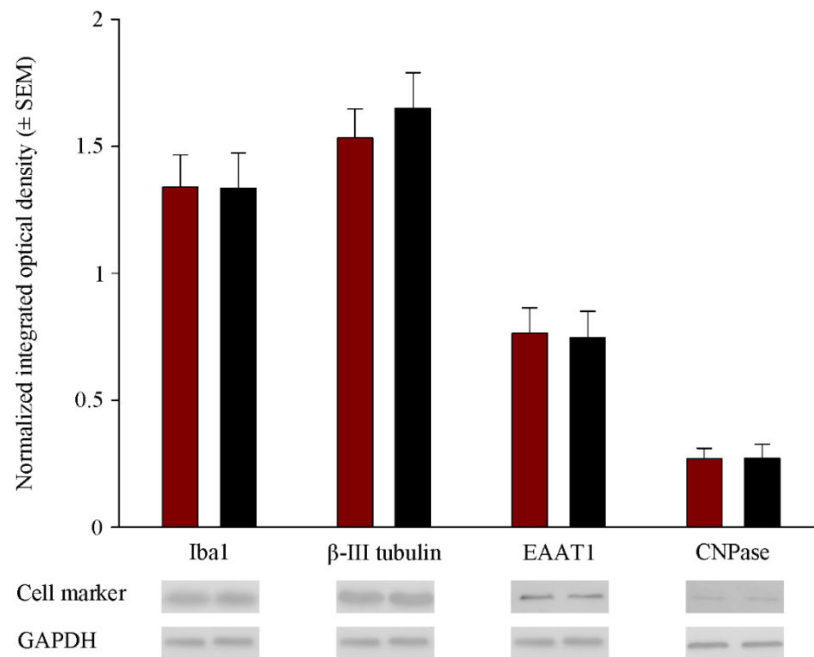
Figure 7. Quantitative western blot analyses of the main cell type markers from control and RST-treated newborn rat brains. Controls (red column) and RST-treated (black column) samples were analyzed quantitatively on western blots for microglial, neuronal, astrocyte, and oligodendrocyte markers. Protein samples (15–30 μg) were separated by gel electrophoresis, transferred to nitrocellulose membranes, and assayed for reactivity toward the Iba1 (microglia marker), beta III tubulin (neuron-specific marker), EAAT1 (astrocyte marker), CNPase (oligodendrocyte marker), and GAPDH proteins. Error bars indicate integrated optical density values (mean ± SEM) normalized to the values of the internal standard GAPDH. Representative western blot pictures are shown below the graph. No statistically significant differences were found between the control and the RST-treated groups.

These observations were supported by Ki67 fluorescent immunohistochemistry, as proliferation rates in the controls and prenatally RST-exposed rat brains were in the same range (**Figure 8**). Analyses of immunohistochemical data found roughly the same incidence of Ki67-immunopositive cells among the DAPI-labeled cell nuclei for both

control and prenatally RST-treated rats. Out of a total of 4,268 cells analyzed from controls and 3,557 cells analyzed from RST-treated newborns, 554 (12.9%) and 448 (12.5 %) cells were Ki67-positive, respectively.
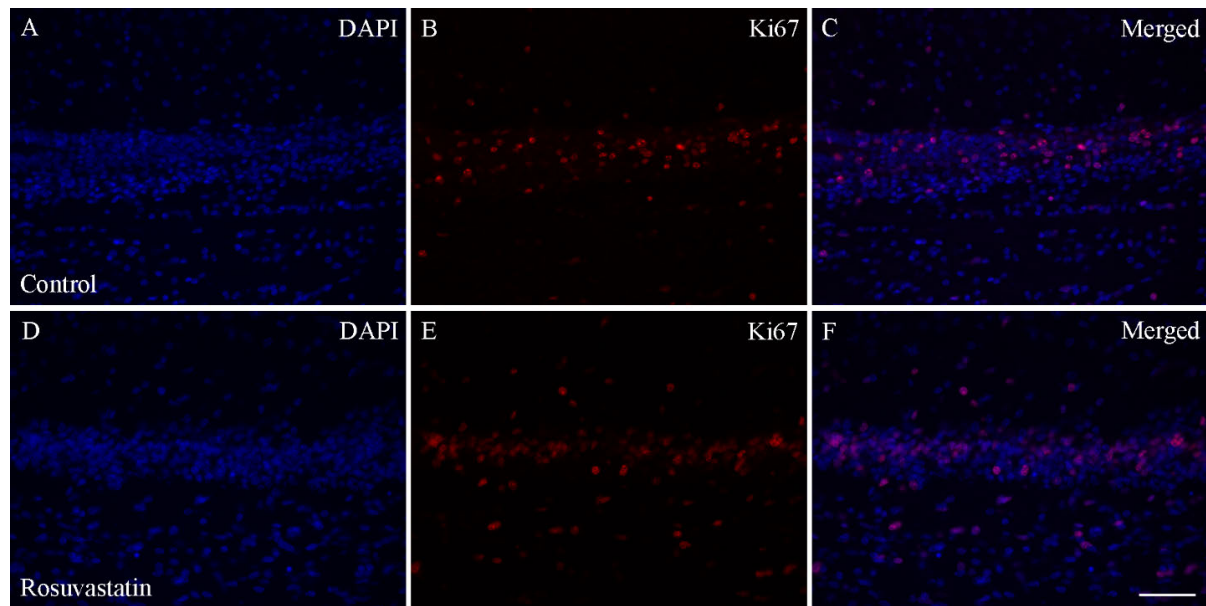

Figure 8. Ki67 immunohistochemistry of the hippocampus in control and prenatally RST-exposed newborn rats. The expression of Ki67 protein in tissue areas was quantified by determining the percentage of Ki67-positive nuclei (red) over the total number of nuclei (positive and negative nuclei). Immunohistochemical data analysis detected highly similar incidences for Ki67-immunopositive cells (**B**, **E**) among the DAPI dye-labeled cell nuclei (blue; **A**, **D**), both for the controls (12.9%) and the prenatally RST-treated rats (12.5%). Merged pictures (**C**, **F**) are shown. Scale bar for all in (**F**): 50 μm.

4.3. *In utero* RST exposure alters histone methylation patterns in the newborn brain

Several antibodies that recognize different methylation sites for H2A, H2B, H3, and H4 histones were used in western blotting experiments (**Table 2**). We found that prenatal RST treatment induced a general, nonsignificant increase in H2AK118me1, H2BK5me1, H3, H3K9me3, H3K27me3, H3K36me2, H4, H4K20me2, and H4K20me3 levels, to 101.0%–111.7% of the control levels (**Figure 9**). However, the levels of histone H3 mono- and tri-methylation at Lys 4 (H3K4me1 and H3K4me3) were significantly elevated (134.3% ± 1.6% and 127.8% ± 8.5%, respectively) when compared to the control values. These modifications are known to play roles in transcription activation.
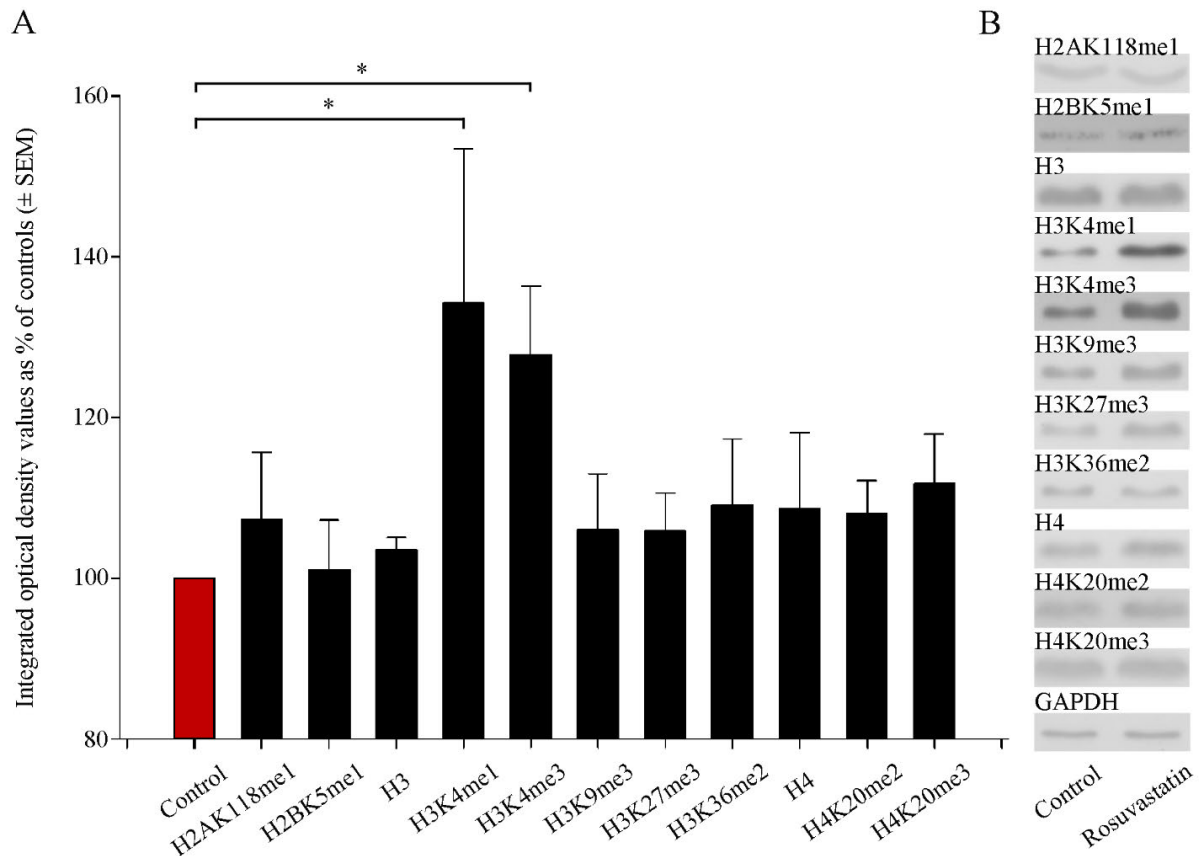
Figure 9. Quantitative western blot analyses of histone methylation patterns in newborn rat brains. (**A**) The protein content from vehicle-treated controls and RST-treated newborns was determined and assayed by western blotting. Gel-loaded protein samples were separated by gel electrophoresis, transferred to nitrocellulose membranes and assayed for immunoreactivity using antibodies that recognize different histone methylations. Grayscale digital images of the immunoblots were scanned and processed at identical settings to allow comparisons to be made between western blots obtained from different samples. Integrated optical density values were calculated as the percentage of vehicle-treated control values that had been normalized to the GAPDH internal standards. Prenatal RST exposure induced a general increase in Lys methylated sites of several histone proteins. A quantitative analysis showed that the histone H3 mono- and tri-methylation at Lys 4 (H3K4me1 and H3K4me3) increased significantly (134.3% and 127.8% of vehicle-treated controls, respectively). (**B**) Representative western blot images of immunoreactivity toward antibodies specific to methylation sites and states, together with the GAPDH immunoreactive bands that served as inner standards. Data were analyzed using the Mann–Whitney rank sum test. Values are presented as the mean ± SEM, where *p* < 0.05 is considered significant. **p* < 0.03.

4.4. The increase in H3K4me1 and H3K4me3 is localized mainly to neuronal cell nuclei

Cell-specific markers were used to localize the increased H3K4me1- and -me3-immunopositivities within the newborn brain. Most of the fluorescent immunoreactivity for these methylation marks was detected in NeuN-immunopositive neuronal cell nuclei, which constitute the vast majority of the tissue parenchyma at this time of postembryonic development (**Figures 10–12**).
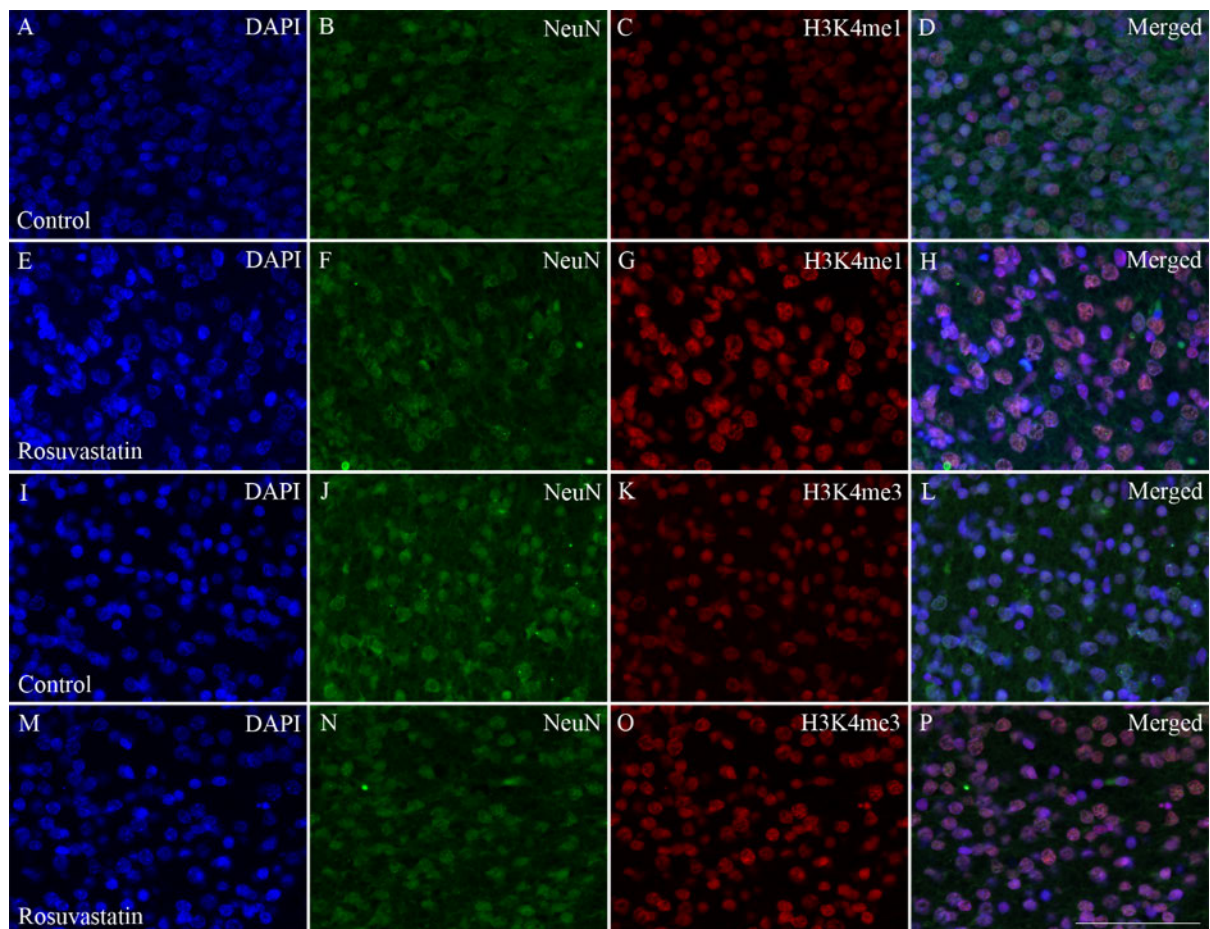

Figure 10. Colocalization of H3K4 methylation patterns and NeuN immunoreactivity in neurons of the newborn brain. DAPI-labeled cell nuclei are shown in blue (**A**, **E**, **I**, **M**). Immunoreactivity of the neuron-specific marker NeuN (**B**, **F**, **J**, **N**; shown here in green) and the histone methylation markers H3K4me1 and H3K4me3 (**C**, **G** and **K**, **O**, respectively; shown here in red) were colocalized in merged images (**D**, **H**, **L**, **P**). These immunohistochemical data were consistent with the results of western analyses as the immunofluorescent signal is more intensive on the sections from RST-exposed newborns (**E**–**H**; **M**–**P**) compared to controls (**A**–**D**; **I**–**L**). Scale bar for all in (**P**): 75 μm.
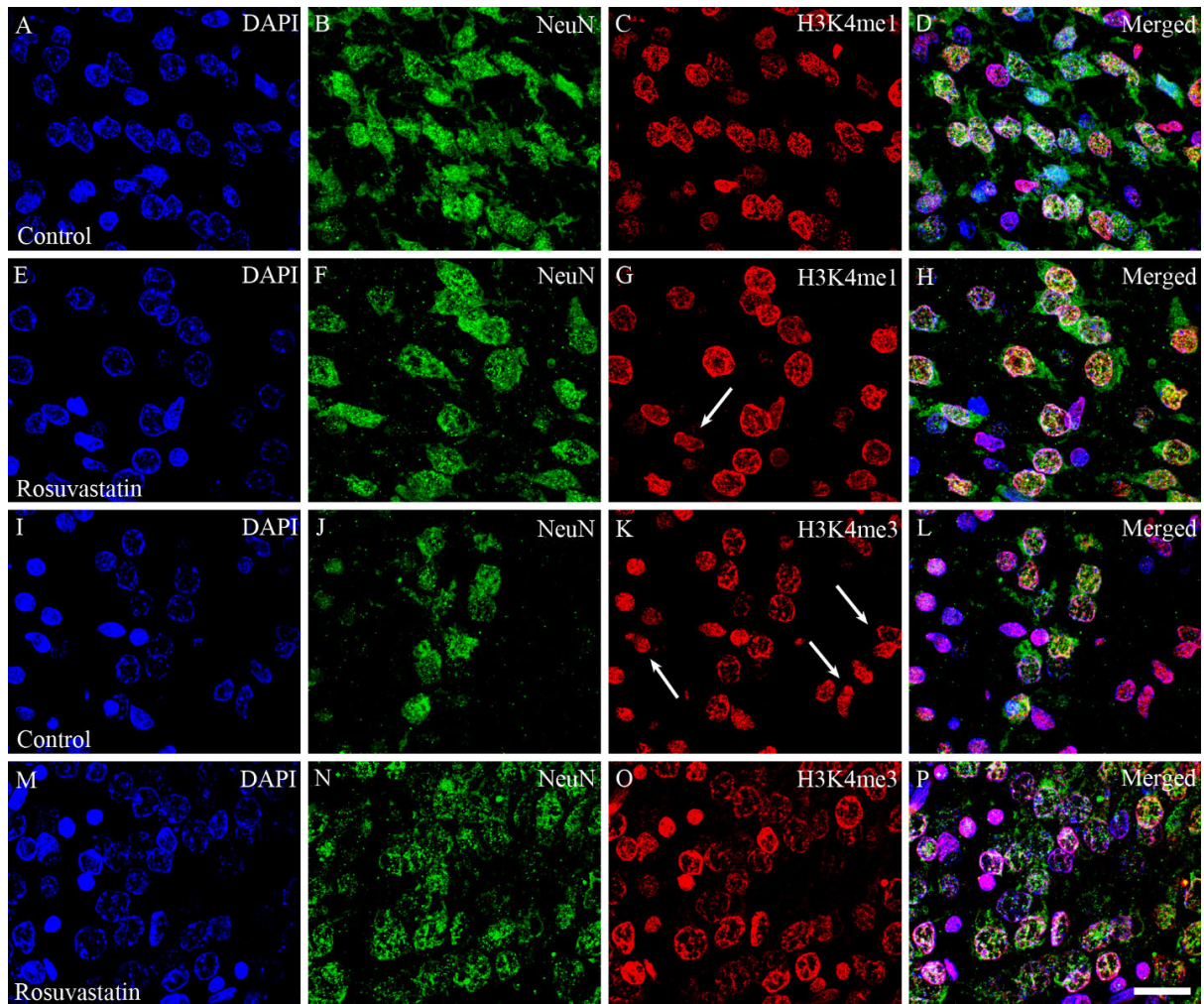
Figure 11. Laser confocal microscopy images of H3K4me1 and H3K4me3 immunoreactivities in neuronal nuclei. Paraffin sections of brains from control (**A–D**; **I–L**) and RST-treated newborn rats (**E–H**; **M–P**) were immunostained for NeuN (shown here in green) and H3K4me1 or H3K4me3 (shown here in red) and visualized by confocal microscopy. Cell nuclei were labeled with DAPI (blue). Note the overwhelmingly neuronal localization of the histone methylation marks. Some non-neuronal cells, notably in panel (**K**) (arrows), also display H3K4me3 marks. Scale bar for all in (**P**): 20 μm.
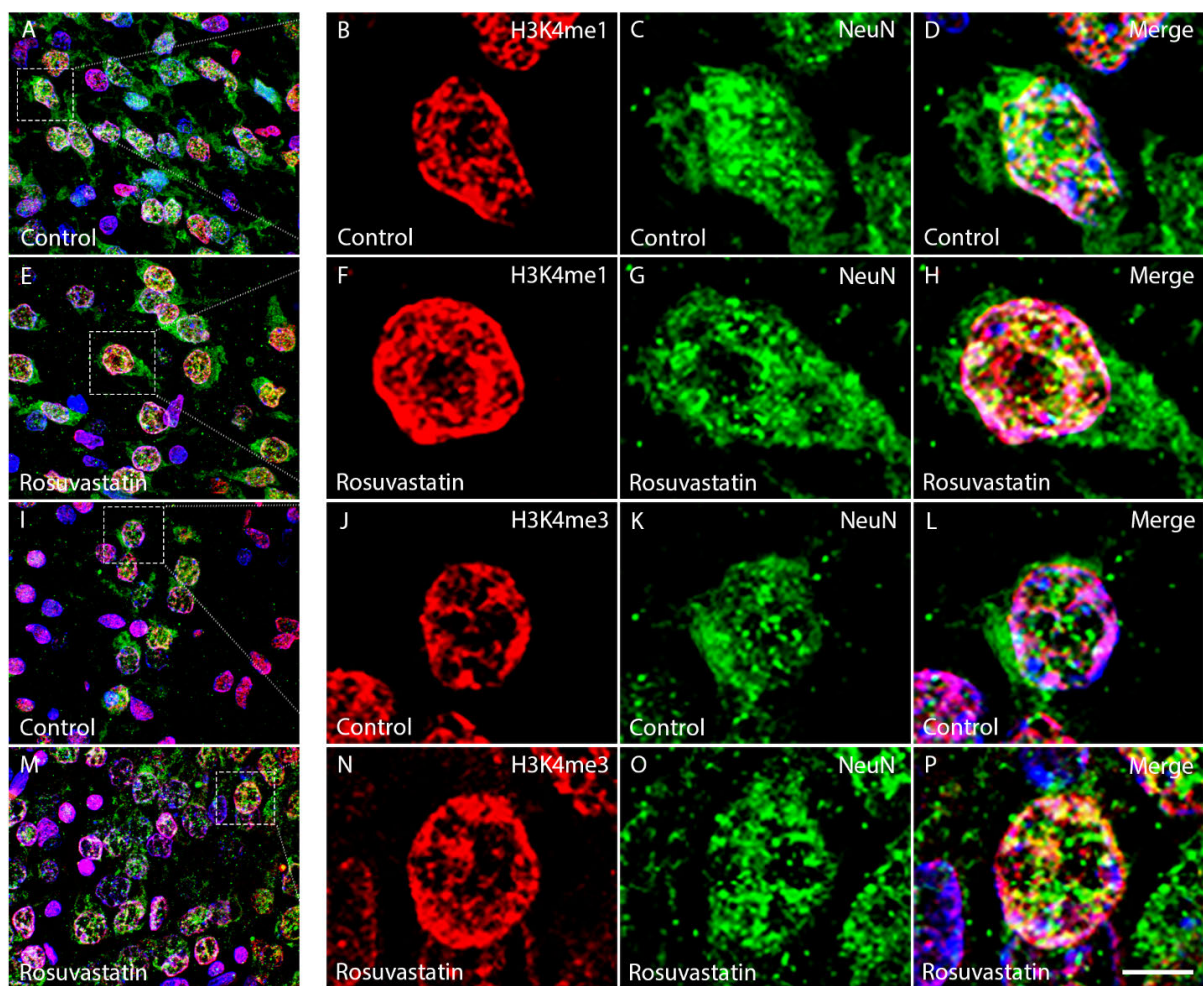
Figure 12. Laser confocal microscopy images of H3K4me1 and H3K4me3 immunoreactivities enlarged to neuronal nuclei. Immunostainings were performed both in paraffin sections of brains from control (**A**–**D**; **I**–**L**) and RST-treated newborn rats (**E**–**H**; **M**–**P**). Co-immunostaining with NeuN (green) and H3K4me1 (red) or H3K4me3 (red), respectively. Staining with DAPI (blue) was used to visualize cell nuclei. As regards distribution, H3K4me1/me3 immunoreactivity was localized to transcriptionally active euchromatin that was not overlapping with DAPI-labeled heterochromatin. Scale bar in (**P**): 5 μm.

Interestingly, besides neurons, few Iba1-positive microglia (**Figures 13** and **14**) and GFAP-positive astrocytes (**Figure 15**) exhibited increased H3K4me1and H3K4me3 immunopositive signals, although the numbers of these cells in the neonatal brain were negligible. These glial cells, especially microglia, display smaller nuclei with more compact chromatin, and they are smaller than the neurons in the newborn rat brain. Hardly any CNPase-positive oligodendrocytes were detected (data not shown), as myelogenesis occurs mainly postnatally.
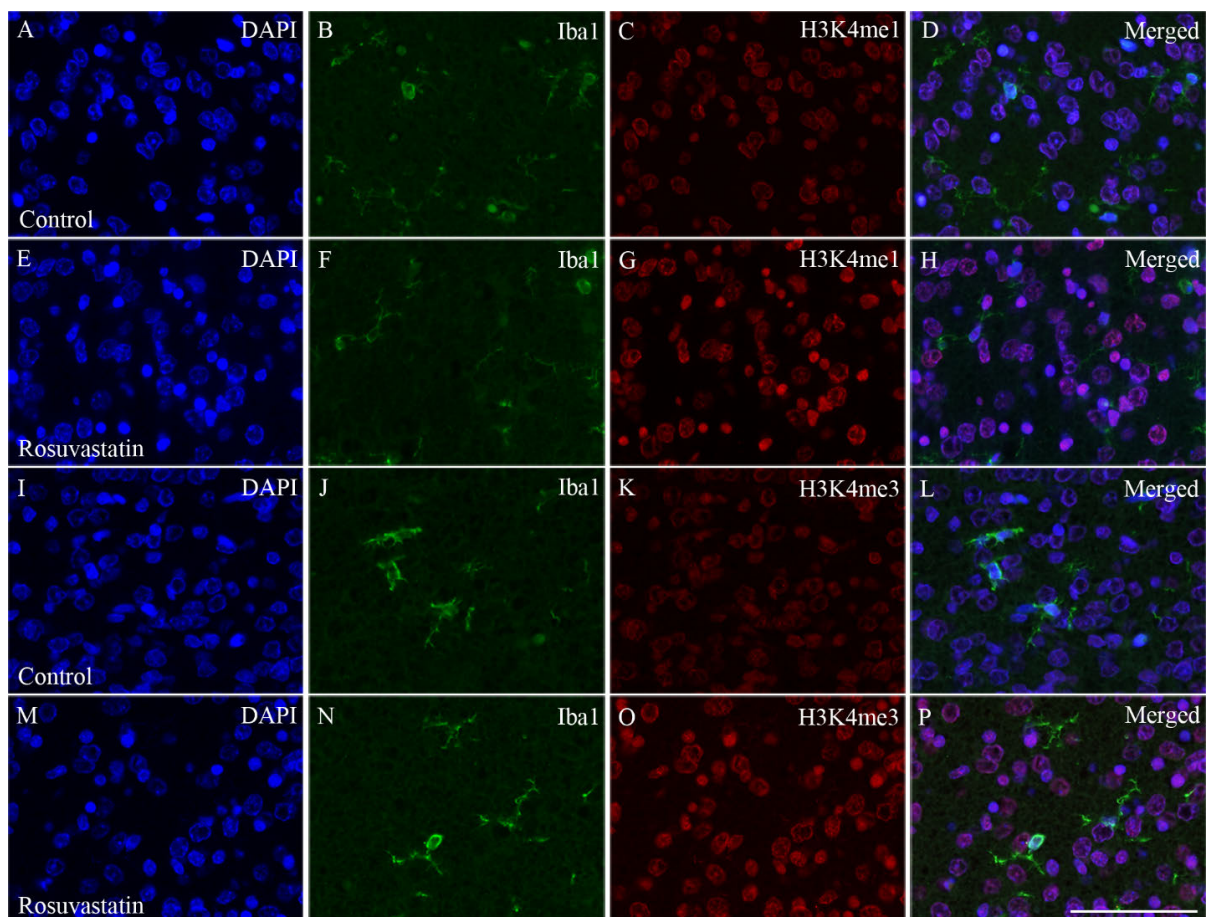
Figure 13. Colocalization of H3K4 methylation patterns and Iba1 immunoreactivity in microglial cells of the newborn rat brain. At birth, the majority of the cells are neurons. Microglia are unevenly distributed and located in specific "hotspots" such as the ventricular zone. Due to their overwhelmingly neuronal localization, H3K4me1 and H3K4me3 immunoreactivities (shown here in red) are more intensive on the sections cut from RST-treated newborn brain tissue (**E–H**; **M–P**) as compared to control newborns (**A–D**; **I–L**). A few H3K4 methylated cell nuclei formed part of Iba1-positive microglia (shown here in green). DAPI-labeled nuclei are shown in blue (**A, E, I, M**). Scale bar for all in (**P**): 75 μm.
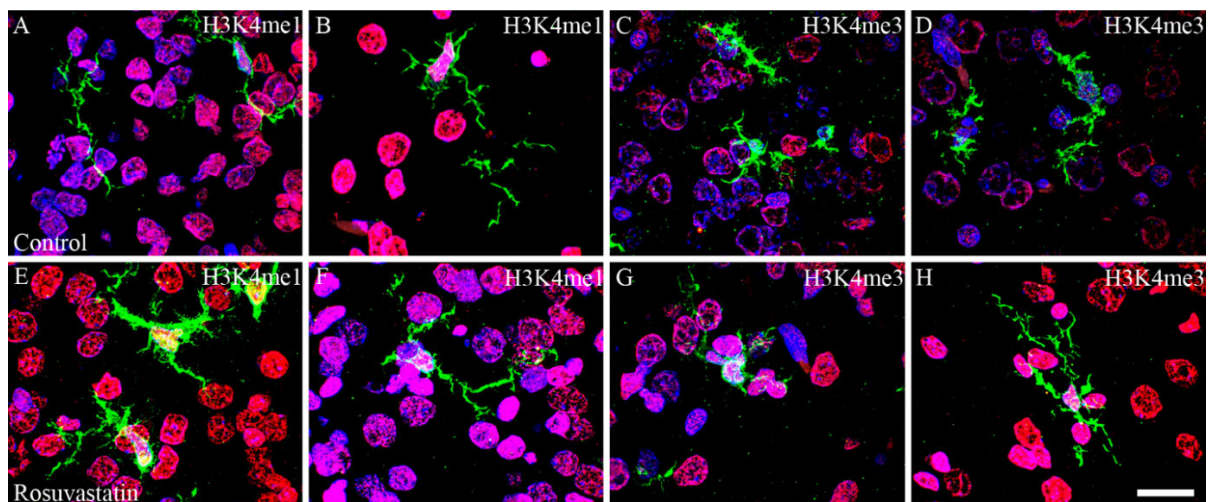
Figure 14. Laser confocal microscopy images of H3K4me1 and H3K4me3 immunoreactivities in microglial nuclei. Newborn brain sections of control (**A–D**) and RST-treated rats (**E–H**) were immunostained for Iba1 (green) and H3K4me1 and H3K4me3 (red), and visualized by confocal microscopy. DAPI-labeled cell nuclei are blue. Note the very few microglia that colocalize with the histone methylation marks in the merged pictures. Scale bar for all in (**H**): 20 μm.
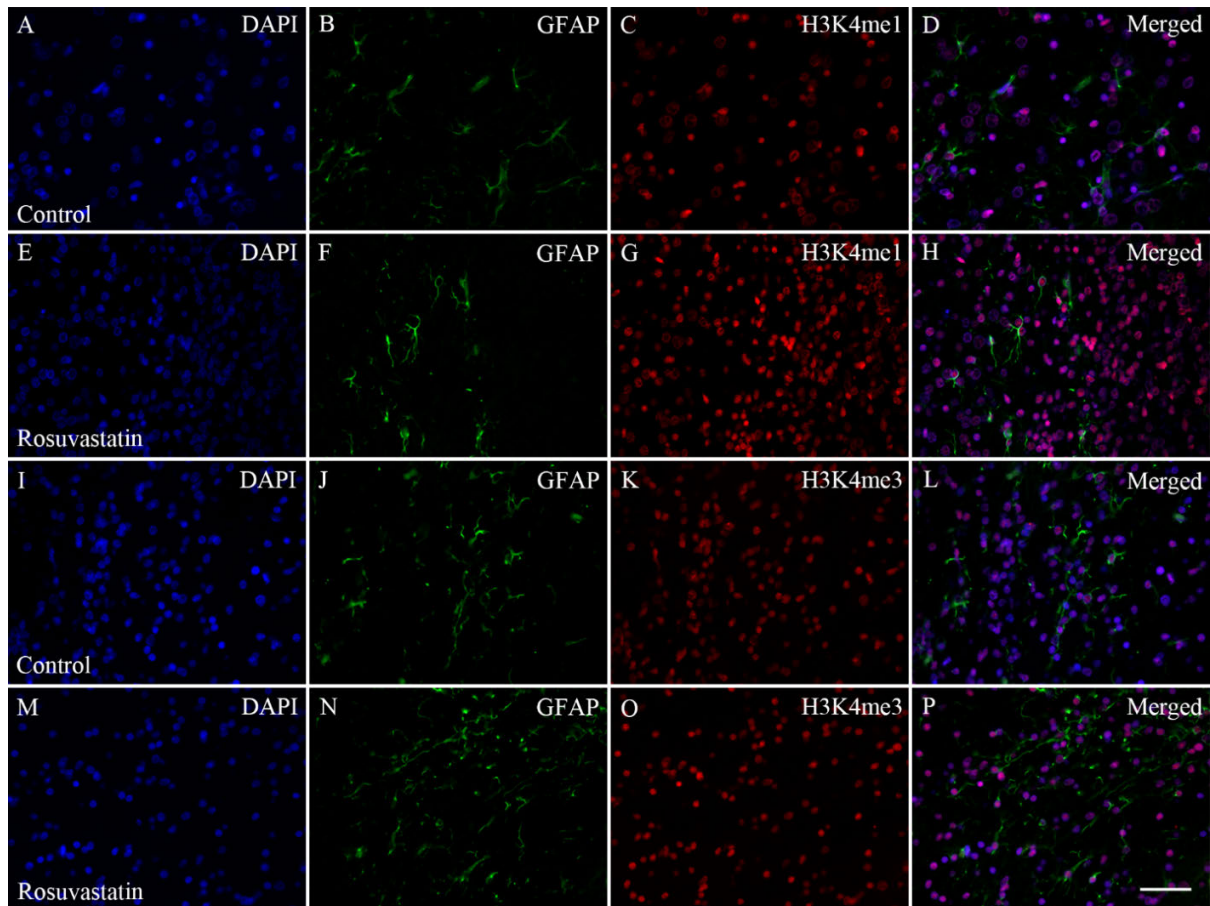

Figure 15. Double immunofluorescence staining for H3K4me1 and H3K4me3 in GFAP-positive astrocytes in the cortex. In the neonatal rat brain GFAP-positive cells (green; **B**, **F**, **J**, **N**) are unevenly distributed. DAPI-labeled cell nuclei are shown in blue (**A**, **E**, **I**, **M**), and H3K4me1 and H3K4me3 marks are shown in red. Scale bar for all in (**P**): 50 μm.

5. DISCUSSION

Although limited data exist on the effect of statins in pregnancy, there is no specific pattern of congenital anomalies associated with statin use (Morton and Thangaratinam, 2013). Exposure to lipophilic statins is hypothesized to be of greater risk to the fetus than hydrophilic statins, because of their greater ability to reach the fetus in larger

concentrations as a result of placental transport (Lecarpentier et al., 2012). As RST is relatively hydrophilic, its transplacental passage is probably reduced; nevertheless, data are only sparsely available on the transplacental transport (Lecarpentier et al., 2012). The risk of major congenital abnormalities from exposure to statins in pregnancy is similar to the background risk of the population and no specific pattern of abnormalities was observed in existing studies (Morton and Thangaratinam, 2013). The paucity of information is due to the fact that findings were limited by the poor quality and reporting of existing studies. Consequently, in a prospective, observational cohort study, Taguchi et al. (2008) found no evidence of major malformations, spontaneous or therapeutic abortions, or stillbirths, but noted a younger gestational age at birth and lower birth weight for patients using RST.

Animal models have provided some evidence for the teratogenic effects of lipophilic statins on pregnancy outcomes, including decreased fetal body weight, survival rate, and unusual neonatal development (Emami et al. 2013). Some malformations were reported in fetuses after pregnant mothers were exposed to lipophilic statins (such as simvastatin, lovastatin, atorvastatin, cerivastatin, and fluvastatin) compared to hydrophilic statins (pravastatin and RST) (Lecarpentier et al., 2012; Morton and Thangaratinam, 2013). For example, Beverly et al. (2019) demonstrated that *in utero* exposure to simvastatin reduced offspring viability and permanently disrupted reproductive tract development in males. Dostal et al. (1994) reported developmental toxicity at maternally toxic doses of atorvastatin in rats and rabbits, but no evidence of teratogenicity. Neither the rat nor the rabbit showed significant differences between the control and treated groups in the incidence of fetal loss, *in utero* growth or congenital malformations when used at doses potentially toxic for the dam. Despite this, the results of Henck et al. (1998), in contrast, indicated that pre- and postnatal administration of atorvastatin to female rats produced developmental toxicity in their offspring via *in utero* and/or lactational exposure, either in the presence or absence of maternal toxicity.

About half of all pregnancies are unplanned (Koren et al., 1998), with concomitant chances of exposure to statins. The risk to the fetus needs to be weighed against the risk to the mother. The effect of prolonged exposure of the mother to a hypercholesteremic environment throughout pregnancy and lactation on her cardiovascular status is a subject of concern (Morton and Thangaratinam, 2013). Occasionally, studies have also reported beneficial effects from statin use. For example, increasing evidence suggests

that hypercholesterolemia during pregnancy initiates pathogenic events in the fetus and, thus, increases the risk of cardiovascular disease in the offspring (Napoli et al., 1997). In such cases, statin use during pregnancy could be beneficial. For example, Elahi et al. (2008) demonstrated that statin treatment in hypercholesterolemic pregnant mice reduced certain cardiovascular risk factors in their offspring. Statins also proved beneficial in preventing preeclampsia, thus ameliorating the risks of structural abnormalities to the fetus (Morton and Thangaratinam, 2013). Preeclampsia is a common hypertensive disorder of pregnancy associated with quite large neonatal and maternal morbidities and mortalities. Due to the immunomodulatory and antiinflammatory effects, along with other pleiotropic actions on free oxygen radical formation and smooth muscle cell proliferation, they make statins highly promising candidates for the prevention and treatment of preeclampsia (Smith and Costtantine, 2020).

Based on the sporadic human data available, and because of the potential teratogenic *in utero* effects of statins observed in initial animal experiments (Henck et al., 1998; Faqi et al., 2012), the use of statins in human pregnancy is currently not recommended primarily as a precaution. A reconsideration of the use of statins in high-risk mothers, therefore, seems to be required, but this remains controversial. Bearing this in mind, we therefore restricted the use of statin to the second half of pregnancy.

Mammalian embryonic development involves precise molecular interactions between intrinsic factors such as genetics and epigenetics, and extrinsic maternal factors, such as environmental perturbations, drugs, or even maternal nutrition, as nutritional components could influence the epigenetic landscape in the fetus and hence developmental processes (Li, 2018). Indeed, development is governed by a carefully orchestrated program of gene expression controlled by both genetic and epigenetic factors. Numerous environmental factors could elicit long-term consequences for the adult phenotype and they might influence and promote adult-onset diseases. However, the timing of exposure is crucial to achieve such long-lasting effects (Li, 2018). Therefore, an additional consideration for environmental influences is the developmental stage of exposure. Exposures during a crucial time of development can alter genome activity associated with differentiation of cells and tissues. This altered program and gene expression profile could then promote an abnormal physiology and disease in later stages of the development (Skinner et al., 2010). Epigenetic regulation includes both long-lasting changes in gene activity and transient changes in the regulation of gene

expression. Euchromatin allows transcription factors to interact with gene promoters and activate lineage-specific genes, while heterochromatin remains inaccessible to transcriptional activation (Kouzarides, 2007). Furthermore, diet is now recognized as a major environmental factor that may contribute to regulate physiological and pathophysiological aspects of homeostasis, metabolism, and gene expression (Johnson, 2017; Khambadkone et al., 2020). It was therefore necessary to exclude any interference of liver pâté, the vehicle for RST, on epigenetic mechanisms. Our data ruled out potential effects of this diet supplement on histone methylation patterns, as they did not significantly change their levels between the absolute and vehicle-treated control newborn rat brains.

The nervous system comprises several different cell types that are defined by morphology, function, anatomical location, and specific patterns of gene expression. The determination of these complex and highly regulated cell fates requires the spatial and temporal coordination of transcription in the proper order, number, and location. During development, differentiated cell types are generated from dividing progenitor/precursor cells (Kilpatrick et al., 1995). During lineage commitment, cells sustain cascades of gene activation and repression to generate specific cell types that execute highly specialized functions. Differentiation is associated with pronounced changes in patterns of gene expression, cell morphology and function. In the developing mammalian brain, neurons are generated first, followed by the supporting glia. Lineage studies indicate that the developing brain contains multipotent progenitor cells capable of generating both neurons and glia, namely astrocytes and oligodendrocytes, and that cell fate restriction may be a consequence of a series of gene expression events and extracellular signals acting on multipotent progenitors (Morrow et al., 2001). Hence, the sequential generation of neuronal and glial cells in the brain appears to be regulated by developmentally controlled genetic mechanisms and extracellular factors that can induce a cell fate switch followed by terminal differentiation (Morrow et al., 2001). As **Figure 16** shows, neurogenesis begins at embryonic day (E)12, peaks at E14, and decreases by E17 in rats (Sauvageot and Stiles, 2002). On postnatal day 1, the newborn rat brain is a tissue populated mostly by neurons that are complemented gradually with non-neuronal cells. Bandeira et al. (2009) reported that over 90% of the cells were neurons at this stage, and only about 6% of the cells had non-neuronal phenotypes. They also showed that the

neuronal population initially present at birth was further reduced by apoptosis and that the number of non-neuronal, mostly glial cells increased.

Neurons and glial cells worked together to achieve proper neuronal development and normal brain function. Glial cells actively direct CNS development in various ways. Glia are essential for brain function during development and in the adult brain as well (Reemst et al., 2016; Lago-Baldaia et al., 2020). The main glial subsets in CNS are microglia, astrocytes and oligodendrocytes. These cells are actively involved in many aspects of the nervous system, hence due to their important roles in developmental processes, dysfunction of glial cells during brain development might contribute to neurodevelopmental disorders and potentially even late-onset neuropathology (Reemst et al., 2016). The generation of astrocytes and oligodendrocytes occurs in a temporally distinct, yet overlapping, pattern. Astrocytes arise during later embryonic life (**Figure 16**). They originate from the neural lineage and they are mainly produced during the final stages of neurogenesis. In mice, astrogenesis starts around embryonic age 18 (E18) and lasts at least until approximately postnatal day 7 (Reemst et al., 2016); nevertheless, the cells can use their mitotic potential and differentiate when needed. Oligodendrocytes are responsible for myelination of axons thereby contribute to white matter development. Although oligodendrocytogenesis peaks at postnatal day 14, oligodendrocyte precursors appear somewhat earlier (Sauvageot and Stiles, 2002). During development, oligodendrocyte precursor cells are generated in multiple waves, originating from distinct brain regions (van Tilborg et al., 2018).

Microglia, the resident immune cells of the CNS, are derived from macrophage-like cells of mesodermal origin (Prinz and Priller, 2014). These cells infiltrate the brain in the early stages of embryonic development and develop side by side with the neurons (**Figure 16**). Microglial cells are the first "glial" cells observed in the brain, during the critical period of early brain development, when the first wave of synaptogenesis occurs (Reemst et al., 2016). In mice, the first microglia progenitors are detected in the brain around embryonic age E9 (Ginhoux et al., 2010).

Recently, Matcovitch-Natan et al. (2016) identified a stepwise developmental program of microglia in synchrony with the developing brain. They found that a subset of the genes that were expressed at the pre-microglia stage (from embryonic day 14 to a few days after birth) was related to the neuronal migration, neurogenesis, and cytokine secretion. This is the phase when microglia adopt a role in synaptic pruning and neuronal

maturation. Perturbation of the microglial environment during development may alter the strict timing of developmental programs, lead to misplaced expression, disrupt neuronal development, and cause brain disorders at later stages in life (Matcovich-Natan et al., 2016). As we recently demonstrated, cellular abundancy in the newborn brain tissue is also reflected in the cellular composition of the primary cultures from which subsequent cultures are made (Dulka et al., 2021).
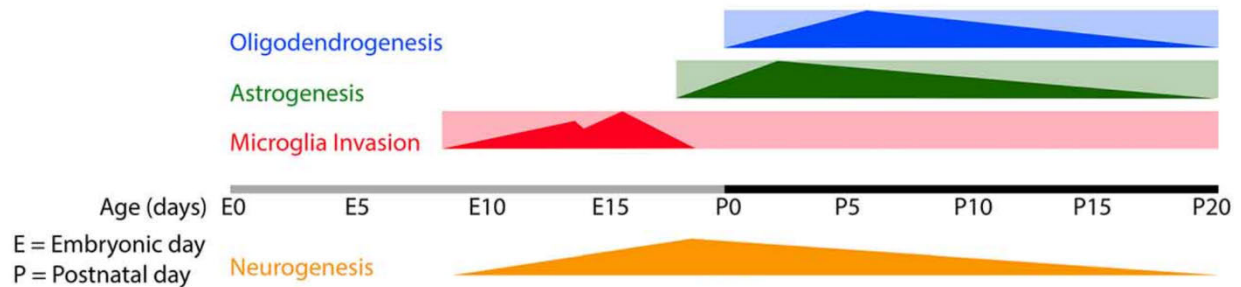

Figure 16. Timeline of developmental processes in the developing rodent brain. Triangles indicate the onset and peaks of the given developmental processes (adapted from Reemst et al., 2016).

We did not find any signs of RST histotoxicity or changes in the cellular compositions of newborn brains through light microscopy. This supports the opinion that the use of statins in pregnancy poses no risks of developing fetal CNS abnormalities. It should be added that most of the histone methylation marks we detected in this study were localized to neurons, and to a much smaller extent, to microglia. Astrocytes and oligodendrocytes develop and populate the newborn brain at later stages of development.

The dysregulation of chromatin decreases viability and physiological cell functions and leads to various neurodevelopmental and psychiatric diseases (Shen et al., 2014). Our intention was to assess the changes of PTMs of the chromatin in the brains of the newborn rats whose mothers had been treated with RST; specifically, we narrowed our attention to histone methylation. During embryonal development, the histone methylation landscape of the brain cells is sensitive to a wide range of environmental cues. Alterations in histone methylation have recently been linked not only to a number of neurological and psychiatric disorders but also to proper brain development and function (Akbarian and Huang, 2009; Peter and Akbarian, 2011).

38

In this study, we focused on methylations of the Lys (K) residues of the four core histones. A recent study on the epigenetic silencing of inflammation-related genes demonstrated that repressive histone marks (e.g., H3K27me3) correlated with a silencing of their expression (Maleszewska et al., 2021). Similar to H3K27, the methylation of H3K9 was shown to be involved in heterochromatin formation and transcriptional silencing (Bannister et al., 2001). H3K9me3 is a typical mark of constitutive heterochromatin, while H3K27me3 is usually enriched in facultative heterochromatin (Saksouk et al., 2015). H3K9me3 modification is associated with changes in gene transcription by alterations to the chromatin structure. Another distinct feature of heterochromatin is a strong enrichment of H4K20me2/3; in fact, H3K9me3 is required for the induction of H4K20me2/3 (Saksouk et al., 2015). Hence, the H4K20 histone methyl mark is associated with gene repression (Vermeulen et al., 2010). Besides H3 and H4, there are only a few known methylation marks in H2A and H2B; for instance, Barski et al. (2007) reported that H2BK5me1 is an activation mark associated with the active promoters downstream of transcription start sites. Interestingly, to the best of our knowledge, no data are available on the Lys methylation of H2A, especially for H2AK118. Taken together, these examples suggest that even closely related histone Lys methylation markings are potentially associated with contrasting chromatin states.

Other methylation sites are also known to be strong epigenetic marks. The methylation of histone H3 Lys 36 (H3K36) plays an important role in the partitioning of chromatin into distinct domains, as well as in the regulation of a wide range of biological processes and it is also implicated in the repair of double-strand DNA breaks (Li et al., 2019; Sun et al., 2020). H3K36me2 regulates the distribution of H3K27me3 (Li et al., 2019), a characteristic of heterochromatin. Interestingly, H3K36 sites correlate positively with gene expression similar to H3K4me1/3 methylation. H3K4me1 and H3K4me3 marks, commonly located in euchromatin, are broadly associated with transcriptional regulation and the epigenetic tagging of promoters and enhancer sequences, and they are known to allow the DNA to adopt a more "open" conformation and recruit chromatin-modifying factors (Barski et al., 2007). H3K4 methylation has been observed in genes that are important for the regulation of cell differentiation, proliferation, and apoptosis (Batista and Helguero, 2018); for example, homeobox genes, known for their roles in embryonic development, are regulated by H3K4 methylation (Malik and Bhaumik, 2010). H3K4me3 is almost always associated with RNA polymerase II occupancy of the

promoters at the sites of active gene expression (Guenther et al., 2005). The proper regulation of H3K4 methylation is pivotal for healthy brain development, as mutations associated with the loss and gain of H3K4 methylation could potentially result in intellectual disability, autism, microcephaly, seizure disorders, and other neurological diseases in early childhood (Shen et al., 2014). Perhaps this epigenetic mark is involved more broadly in the pathophysiology of some neurodevelopmental disorders, as multiple regulators of H3K4 methylation are associated with neurodevelopmental diseases (Jones et al., 2012; Najmabadi et al., 2011). Consequently, there is further evidence that the epigenetic fine-tuning of the H3K4 methyl markings in the brain is crucial for orderly neurodevelopment. There can be little doubt that the H3K4 methylation landscape of brain cells is sensitive to a wide range of environmental perturbations (Shen et al., 2014); indeed, the H3K4me3 mark undergoes global and gene-specific alterations in the hippocampus of fear-conditioned animals. Gupta et al. (2010) found that H3K4me3 was upregulated in the rat hippocampus 1 h after contextual fear conditioning and that this increase was reversible. Furthermore, the activation of the maternal immune system by the viral RNA mimic polyriboinosinic-polyribocytidilic acid, which leads to behavioral deficits in the adult offspring, could result in robust but transient changes in H3K4 methylation at the genes encoding cytokines and other signaling molecules in the fetal brain (Connor et al., 2012). Prenatal exposure to the alkylating and antimitotic agent methylazoxymethanol, which leads to several anatomical and behavioral abnormalities in adulthood similar to those observed in patients with schizophrenia, resulted in decreased H3K4 methylation in the adult prefrontal cortex (Maćkowiak et al. 2014). Loss-of-function mutations in a H3K4 demethylase have been linked to mental retardation and autism spectrum disorders (Peter and Akbarian, 2011), while a H3K4 methyltransferase mutation shows distinct abnormalities in hippocampal plasticity and signaling (Kim et al., 2007). Multiple methyltransferases and demethylases were recently implicated in neurodevelopment and major psychiatric diseases, and these types of chromatin-modifying enzymes could emerge as novel targets for the treatment of mood and psychosis spectrum disorders (Peter and Akbarian, 2011). Interestingly, statins, in general, did not directly inhibit the activity of the major epigenetic modifying enzymes, such as "writers" or "readers" (Bridgeman et al., 2019).

The examples given above further illustrate the complex regulation of histone Lys methylation. These epigenetic modifications, especially in the case of the histone H3, are

involved in a wide range of biological processes, including the activation and repression of transcription; nevertheless, one methyl mark by itself might still have a limited biological message (Trojer and Reinberg, 2006; Kimura, 2013). As discussed above, H3K4me is a mark that, on a genome-wide scale, is associated broadly with transcriptional activation and the epigenetic tagging of promoters and enhancers (Barski et al., 2007). As multiple regulators of H3K4 methylation are associated with neurodevelopmental disease, and H3K4 methylation is subject to dynamic changes during the extended period of development and maturation of the brain, it might be that this epigenetic mark is more broadly involved in the pathophysiology of some CNS abnormalities (Shen et al., 2014).

The present study showed that prenatal RST administration from embryonic day 11 led to regulation of the methylation processes at K4 of histone H3 during CNS development. RST selectively affected methylated forms of H3K4, namely it increased the levels of both the mono- and trimethylated forms of H3K4 in the newborn brain. The epigenetic changes elicited by RST are not good or bad unless definitely proven either way. Although there are no such data available yet on humans, these data could contain a message. Prenatal statin therapies, should be used with caution and warrant further investigation until a clearest picture of their precise effects on the epigenetic spectrum emerges.

6. CONCLUSION

In this study, we provided evidence that in newborn rat brains prenatal exposure to RST alters the methylation landscape in general, and the H3K4me1 and H3K4me3 histone modifications in particular, in newborn rat brains. We did not find any histological structural alteration in newborn brains that could be related to RST treatment. However, we found that RST significantly elevated the levels of H3K4me1 and H3K4me3 marks compared to the controls. The elevation of these methylation marks was most dominant in neurons after RST treatment. As statins, in general, did not directly inhibit the activity of the major epigenetic modifying enzymes, it remains to be determined in future studies whether the changes observed in the H3K4 methylation patterns: (1) are linked to specific loci or are genome-wide, (2) reflect an adaptive or maladaptive response to RST, or (3) represent the outcomes of secondary or tertiary processes in response to RST

treatment. The identification of the genomic sequences involved in the control of the embryonic development of offspring whose mothers had been treated with RST remains a formidable challenge. The epigenetic changes elicited by RST are possibilities that should be taken on board. Although there are no such data available yet on humans, our data could provide an adverse message.

We think that changes in histone marks, more precisely the elevated levels of H3K4me1/me3 may be responsible for weakening heterochromatin structure and inducing a "relaxed" state of chromatin in the developing brain cells. This might allow heterochromatinization of new genomic loci, and perhaps lead to or reflect a new program of gene expression. The precise mechanisms underlying this process requires further study.

7. THE MAIN FINDINGS OF THE STUDY

1) We demonstrated that RST induced molecular epigenetic events in the brains of newborn rats when pregnant mothers were treated daily with oral RST from the 11th day of pregnancy for 10 days (or until delivery);

2) By analyzing cell-type-specific markers in the newborn brains we demonstrated that prenatal RST administration did not affect the light microscopic cytoarchitecture and cell type ratios of the nervous tissue as compared to the controls;

3) We found that prenatal RST administration induced a general, nonsignificant increase in H2AK118me1, H2BK5me1, H3, H3K9me3, H3K27me3, H3K36me2, H4, H4K20me2, and H4K20me3 levels, as compared to the controls;

4) We found that significant changes were detected in the number of H3K4me1 and H3K4me3 sites (134.3% ± 19.2% and 127.8% ± 8.5% of the controls, respectively), which are generally recognized as transcriptional activators;

5) Using fluorescent/confocal immunohistochemistry for cell-type-specific markers and histone methylation marks on tissue sections, we demonstrated that most of the increase at these sites belonged to neuronal cell nuclei;

6) We concluded that prenatal RST treatment induced epigenetic changes that might affect neuronal differentiation and development, and such possibilities should be taken into account when human RST therapy is recommended.

8. ACKNOWLEDGMENTS

9. REFERENCES

Afshari AR, Mollazadeh H, Henney NC, Jamialahmad T, Sahebkar A (2020) Effects of statins on brain tumors: a review. Semin Cancer Biol. S1044-579X(20)30173-5. doi: 10.1016/j.semcancer.2020.08.002.

Akbarian S, Huang HS (2009) Epigenetic regulation in human brain-focus on histone lysine methylation. Biol Psychiatry. 65(3):198-203. doi: 10.1016/j.biopsych.2008.08.015.

Asztalos BF, Le Maulf F, Dallal GE, Stein E, Jones PH, Horvath KV, McTaggart F, Schaefer EJ (2007) Comparison of the effects of high doses of rosuvastatin versus atorvastatin on the subpopulations of high-density lipoproteins. Am J Cardiol. 99(5):681-5. doi: 10.1016/j.amjcard.2006.09.117.

Bandeira F, Lent R, Herculano-Houzel S (2009) Changing numbers of neuronal and non-neuronal cells underlie postnatal brain growth in the rat. Proc Natl Acad Sci U S A. 106(33):14108-13. doi: 10.1073/pnas.0804650106.

Bannister AJ, Zegerman P, Partridge JF, Miska EA, Thomas JO, Allshire RC, Kouzarides T (2001) Selective recognition of methylated lysine 9 on histone H3 by the HP1 chromo domain. Nature. 410(6824):120-4. doi: 10.1038/35065138.

Bannister AJ, Kouzarides T (2011) Regulation of chromatin by histone modifications. Cell Res. 21(3):381-95. doi: 10.1038/cr.2011.22.

Barski A, Cuddapah S, Cui K, Roh TY, Schones DE, Wang Z, Wei G, Chepelev I, Zhao K (2007) High-resolution profiling of histone methylations in the human genome. Cell. 129(4):823-37. doi: 10.1016/j.cell.2007.05.009.

Batista IAA, Helguero LA (2018) Biological processes and signal transduction pathways regulated by the protein methyltransferase SETD7 and their significance in cancer. Signal Transduct Target Ther. 3:19. doi: 10.1038/s41392-018-0017-6.

Beverly BEJ, Furr JR, Lambright CS, Wilson VS, McIntyre BS, Foster PMD, Travlos G, Earl Gray L Jr (2019) *In utero* exposure to simvastatin reduces postnatal survival and permanently alters reproductive tract development in the Crl:CD(SD) male rat. Toxicol Appl Pharmacol. 365:112-123. doi: 10.1016/j.taap.2019.01.001.

Bhaumik SR, Smith E, Shilatifard A (2007) Covalent modifications of histones during development and disease pathogenesis. Nat Struct Mol Biol. 14(11):1008-16. doi: 10.1038/nsmb1337.

Biswas S, Rao CM (2018) Epigenetic tools (The Writers, The Readers and The Erasers) and their implications in cancer therapy. Eur J Pharmacol. 837:8-24. doi: 10.1016/j.ejphar.2018.08.021.

Bowman GD, Poirier MG (2015) Post-translational modifications of histones that influence nucleosome dynamics. Chem Rev. 115(6):2274-95. doi: 10.1021/cr500350x.

Brewer LM, Sheardown SA, Brown NA (1993) HMG-CoA reductase mRNA in the post-implantation rat embryo studied by in situ hybridization. Teratology. 47(2):137-46. doi: 10.1002/tera.1420470206.

Bridgeman S, Northrop W, Ellison G, Sabapathy T, Melton PE, Newsholme P, Mamotte CDS (2019) Statins Do Not Directly Inhibit the Activity of Major Epigenetic Modifying Enzymes. Cancers (Basel). 11(4):516. doi: 10.3390/cancers11040516.

Connor CM, Dincer A, Straubhaar J, Galler JR, Houston IB, Akbarian S (2012) Maternal immune activation alters behavior in adult offspring, with subtle changes in the cortical transcriptome and epigenome. Schizophr Res. 140(1-3):175-84. doi: 10.1016/j.schres.2012.06.037.

Danielewicz H, Gurgul A, Dębińska A, Myszczyszyn G, Szmatoła T, Myszkal A, Jasielczuk I, Drabik-Chamerska A, Hirnle L, Boznański A (2020) Maternal atopy and offspring epigenome-wide methylation signature. Epigenetics. 16(6):629-641. doi: 10.1080/15592294.2020.1814504.

Dostal LA, Schardein JL, Anderson JA (1994) Developmental toxicity of the HMG-CoA reductase inhibitor, atorvastatin, in rats and rabbits. Teratology. 50(6):387-94. doi: 10.1002/tera.1420500604.

Dulka K, Nacsa K, Lajkó N, Gulya K (2021) Quantitative morphometric and cell-type-specific population analysis of microglia-enriched cultures subcloned to high purity from newborn rat brains. IBRO Neurosci Rep. 10:119-129. doi: 10.1016/j.ibneur.2021.01.007.

Elahi MM, Cagampang FR, Anthony FW, Curzen N, Ohri SK, Hanson MA (2008) Statin treatment in hypercholesterolemic pregnant mice reduces cardiovascular risk factors in their offspring. Hypertension. 51(4):939-44. doi: 10.1161/HYPERTENSIONAHA.107.100982.

Emami F, Asl BM, Seydi E, Zargar M, Naserzadeh P, Pourahmad J (2013) Embryotoxic effects of atorvastatin on mouse fetus. Iran. J. Pharm. Sci. 9, 13–23.

Famer D, Wahlund LO, Crisby M (2010) Rosuvastatin reduces microglia in the brain of wild type and ApoE knockout mice on a high cholesterol diet; implications for prevention of stroke and AD. Biochem Biophys Res Commun. 402(2):367-72. doi: 10.1016/j.bbrc.2010.10.035.

Faqi AS, Prohaska D, Lopez R, McIntyre G (2012) Developmental toxicity of the HMG-CoA reductase inhibitor (PPD10558) in rats and rabbits. Birth Defects Res B Dev Reprod Toxicol. 95(1):23-37. doi: 10.1002/bdrb.20337.

Gachpazan M, Kashani H, Khazaei M, Hassanian SM, Rezayi M, Asgharzadeh F, Ghayour-Mobarhan M, Ferns GA, Avan A (2019) The Impact of Statin Therapy on the Survival of Patients with Gastrointestinal Cancer. Curr Drug Targets. 20(7):738-747. doi: 10.2174/1389450120666181211165449.

Ginhoux F, Greter M, Leboeuf M, Nandi S, See P, Gokhan S, Mehler MF, Conway SJ, Ng LG, Stanley ER, Samokhvalov IM, Merad M (2010) Fate mapping analysis reveals that adult microglia derive from primitive macrophages. Science. 330(6005):841-5. doi: 10.1126/science.1194637.

Godfrey LM, Erramouspe J, Cleveland KW (2012) Teratogenic risk of statins in pregnancy. Ann Pharmacother. 46(10):1419-24. doi: 10.1345/aph.1R202.

Goldberg AD, Allis CD, Bernstein E (2007) Epigenetics: a landscape takes shape. Cell. 128(4):635-8. doi: 10.1016/j.cell.2007.02.006.

Gómez-Díaz E, Jordà M, Peinado MA, Rivero A (2012) Epigenetics of host-pathogen interactions: the road ahead and the road behind. PLoS Pathog. 8(11):e1003007. doi: 10.1371/journal.ppat.1003007.

Greer EL, Shi Y (2012) Histone methylation: a dynamic mark in health, disease and inheritance. Nat Rev Genet. 13(5):343-57. doi: 10.1038/nrg3173.

Guenther MG, Jenner RG, Chevalier B, Nakamura T, Croce CM, Canaani E, Young RA (2005) Global and Hox-specific roles for the MLL1 methyltransferase. Proc Natl Acad Sci U S A. 102(24):8603-8. doi: 10.1073/pnas.0503072102.

Gupta S, Kim SY, Artis S, Molfese DL, Schumacher A, Sweatt JD, Paylor RE, Lubin FD (2010) Histone methylation regulates memory formation. J Neurosci. 30(10):3589-99. doi: 10.1523/JNEUROSCI.3732-09.2010.

Halaburkova A, Cahais V, Novoloaca A, Araujo MGDS, Khoueiry R, Ghantous A, Herceg Z (2020) Pan-cancer multi-omics analysis and orthogonal experimental assessment

of epigenetic driver genes. Genome Res. 30(10):1517-1532. doi: 10.1101/gr.268292.120.

Henck JW, Craft WR, Black A, Colgin J, Anderson JA (1998) Pre- and postnatal toxicity of the HMG-CoA reductase inhibitor atorvastatin in rats. Toxicol Sci. 41(1):88-99. doi: 10.1006/toxs.1997.2400.

Henn L, Szabó A, Imre L, Román Á, Ábrahám A, Vedelek B, Nánási P, Boros IM (2020) Alternative linker histone permits fast paced nuclear divisions in early Drosophila embryo. Nucleic Acids Res. 48(16):9007-9018. doi: 10.1093/nar/gkaa624.

Hyun K, Jeon J, Park K, Kim J (2017) Writing, erasing and reading histone lysine methylations. Exp Mol Med. 49(4):e324. doi: 10.1038/emm.2017.11.

Johnson IT (2017) The cancer risk related to meat and meat products. Br Med Bull. 121(1):73-81. doi: 10.1093/bmb/ldw051.

Jones KD, Couldwell WT, Hinton DR, Su Y, He S, Anker L, Law RE (1994) Lovastatin induces growth inhibition and apoptosis in human malignant glioma cells. Biochem Biophys Res Commun. 205(3):1681-7. doi: 10.1006/bbrc.1994.2861.

Jones WD, Dafou D, McEntagart M, Woollard WJ, Elmslie FV, Holder-Espinasse M, Irving M, Saggar AK, Smithson S, Trembath RC, Deshpande C, Simpson MA (2012) De novo mutations in MLL cause Wiedemann-Steiner syndrome. Am J Hum Genet. 91(2):358-64. doi: 10.1016/j.ajhg.2012.06.008.

Karlic H, Haider F, Thaler R, Spitzer S, Klaushofer K, Varga F (2017) Statin and Bisphosphonate Induce Starvation in Fast-Growing Cancer Cell Lines. Int J Mol Sci. 18(9):1982. doi: 10.3390/ijms18091982.

Kata D, Földesi I, Feher LZ, Hackler L Jr, Puskas LG, Gulya K (2016) Rosuvastatin enhances anti-inflammatory and inhibits pro-inflammatory functions in cultured microglial cells. Neuroscience. 314:47-63. doi: 10.1016/j.neuroscience.2015.11.053.

Khambadkone SG, Cordner ZA, Dickerson F, Severance EG, Prandovszky E, Pletnikov M, Xiao J, Li Y, Boersma GJ, Talbot CC Jr, Campbell WW, Wright CS, Siple CE, Moran TH, Tamashiro KL, Yolken RH (2020) Nitrated meat products are associated with mania in humans and altered behavior and brain gene expression in rats. Mol Psychiatry. 25(3):560-571. doi: 10.1038/s41380-018-0105-6.

Kilpatrick TJ, Richards LJ, Bartlett PF (1995) The regulation of neural precursor cells within the mammalian brain. Mol Cell Neurosci. 6(1):2-15. doi: 10.1006/mcne.1995.1002.

Kim SY, Levenson JM, Korsmeyer S, Sweatt JD, Schumacher A (2007) Developmental regulation of Eed complex composition governs a switch in global histone modification in brain. J Biol Chem. 282(13):9962-9972. doi: 10.1074/jbc.M608722200.

Kimura H (2013) Histone modifications for human epigenome analysis. J Hum Genet. 58(7):439-45. doi: 10.1038/jhg.2013.66.

Klein BJ, Krajewski K, Restrepo S, Lewis PW, Strahl BD, Kutateladze TG (2018) Recognition of cancer mutations in histone H3K36 by epigenetic writers and readers. Epigenetics. 13(7):683-692. doi: 10.1080/15592294.2018.1503491.

Koren G, Pastuszak A, Ito S. Drugs in pregnancy (1998) N Engl J Med. 338(16):1128-37. doi: 10.1056/NEJM199804163381607.

Kornberg RD, Lorch Y (1999) Twenty-five years of the nucleosome, fundamental particle of the eukaryote chromosome. Cell. 98(3):285-94. doi: 10.1016/s0092-8674(00)81958-3.

Kostapanos MS, Milionis HJ, Elisaf MS (2010) Rosuvastatin-associated adverse effects and drug-drug interactions in the clinical setting of dyslipidemia. Am J Cardiovasc Drugs. 10(1):11-28. doi: 10.2165/13168600-000000000-00000.

Kouzarides T (2007) Chromatin modifications and their function. Cell. 128(4):693-705. doi: 10.1016/j.cell.2007.02.005.

Kumar S, Chinnusamy V, Mohapatra T (2018) Epigenetics of Modified DNA Bases: 5-Methylcytosine and Beyond. Front Genet. 9:640. doi: 10.3389/fgene.2018.00640.

Kurata T, Miyazaki K, Kozuki M, Morimoto N, Ohta Y, Ikeda Y, Abe K (2012) Atorvastatin and pitavastatin reduce senile plaques and inflammatory responses in a mouse model of Alzheimer's disease. Neurol Res. 34(6):601-10. doi: 10.1179/1743132812Y.0000000054.

Lago-Baldaia I, Fernandes VM, Ackerman SD (2020) More Than Mortar: Glia as Architects of Nervous System Development and Disease. Front Cell Dev Biol. 8:611269. doi: 10.3389/fcell.2020.611269.

Lajkó N, Kata D, Szabó M, Mátyás A, Dulka K, Földesi I, Fülöp F, Gulya K, Vécsei L, Mihály A (2020) Sensitivity of rodent microglia to kynurenines in models of epilepsy and inflammation *in vivo* and *in vitro*: Microglia activation is inhibited by kynurenic acid and the synthetic analogue SZR104. Int J Mol Sci. 21(23):9333. doi: 10.3390/ijms21239333.

Lecarpentier E, Morel O, Fournier T, Elefant E, Chavatte-Palmer P, Tsatsaris V (2012) Statins and pregnancy: between supposed risks and theoretical benefits. Drugs. 72(6):773-88. doi: 10.2165/11632010-000000000-00000.

Legradi A, Dulka K, Jancsó G, Gulya K (2020) Orofacial skin inflammation increases the number of macrophages in the maxillary subregion of the rat trigeminal ganglion in a corticosteroid-reversible manner. Cell Tissue Res. 382(3):551-561. doi: 10.1007/s00441-020-03244-3.

Li Y (2018) Epigenetic Mechanisms Link Maternal Diets and Gut Microbiome to Obesity in the Offspring. Front Genet. 9:342. doi: 10.3389/fgene.2018.00342.

Li J, Ahn JH, Wang GG (2019) Understanding histone H3 lysine 36 methylation and its deregulation in disease. Cell Mol Life Sci. 76(15):2899-2916. doi: 10.1007/s00018-019-03144-y.

Lowry OH, Rosebrough NJ, Farr AL, Randall RJ (1951) Protein measurement with the Folin phenol reagent. J Biol Chem. 193(1): 265–275. PMID: 14907713.

Luo B, Li B, Wang W, Liu X, Liu X, Xia Y, Zhang C, Zhang Y, Zhang M, An F (2014) Rosuvastatin alleviates diabetic cardiomyopathy by inhibiting NLRP3 inflammasome and MAPK pathways in a type 2 diabetes rat model. Cardiovasc Drugs Ther. 28(1):33-43. doi: 10.1007/s10557-013-6498-1.

Lwin EMP, Leggett C, Ritchie U, Gerber C, Song Y, Hague W, Turner S, Upton R, Garg S (2018) Transfer of rosuvastatin into breast milk: liquid chromatography-mass spectrometry methodology and clinical recommendations. Drug Des Devel Ther. 12:3645-3651. doi: 10.2147/DDDT.S184053.

Maćkowiak M, Bator E, Latusz J, Mordalska P, Wędzony K (2014) Prenatal MAM administration affects histone H3 methylation in postnatal life in the rat medial prefrontal cortex. Eur Neuropsychopharmacol. 24(2):271-89. doi: 10.1016/j.euroneuro.2013.05.013.

Maleszewska M, Steranka A, Smiech M, Kaza B, Pilanc P, Dabrowski M, Kaminska B (2021) Sequential changes in histone modifications shape transcriptional responses underlying microglia polarization by glioma. Glia. 69(1):109-123. doi: 10.1002/glia.23887.

Malik S, Bhaumik SR (2010) Mixed lineage leukemia: histone H3 lysine 4 methyltransferases from yeast to human. FEBS J. 277(8):1805-21. doi: 10.1111/j.1742-4658.2010.07607.x.

Matcovitch-Natan O, Winter DR, Giladi A, Vargas Aguilar S, Spinrad A, Sarrazin S, Ben-Yehuda H, David E, Zelada González F, Perrin P, Keren-Shaul H, Gury M, Lara-Astaiso D, Thaiss CA, Cohen M, Bahar Halpern K, Baruch K, Deczkowska A, Lorenzo-Vivas E, Itzkovitz S, Elinav E, Sieweke MH, Schwartz M, Amit I (2016) Microglia development follows a stepwise program to regulate brain homeostasis. Science. 353(6301):aad8670. doi: 10.1126/science.aad8670.

McTaggart F, Buckett L, Davidson R, Holdgate G, McCormick A, Schneck D, Smith G, Warwick M (2001) Preclinical and clinical pharmacology of Rosuvastatin, a new 3-hydroxy-3-methylglutaryl coenzyme A reductase inhibitor. Am J Cardiol. 87(5A):28B-32B. doi: 10.1016/s0002-9149(01)01454-0.

Monk D, Mackay DJG, Eggermann T, Maher ER, Riccio A (2019) Genomic imprinting disorders: lessons on how genome, epigenome and environment interact. Nat Rev Genet. 20(4):235-248. doi: 10.1038/s41576-018-0092-0.

Morton S, Thangaratinam S (2013) Statins in pregnancy. Curr Opin Obstet Gynecol. 25(6):433-40. doi: 10.1097/GCO.0000000000000026.

Morrow T, Song MR, Ghosh A (2001) Sequential specification of neurons and glia by developmentally regulated extracellular factors. Development. 128(18):3585-94. PMID: 11566862.

Najmabadi H, Hu H, Garshasbi M, Zemojtel T, Abedini SS, Chen W, Hosseini M, Behjati F, Haas S, Jamali P, Zecha A, Mohseni M, Püttmann L, Vahid LN, Jensen C, Moheb LA, Bienek M, Larti F, Mueller I, Weissmann R, Darvish H, Wrogemann K, Hadavi V, Lipkowitz B, Esmaeeli-Nieh S, Wieczorek D, Kariminejad R, Firouzabadi SG, Cohen M, Fattahi Z, Rost I, Mojahedi F, Hertzberg C, Dehghan A, Rajab A, Banavandi MJ, Hoffer J, Falah M, Musante L, Kalscheuer V, Ullmann R, Kuss AW, Tzschach A, Kahrizi K, Ropers HH (2011) Deep sequencing reveals 50 novel genes for recessive cognitive disorders. Nature. 478(7367):57-63. doi: 10.1038/nature10423.

Napoli C, D'Armiento FP, Mancini FP, Postiglione A, Witztum JL, Palumbo G, Palinski W (1997) Fatty streak formation occurs in human fetal aortas and is greatly enhanced by maternal hypercholesterolemia. Intimal accumulation of low density lipoprotein and its oxidation precede monocyte recruitment into early atherosclerotic lesions. J Clin Invest. 100(11):2680-90. doi: 10.1172/JCI119813.

Ohashi K, Osuga J, Tozawa R, Kitamine T, Yagyu H, Sekiya M, Tomita S, Okazaki H, Tamura Y, Yahagi N, Iizuka Y, Harada K, Gotoda T, Shimano H, Yamada N, Ishibashi S (2003)

Early embryonic lethality caused by targeted disruption of the 3-hydroxy-3-methylglutaryl-CoA reductase gene. J Biol Chem. 278(44):42936-41. doi: 10.1074/jbc.M307228200.

Passarge E (1979) Emil Heitz and the concept of heterochromatin: longitudinal chromosome differentiation was recognized fifty years ago. Am J Hum Genet. 31(2):106-15. PMID: 377956; PMCID: PMC1685768.

Peter CJ, Akbarian S (2011) Balancing histone methylation activities in psychiatric disorders. Trends Mol Med. 17(7):372-9. doi: 10.1016/j.molmed.2011.02.003.

Plass C, Pfister SM, Lindroth AM, Bogatyrova O, Claus R, Lichter P (2013) Mutations in regulators of the epigenome and their connections to global chromatin patterns in cancer. Nat Rev Genet. 14(11):765-80. doi: 10.1038/nrg3554.

Prinz M, Priller J (2014) Microglia and brain macrophages in the molecular age: from origin to neuropsychiatric disease. Nat Rev Neurosci. 15(5):300-12. doi: 10.1038/nrn3722.

Reemst K, Noctor SC, Lucassen PJ, Hol EM (2016) The Indispensable Roles of Microglia and Astrocytes during Brain Development. Front Hum Neurosci. 10:566. doi: 10.3389/fnhum.2016.00566.

Relton CL, Davey Smith G (2010) Epigenetic epidemiology of common complex disease: prospects for prediction, prevention, and treatment. PLoS Med. 7(10):e1000356. doi: 10.1371/journal.pmed.1000356.

Saksouk N, Simboeck E, Déjardin J (2015) Constitutive heterochromatin formation and transcription in mammals. Epigenetics Chromatin. 8:3. doi: 10.1186/1756-8935-8-3.

Satoh M, Tabuchi T, Itoh T, Nakamura M (2014) NLRP3 inflammasome activation in coronary artery disease: results from prospective and randomized study of treatment with atorvastatin or rosuvastatin. Clin Sci (Lond). 126(3):233-41. doi: 10.1042/CS20130043.

Sauvageot CM, Stiles CD (2002) Molecular mechanisms controlling cortical gliogenesis. Curr Opin Neurobiol. 12(3):244-9. doi: 10.1016/s0959-4388(02)00322-7.

Schäfer A, Baric RS (2017) Epigenetic Landscape during Coronavirus Infection. Pathogens. 6(1):8. doi: 10.3390/pathogens6010008.

Schneider CA, Rasband WS, Eliceiri KW (2012) NIH Image to ImageJ: 25 years of image analysis. Nat Methods. 9(7):671-5. doi: 10.1038/nmeth.2089.

Shahbazian MD, Grunstein M (2007) Functions of site-specific histone acetylation and deacetylation. Annu Rev Biochem. 76:75-100. doi: 10.1146/annurev.biochem.76.052705.162114.

Shen E, Shulha H, Weng Z, Akbarian S (2014) Regulation of histone H3K4 methylation in brain development and disease. Philos Trans R Soc Lond B Biol Sci. 369(1652):20130514. doi: 10.1098/rstb.2013.0514.

Skinner MK, Manikkam M, Guerrero-Bosagna C (2010) Epigenetic transgenerational actions of environmental factors in disease etiology. Trends Endocrinol Metab. 21(4):214-22. doi: 10.1016/j.tem.2009.12.007.

Smith DD, Costantine MM (2020) The role of statins in the prevention of preeclampsia. Am J Obstet Gynecol. S0002-9378(20)30868-1. doi: 10.1016/j.ajog.2020.08.040.

Sun Z, Zhang Y, Jia J, Fang Y, Tang Y, Wu H, Fang D (2020) H3K36me3, message from chromatin to DNA damage repair. Cell Biosci. 10:9. doi: 10.1186/s13578-020-0374-z.

Surani MA, Kimber SJ, Osborn JC (1983) Mevalonate reverses the developmental arrest of preimplantation mouse embryos by Compactin, an inhibitor of HMG Co A reductase. J Embryol Exp Morphol. 75:205-23. PMID: 6886611.

Szabo M, Dulka K, Gulya K (2016) Calmodulin inhibition regulates morphological and functional changes related to the actin cytoskeleton in pure microglial cells. Brain Res Bull. 120:41-57. doi: 10.1016/j.brainresbull.2015.11.003.

Taguchi N, Rubin ET, Hosokawa A, Choi J, Ying AY, Moretti ME, Koren G, Ito S (2008) Prenatal exposure to HMG-CoA reductase inhibitors: effects on fetal and neonatal outcomes. Reprod Toxicol. 26(2):175-7. doi: 10.1016/j.reprotox.2008.06.009.

Taylor F, Huffman MD, Macedo AF, Moore TH, Burke M, Davey Smith G, Ward K, Ebrahim S (2013) Statins for the primary prevention of cardiovascular disease. Cochrane Database Syst Rev. 2013(1):CD004816. doi: 10.1002/14651858.CD004816.pub5.

Thorogood M, Seed M, De Mott K (2009) Guideline Development Group. Management of fertility in women with familial hypercholesterolaemia: summary of NICE guidance. BJOG. 116(4):478-9. doi: 10.1111/j.1471-0528.2008.02084.x.

Treasure CB, Klein JL, Weintraub WS, Talley JD, Stillabower ME, Kosinski AS, Zhang J, Boccuzzi SJ, Cedarholm JC, Alexander RW (1995) Beneficial effects of cholesterol-lowering therapy on the coronary endothelium in patients with coronary artery disease. N Engl J Med. 332(8):481-7. doi: 10.1056/NEJM199502233320801.

Trojer P, Reinberg D (2006) Histone lysine demethylases and their impact on epigenetics. Cell. 125(2):213-7. doi: 10.1016/j.cell.2006.04.003.

Tronick E, Hunter RG (2016) Waddington, Dynamic Systems, and Epigenetics. Front Behav Neurosci. 10:107. doi: 10.3389/fnbeh.2016.00107.

Vaiserman AM (2013) Long-term health consequences of early-life exposure to substance abuse: an epigenetic perspective. J Dev Orig Health Dis. 4(4):269-79. doi: 10.1017/S2040174413000123.

Van der Most PJ, Dolga AM, Nijholt IM, Luiten PG, Eisel UL (2009) Statins: mechanisms of neuroprotection. Prog Neurobiol. 88(1):64-75. doi: 10.1016/j.pneurobio.2009.02.002.

van Tilborg E, de Theije CGM, van Hal M, Wagenaar N, de Vries LS, Benders MJ, Rowitch DH, Nijboer CH (2018) Origin and dynamics of oligodendrocytes in the developing brain: Implications for perinatal white matter injury. Glia. 66(2):221-238. doi: 10.1002/glia.23256.

Venkatesh S, Workman JL (2015) Histone exchange, chromatin structure and the regulation of transcription. Nat Rev Mol Cell Biol. 16(3):178-89. doi: 10.1038/nrm3941.

Vermeulen M, Eberl HC, Matarese F, Marks H, Denissov S, Butter F, Lee KK, Olsen JV, Hyman AA, Stunnenberg HG, Mann M (2010) Quantitative interaction proteomics and genome-wide profiling of epigenetic histone marks and their readers. Cell. 142(6):967-80. doi: 10.1016/j.cell.2010.08.020.

Wierzbicki AS, Poston R, Ferro A (2003) The lipid and non-lipid effects of statins. Pharmacol Ther. 99(1):95-112. doi: 10.1016/s0163-7258(03)00055-x.

Woodcock CL, Ghosh RP (2010) Chromatin higher-order structure and dynamics. Cold Spring Harb Perspect Biol. 2(5):a000596. doi: 10.1101/cshperspect.a000596.

Yun M, Wu J, Workman JL, Li B (2011) Readers of histone modifications. Cell Res. 21(4):564-78. doi: 10.1038/cr.2011.42.

Zhou X, Ma H (2008) Evolutionary history of histone demethylase families: distinct evolutionary patterns suggest functional divergence. BMC Evol Biol. 8:294. doi: 10.1186/1471-2148-8-294.

Zipp F, Waiczies S, Aktas O, Neuhaus O, Hemmer B, Schraven B, Nitsch R, Hartung HP (2007) Impact of HMG-CoA reductase inhibition on brain pathology. Trends Pharmacol Sci. 28(7):342-9. doi: 10.1016/j.tips.2007.05.001.

10. APPENDIX

I) **Dulka K**, Szabo M, Lajkó N, Belecz I, Hoyk Z, Gulya K (2021) Epigenetic consequences of *in utero* exposure to rosuvastatin: Alteration of histone methylation patterns in newborn rat brains. **Int J Mol Sci**. 22(7):3412. doi: 10.3390/ijms22073412. (**IF: 5.923**) (Q1)

II) **Dulka K**, Szabo M, Lajko N, Belecz I, Hoyk Z, Gulya K (2020) Prenatal exposure to rosuvastatin changes histone methylation patterns in the newborn rat brain. **12th FENS 2020 Virtual Forum of Neuroscience**, 2020.07.11-15. *(e-poster)*

I.

Article

Epigenetic Consequences of in Utero Exposure to Rosuvastatin: Alteration of Histone Methylation Patterns in Newborn Rat Brains

Karolina Dulka [1], **Melinda Szabo** [1], **Noémi Lajkó** [1], **István Belecz** [2], **Zsófia Hoyk** [3] **and Karoly Gulya** [1,*]

1   Department of Cell Biology and Molecular Medicine, University of Szeged, 6720 Szeged, Hungary;
    dulka.karolina@med.u-szeged.hu (K.D.); szabo.melinda.1@med.u-szeged.hu (M.S.);
    lajko.noemi@med.u-szeged.hu (N.L.)
2   Department of Medical Biology, University of Szeged, 6720 Szeged, Hungary; belecz.istvan@med.u-szeged.hu
3   Biological Barriers Research Group, Institute of Biophysics, Biological Research Center,
    Eötvös Loránd Research Network, 6726 Szeged, Hungary; hoyk.zsofia@brc.hu
*   Correspondence: gulyak@bio.u-szeged.hu

Abstract: Rosuvastatin (RST) is primarily used to treat high cholesterol levels. As it has potentially harmful but not well-documented effects on embryos, RST is contraindicated during pregnancy. To demonstrate whether RST could induce molecular epigenetic events in the brains of newborn rats, pregnant mothers were treated daily with oral RST from the 11th day of pregnancy for 10 days (or until delivery). On postnatal day 1, the brains of the control and RST-treated rats were removed for Western blot or immunohistochemical analyses. Several antibodies that recognize different methylation sites for H2A, H2B, H3, and H4 histones were quantified. Analyses of cell-type-specific markers in the newborn brains demonstrated that prenatal RST administration did not affect the composition and cell type ratios as compared to the controls. Prenatal RST administration did, however, induce a general, nonsignificant increase in H2AK118me1, H2BK5me1, H3, H3K9me3, H3K27me3, H3K36me2, H4, H4K20me2, and H4K20me3 levels, compared to the controls. Moreover, significant changes were detected in the number of H3K4me1 and H3K4me3 sites (134.3% $\pm$ 19.2% and 127.8% $\pm$ 8.5% of the controls, respectively), which are generally recognized as transcriptional activators. Fluorescent/confocal immunohistochemistry for cell-type-specific markers and histone methylation marks on tissue sections indicated that most of the increase at these sites belonged to neuronal cell nuclei. Thus, prenatal RST treatment induces epigenetic changes that could affect neuronal differentiation and development.

Keywords: epigenetics; H3K4me1; H3K4me3; histone methylation; immunohistochemistry; in utero; prenatal; rosuvastatin; Western blot

1. Introduction

Statins (3-hydroxy-3-methylglutaryl coenzyme A (HMG-CoA) reductase inhibitors) are a class of lipid-lowering agents used in the treatment of high cholesterol levels [1]. Apart from the inhibition of cholesterol synthesis, reduction of levels of low-density lipoproteins and triglycerides, and stimulation of the expression of high-density lipoproteins, they also strongly modulate the inflammatory cells surrounding atherosclerotic plaques [2,3]. Statins may also have beneficial effects on the central nervous system (CNS) [4–6]. In vitro [7] and animal studies [8,9] have demonstrated that statins can attenuate neuroinflammation. Furthermore, statins have long been known to induce apoptosis in various cancer cell lines [10,11], and are associated with antitumor properties [12,13].

Besides their beneficial properties, statins also have numerous adverse effects [14]. As a result of their potentially harmful, but not well documented effects on the embryo, it is recommended that statin treatment be discontinued three months before attempting to become pregnant and that statins should not be used during pregnancy or breastfeeding [15]

because of the potential risk of fetal abnormality [16]. Some malformations were reported in fetuses after pregnant mothers were exposed to lipophilic statins (such as simvastatin, lovastatin, atorvastatin, cerivastatin, and fluvastatin) as compared to hydrophilic statins (pravastatin and rosuvastatin (RST)) [17,18]. For example, in a prospective, observational cohort study, Taguchi et al. [19] found no evidence of major malformations, spontaneous or therapeutic abortions, or stillbirths, but noted a younger gestational age at birth and lower birth weights from patients using RST. Animal models provided some evidence for the teratogenic effects of lipophilic statins on pregnancy outcomes, including decreased fetal body weight and survival rate, and unusual neonatal development [20–22].

RST, one of the highest-selling prescription drugs on the market (Crestor; AstraZeneca Pharmaceuticals, LP, Wilmington, DE, USA), exhibits the greatest inhibitory effect on cholesterol biosynthesis [23], and among the statins, it alters the high-density lipoprotein profile most favorably [24]. Only small amounts of RST have been shown to pass into breast milk [25]. In vitro studies, RST strongly inhibited the expression of certain pro-inflammatory genes, while concomitantly vigorously stimulating several anti-inflammatory genes [7]. Its beneficial effects on the expression of inflammasome-related genes in animal models [26] or humans [27] have also been noted.

Histone modification is one of the main mechanisms of epigenetic modification regulating gene expression. This modification requires several different histone-modifying enzymes, including "writers", which attach modifications to histone tails, "erasers", which remove modifications, and "readers", which recognize these modifications [28–31]. The N-terminal tails of histones are subject to a number of highly site- and residue-specific posttranslational modifications, including methylation, acetylation, phosphorylation, ubiquitylation, and SUMOylation, that are implicated in influencing gene expression and genome function, as they coordinate the recruitment of chromatin remodelers and the transcriptional machinery for transcriptional regulation [32]. Of all the known modifications, Lys (K) histone methylation has been regarded as a stable chromatin modification that, together with DNA methylation, defines epigenetic programs [33]. Lys histone methylation has been linked to transcription initiation and elongation and heterochromatin silencing, among other mechanisms. Lys methylation marks, such as H3K4 and H3K36, are implicated in the activation of transcription and are linked to open chromatin, while the H3K9, H3K27, and the H4K20 Lys methylation sites are associated with transcriptional repression, as is characteristic of condensed chromatin [33,34]. The complexity of the methylation patterns of histone proteins and the methylation state at any given Lys residue (unmethylated, mono- (me1), di- (me2), or trimethylated (me3)) further influence gene expression.

As recent studies have emphasized the importance of maternal effects on chromatin structure and the interrelationship between the genome, epigenome, and environment [35,36], our aim was to investigate whether RST elicited molecular epigenetic events such as histone methylation in the brains of the newborn rats whose mothers had been treated chronically with the drug.

2. Results

2.1. Histone Methylation Patterns of Absolute Controls and Vehicle-Treated Controls Did Not Differ Significantly

When investigating epigenetic events in the newborn brain after the administration of RST, we assumed that liver pâté, the vehicle used to deliver RST, would not elicit changes in histone methylation patterns. To reveal such possible effects of the liver pâté, we assayed H2AK118me1, H2BK5me1, H3, H3K4me1, H3K4me3, H3K9me3, H3K27me3, H3K36me2, H4, H4K20me2, and H4K20me3 levels using Western blots from absolute control and vehicle-treated control newborn rat brain samples. Our data showed that liver pâté, as a nutritional supplement, had no significant effect on the methylation patterns of these sites (Figure 1). As all vehicle-based controls had values between 93.2% ± 7.7% and 106.4% ± 10.7% of the absolute controls, with no significant differences among them across at least five separate experiments, we refer to vehicle-treated controls hereafter

as merely "controls", and further data presentation uses the vehicle-based controls as a reference point.
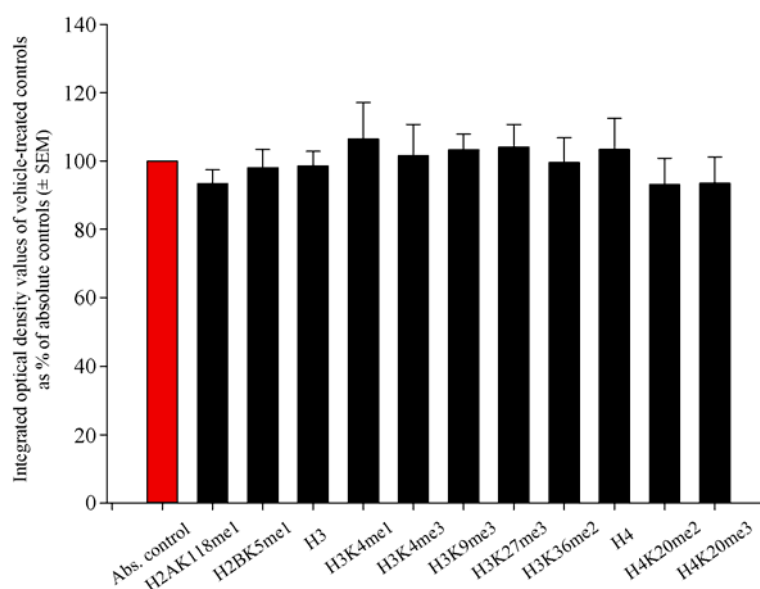

Figure 1. Quantitative Western blot analyses of histone methylation patterns in the brains of absolute control and vehicle-treated newborn rats. Protein contents from the absolute and vehicle-treated controls were determined and assayed on Western blots. Gel-loaded protein samples were separated by gel electrophoresis, transferred to nitrocellulose membranes, and assayed for immunoreactivity with antibodies that recognize core histones and histone methylations. Grayscale digital images of the immunoblots were scanned and processed under identical settings to allow comparisons between Western blots from different samples. Values indicate the means ± SEM from at least 5 separate experiments. Integrated optical density data were analyzed by ANOVA using SigmaPlot. No statistically significant differences were observed between the absolute and vehicle-control samples. Hence, we refer to vehicle-treated controls hereafter as simply "controls", and further data presentation uses the vehicle-based controls as the reference point.

2.2. Prenatal RST Exposure Does Not Affect Cell Composition in the Newborn Brain

RST exposure in utero did not cause structural abnormalities in the newborn brain at the level of light microscopy as evidenced by H&E staining (Figure 2). Double immunofluorescent staining for microglial and neuronal cell markers revealed that the ratios of these cells did not change between the controls and the RST-treated groups (Figure 3). Quantitative Western blot analysis of cell-specific markers corroborated that prenatal exposure to RST did not cause abnormalities in cell composition in newborn brains, as the ratios of these cells did not change significantly between the control and treated groups (Figure 4). These observations were supported by Ki67 fluorescent immunohistochemistry, as proliferation rates in both the control and prenatally RST-exposed rat brains were in the same range (Figure 5). Analyses of the immunohistochemical data detected approximately the same incidence of Ki67-immunopositive cells among the DAPI-labeled cell nuclei of both control and prenatally RST-treated rats. Of a total of 4268 cells analyzed from the controls and 3557 cells analyzed from RST-treated newborns, 554 (12.9%) and 448 (12.5%) cells were Ki67-positive, respectively.

2.3. In Utero RST Exposure Alters Histone Methylation Patterns in the Newborn Brain

Several antibodies that recognize different methylation sites for the H2A, H2B, H3, and H4 histones were used in the Western blotting experiments (Table S2). We found that prenatal RST treatment induced a general, nonsignificant increase in H2AK118me1, H2BK5me1, H3, H3K9me3, H3K27me3, H3K36me2, H4, H4K20me2, and H4K20me3 levels, to 101.0%–111.7% of the control levels (Figure 6). However, the levels of H3 histone mono- and tri-methylation at Lys 4 (H3K4me1 and H3K4me3) were elevated significantly (134.3% $\pm$ 19.2% and 127.8% $\pm$ 8.5%, respectively) compared to the control values. These modifications are known to play roles in transcription activation.
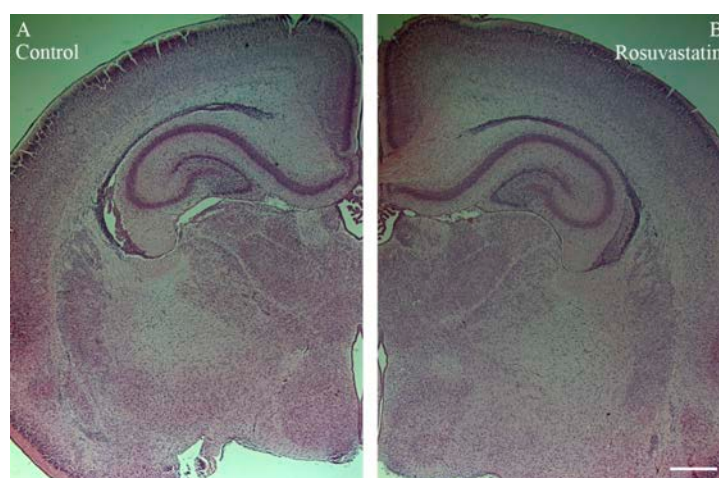

Figure 2. Histological architecture of the newborn rat brain. No differences were observed in paraffin-embedded, H&E-stained tissue sections of control (**A**) and rosuvastatin (RST)-treated newborn (**B**) brains by light microscopy. Scale bar: 1 mm.
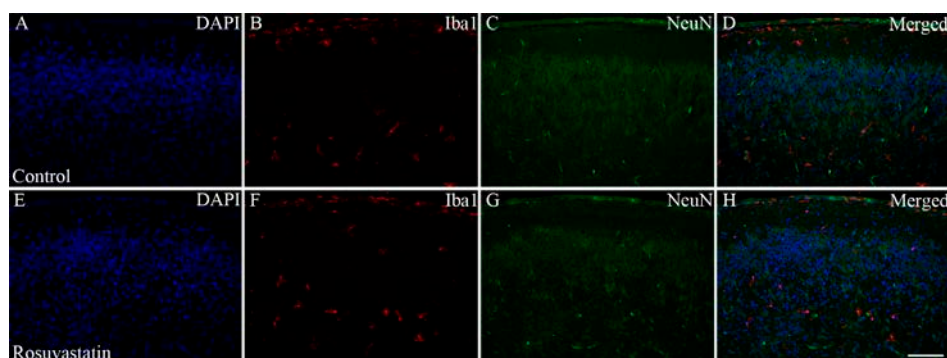

Figure 3. Double immunofluorescent staining for Iba1 and NeuN. Microglia were labeled with the anti-Iba1 antibody/Alexa Fluor 568 goat anti-rabbit IgG complex (red), whereas neurons were detected with the anti-NeuN antibody/Alexa Fluor 488 goat anti-mouse IgG complex (green). Cell nuclei were labeled with DAPI (blue). Representative pictures with lower (20×) magnification show that prenatal exposure to RST did not cause abnormalities in the cytoarchitecture by light microscopy. The ratio of microglia (**B**,**F**) to neurons (**C**,**G**) is similar between the control (**A**–**D**) and RST-treated (**E**–**H**) newborn brains. Scale bar: 100 μm.
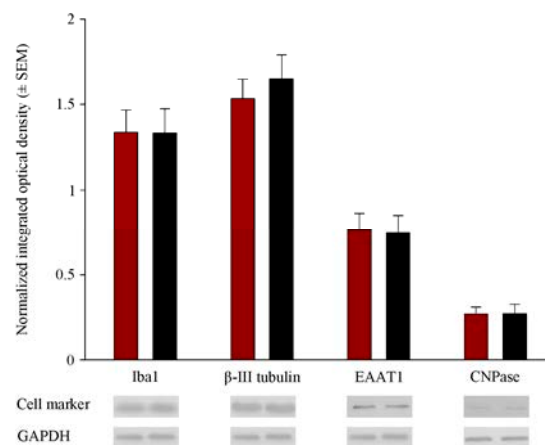
Figure 4. Quantitative Western blot analyses of the main cell types from control and RST-treated newborn rat brains. Controls (red column) and RST-treated (black column) samples were analyzed quantitatively on Western blots for microglial, neuronal, astrocyte, and oligodendrocyte markers. Protein samples (15–30 µg) were separated by gel electrophoresis, transferred to nitrocellulose membranes, and assayed for reactivity toward the Iba1 (microglia marker), beta III tubulin (neuron-specific marker), EAAT1 (astrocyte marker), CNPase (oligodendrocyte marker), and GAPDH proteins. Error bars indicate integrated optical density values (means ± SEM from at least 5 separate experiments) normalized to the values of the internal standard GAPDH. Representative Western blot pictures are shown below the graphs. No statistically significant differences were found between the control and the RST-treated groups.
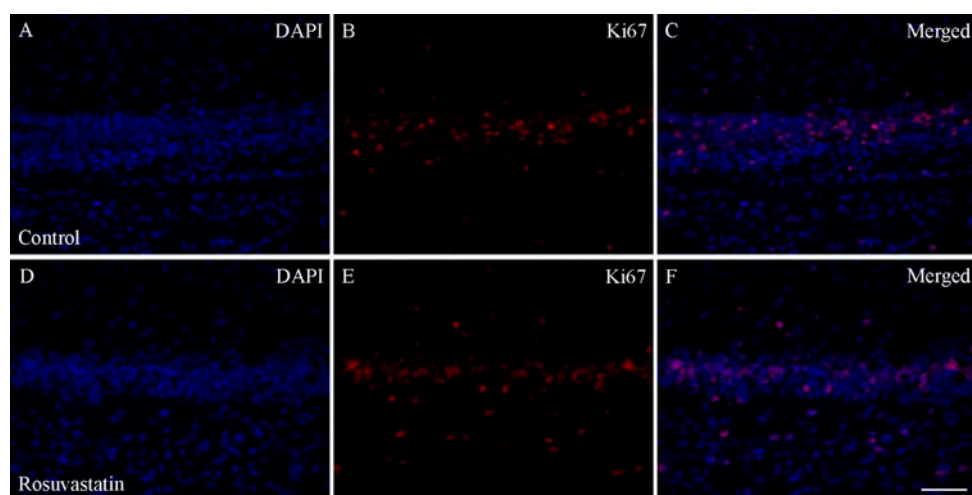

Figure 5. Ki67 immunohistochemistry of the hippocampus in control and prenatally RST-exposed newborn rats. The expression of the Ki67 protein in the tissue areas was quantified by the percentage of Ki67-positive nuclei (red) over the total number of nuclei (positive and negative nuclei). Immunohistochemical data analysis detected highly similar incidences for Ki67-immunopositive cells (**B**,**E**) among the DAPI dye-labeled cell nuclei (blue; **A**,**D**) for both the controls (12.9%) and the prenatally RST-treated rats (12.5%). Merged pictures (**C**,**F**) are shown. Scale bar: 50 µm.
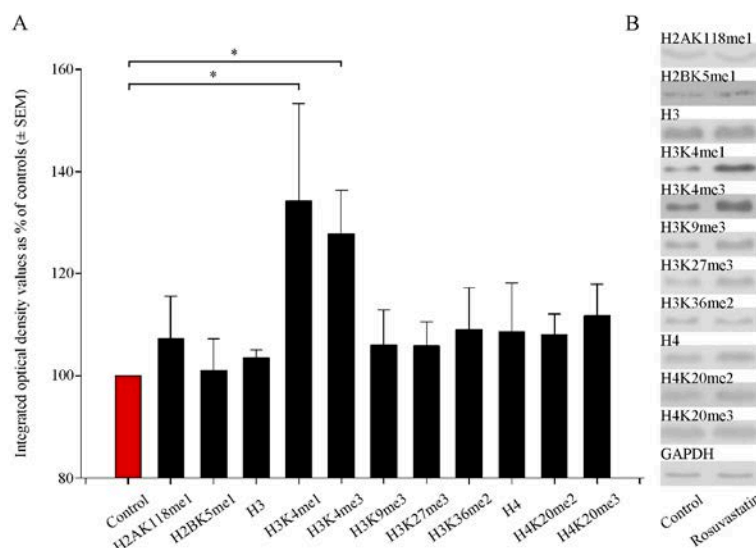
Figure 6. Quantitative Western blot analyses of histone methylation patterns in newborn rat brains. (**A**) Protein contents from the vehicle-treated controls and RST-treated newborns were determined and assayed by Western blot. Gel-loaded protein samples were separated by gel electrophoresis, transferred to nitrocellulose membranes, and assayed for immunoreactivity using antibodies that recognize different histone methylations. Grayscale digital images of the immunoblots were scanned and processed at identical settings to allow comparisons between Western blots from different samples. Integrated optical density values were calculated as the percentage of the vehicle-treated control values that had been normalized to the internal standard GAPDH. Prenatal RST exposure induced a general increase in the Lys-methylated sites of several histone proteins. Quantitative analysis showed that H3 histone mono- and tri-methylation at Lys 4 (H3K4me1 and H3K4me3) increased significantly (134.3% and 127.8% of vehicle-treated controls, respectively). (**B**) Representative Western blot images of immunoreactivity toward antibodies specific to the methylation sites and states, together with the GAPDH immunoreactive bands that served as the internal standards. Data were analyzed with the Mann–Whitney rank–sum test. Values are presented as the means $\pm$ SEM from at least 5 separate experiments, where $p < 0.05$ is considered significant. (* $p < 0.05$).

2.4. The Increase in H3K4me1 and H3K4me3 Is Localized Mainly to Neuronal Cell Nuclei

Cell-specific markers were used to localize the increases in H3K4me1- and -me3-immunopositivity in the cerebral tissue sections. Most of the immunoreactivity was localized to NeuN-positive neuronal cell nuclei, which constitute the vast majority of the parenchyma, and typically displayed the large nuclei of neuronal morphology (Figures 7 and 8). Interestingly, besides neurons, few Iba1-positive microglia (Figures 9 and 10) and GFAP-positive astrocytes (Figure 11) exhibited increased H3K4me1and H3K4me3 immunopositive signals, although the numbers of these cells in the neonatal brain were negligible. These glial cells displayed smaller nuclei with more compact chromatin, and they were smaller than the neurons in the newborn rat brain. Hardly any CNPase-positive oligodendrocytes were detected (data not shown), as myelogenesis occurs predominantly postnatally.
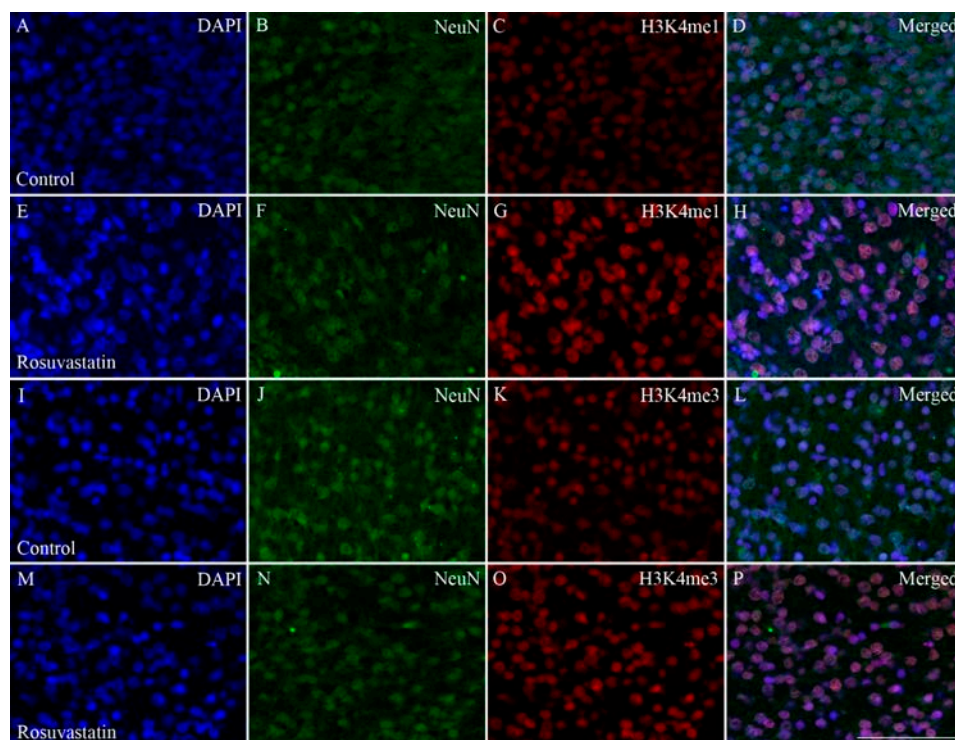
Figure 7. Colocalization of H3K4 methylation patterns and NeuN immunoreactivity in neurons of the newborn brain. DAPI-labeled cell nuclei are shown in blue (**A**,**E**,**I**,**M**). Immunoreactivity of the neuron-specific marker NeuN (**B**,**F**,**J**,**N**; shown here in green) and the histone methylation markers H3K4me1 and H3K4me3 (**C**,**G**,**K**,**O**, respectively; shown here in red) were colocalized in merged images (**D**,**H**,**L**,**P**). These immunohistochemical data corroborated the results of the Western blot analyses, as the immunofluorescent signals of the methylation marks were more intense in the sections from the RST-exposed newborns (**G**,**O**) as compared to the controls (**C**,**K**). Scale bar: 75 μm.
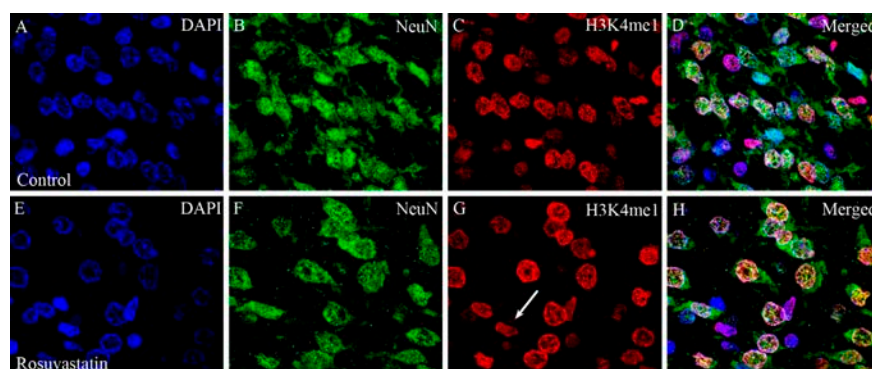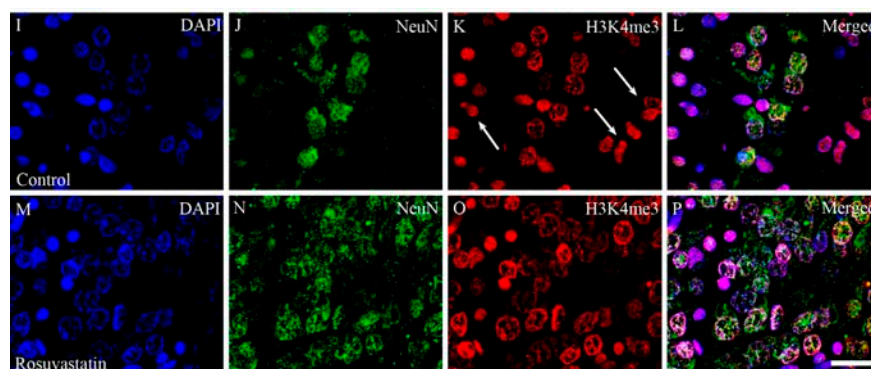

Figure 8. *Cont.*

Figure 8. Laser confocal microscopy images of H3K4me1 and H3K4me3 immunoreactivities in neuronal nuclei. Paraffin sections of brains from the control (**A–D,I–L**) and RST-treated newborn rats (**E–H,M–P**) were immunostained for NeuN (shown here in green) and H3K4me1 or H3K4me3 (shown here in red), then visualized by confocal microscopy. Cell nuclei were labeled with DAPI (blue). Note the overwhelmingly neuronal localization of the histone methylation marks. Some NeuN-negative non-neuronal cells, notably in panels (**G,K**) (white arrows), also display H3K4me1 and H3K4me3 marks. Scale bar: 20 μm.
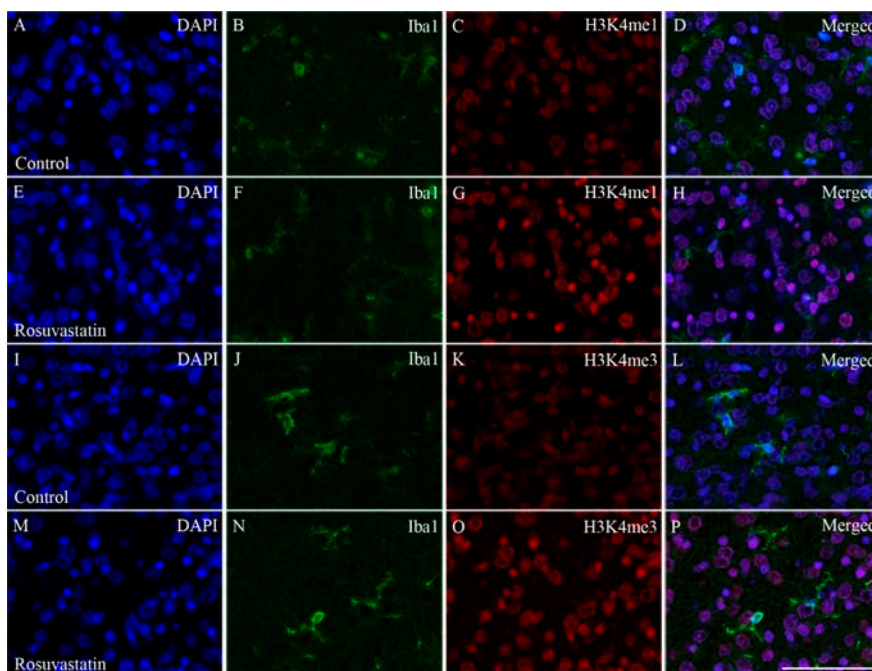

Figure 9. Colocalization of H3K4 methylation patterns and Iba1 immunoreactivity in the microglial cells of the newborn brain. In a newborn rat brain, the majority of the cells are neurons. At birth, microglia are unevenly distributed and located in specific "hotspots" such as the ventricular zone. Due to their overwhelmingly neuronal localization, H3K4me1 and H3K4me3 immunoreactivities (shown here in red) were more intense in the sections cut from the RST-treated newborns (**E–H,M–P**) as compared to the controls (**A–D,I–L**). A few H3K4 methylated cell nuclei belonged to Iba1-positive microglia (shown here in green). DAPI-labeled nuclei are shown in blue (**A,E,I,M**). Scale: 75 μm.
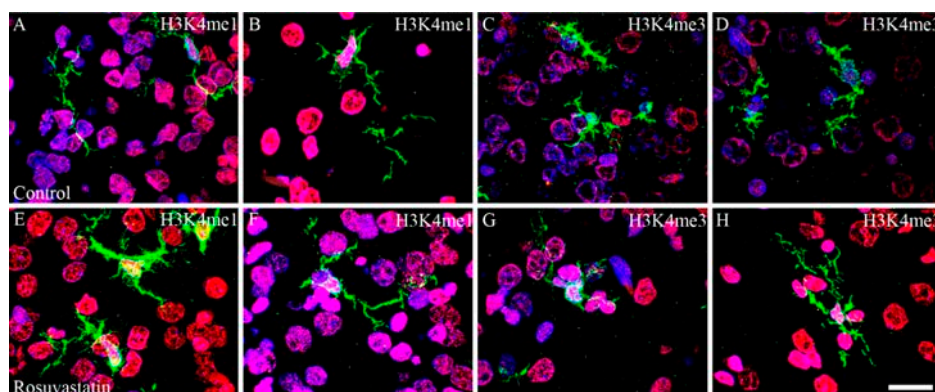
Figure 10. Laser confocal microscopy images of H3K4me1 and H3K4me3 immunoreactivities in microglial nuclei. Newborn brain sections from the control (**A**–**D**) and RST-treated rats (**E**–**H**) were immunostained for Iba1 (green), and H3K4me1 or H3K4me3 (red), then visualized by confocal microscopy. DAPI-labeled cell nuclei are blue. Note in the merged pictures the very few microglia that colocalize with the histone methylation marks. Scale bar: 20 μm.
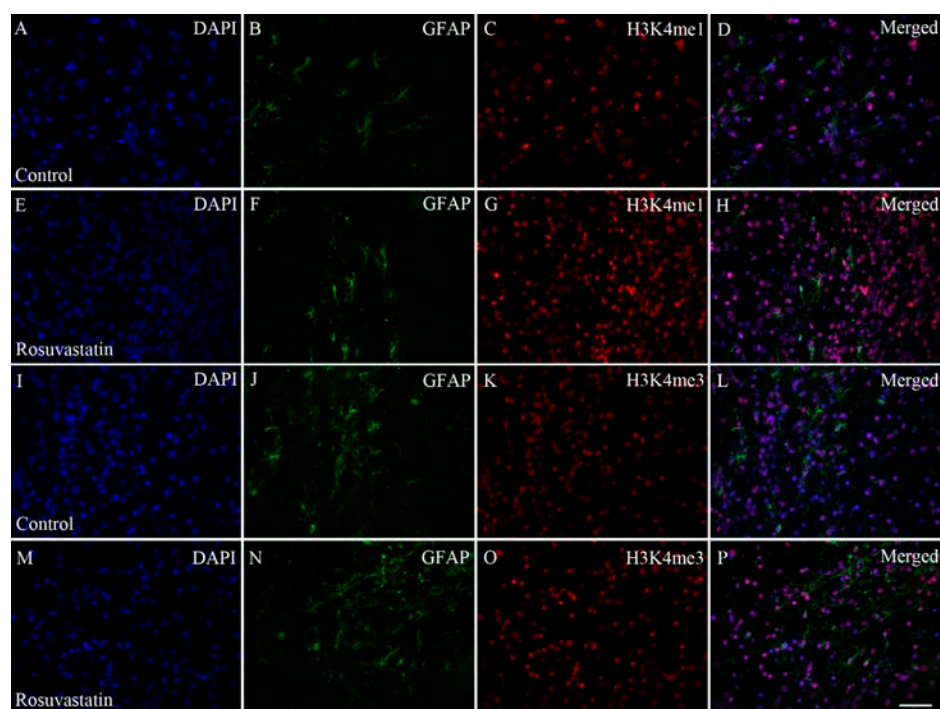
Figure 11. Double immunofluorescence staining for H3K4me1 and H3K4me3 in GFAP-positive astrocytes. In the neonatal rat brains, GFAP-positive cells were few, and unevenly distributed (green; **B**,**F**,**J**,**N**). DAPI-labeled cell nuclei are blue (**A**,**E**,**I**,**M**), and H3K4me1 (**C**,**G**) and H3K4me3 (**K**,**O**) marks are shown here in red. Merged pictures show (**D**,**H**,**L**,**P**) that few GFAP-positive astrocytes exhibited H3K4me1 and H3K4me3 marks. Scale bar: 50 μm.

3. Discussion

Although the beneficial effects of statins are well documented [1], there are some circumstances, including pregnancy, in which their use requires caution. For example, HMG-CoA reductase activity is required for normal placental development in mammals. The inhibition of this enzyme by statins may disrupt membrane synthesis, cellular proliferation and growth, and metabolism and protein glycosylation, which are crucial for the normal development of the placenta [17]. Limited data exist on the effect of statins in pregnancy, and there is no specific pattern of congenital anomalies associated with statin use [18]. Exposure to lipophilic statins is hypothesized to be of greater risk to the fetus than hydrophilic statins, because of their greater ability to reach the fetus in larger concentrations as a result of placental transport [17]. Studies have occasionally reported beneficial effects from statin use; for example, Elahi et al. [37] demonstrated that statin treatment in hypercholesterolemic pregnant mice reduced certain cardiovascular risk factors in their offspring. Statins also proved beneficial in preventing preeclampsia, thus ameliorating the risks of structural abnormalities to the fetus [18,38]. However, the use of statins in human pregnancy is currently not recommended, because of the potential teratogenic effects observed in animal experiments on one hand, and as a precaution owing to the lack of data supporting an indication for their use in pregnancy on the other. Indeed, animal models (rats, mice, rabbits) provide sporadic evidence for the teratogenicity of statins on pregnancy outcomes [21,22,39].

The nervous system comprises several different cell types that are defined by morphology, function, anatomical location, and specific patterns of gene expression. The establishment of these complex and highly regulated cell fates requires the spatial and temporal coordination of gene transcription in the proper order, number, and location. In the developing brain, neurons are generated first, followed by the supporting glia. Lineage studies indicate that the developing brain contains multipotent progenitor cells capable of generating both neurons and glia, and that cell fate restriction may be a consequence of a series of gene expression events and extracellular signals acting on multipotent progenitors [40].

On postnatal day 1, the newborn rat brain is a tissue populated mostly by neurons that are complemented gradually with non-neuronal cells. Bandeira et al. [41] reported that > 90% of the cells are neurons at this stage, and only about 6% of the cells had non-neuronal phenotypes. They also showed that the neuronal population initially present at birth was further reduced by apoptosis and that the number of non-neuronal, mostly glial, cells increased. Neurons and glial cells then worked together to achieve proper neuronal development and normal brain function. Microglia, the resident immune cells of the CNS, infiltrate the embryonic brain early and develop side by side with the neurons. At this early stage, when the first wave of synaptogenesis occurs, microglia are the only major non-neuronal cell type present in the CNS [42]. The generation of astrocytes and oligodendrocytes occurs in a temporally distinct, yet overlapping, pattern. In rats, neurogenesis peaks at embryonic day 14, astrocytogenesis at postnatal day 2 (they are produced largely during the final stage of neurogenesis), and oligodendrocytogenesis at postnatal day 14, although oligodendrocyte precursors appear somewhat earlier [43].

Mammalian embryonic development and subsequent fetal development involve precise molecular interactions between intrinsic factors such as genetics and epigenetics, and extrinsic maternal factors, such as environmental perturbations, drugs, or even maternal nutrition, as nutritional components that could influence the epigenetic landscape in the fetus and thus developmental processes [44]. Euchromatin allows transcription factors to interact with gene promoters and activate lineage-specific genes, while heterochromatin remains inaccessible to transcriptional activation [32]. During embryonal development, the histone methylation landscape of brain cells is sensitive to a wide range of environmental cues. Diet is now recognized as a major environmental factor that may contribute to controlling the physiological and pathophysiological aspects of homeostasis, metabolism, and gene expression [45,46]. It was therefore important to rule out any interference of liver pâté, as the vehicle for RST, on epigenetic mechanisms. We ruled out potential impacts

of this diet supplement on the histone methylation patterns, as they did not significantly change their levels between the absolute and vehicle-treated control newborn rat brains. We did not find any signs of RST histotoxicity or changes in the cellular compositions of newborn brains through light microscopy. It is important to note that most of the histone methylation marks we detected in this study were localized to neurons, and to a much smaller extent, to microglia. Astrocytes and oligodendrocytes develop and populate the newborn brain at later time points.

The dysregulation of chromatin decreases viability and normal cell functions and leads to various neurodevelopmental and psychiatric diseases [47]. H3K4 methylation has been observed in genes that are important for the regulation of cell differentiation, proliferation, and apoptosis [48]; for example, homeobox genes, known for their role in embryonic development, are regulated by H3K4 methylation [49]. H3K4me3 is almost always associated with RNA polymerase II occupancy of the promoters at the sites of active gene expression [50]. H3K4me1 and H3K4me3 marks are commonly located in euchromatin, are broadly associated with transcriptional regulation and the epigenetic tagging of promoters and enhancer sequences, and are known to allow the DNA to adopt a more "open" conformation and recruit chromatin-modifying factors [51]. The proper regulation of H3K4 methylation is pivotal for healthy brain development, as mutations associated with the loss and gain of H3K4 methylation could potentially result in intellectual disability, autism, microcephaly, seizure disorders, and other neurological diseases in early childhood [47]. It is possible that this epigenetic mark is involved more broadly in the pathophysiology of some neurodevelopmental disorders, as multiple regulators of H3K4 methylation are associated with neurodevelopmental diseases [52,53]. There can be little doubt that the H3K4 methylation landscape of brain cells is sensitive to a wide range of environmental perturbations [47]; indeed, the H3K4me3 mark undergoes global and gene-specific alterations in the hippocampus of fear-conditioned animals. Gupta et al. [54] found that H3K4me3 was upregulated in the rat hippocampus 1 h after contextual fear conditioning and that this increase was reversible. Furthermore, the activation of the maternal immune system by the viral mimic polyriboinosinic¬–polyribocytidilic acid, which leads to behavioral deficits in the adult offspring, could result in robust but transient changes in H3K4 methylation at the genes encoding cytokines and other signaling molecules in the fetal brain [55]. Prenatal exposure to the alkylating and antimitotic agent methylazoxymethanol, which leads to several anatomical and behavioral abnormalities in adulthood similar to those observed in patients with schizophrenia, resulted in decreased H3K4 methylation in the adult prefrontal cortex [56].

In this study, we focused on methylations of the Lys (K) residues of the four core histones. These epigenetic modifications, particularly in the case of the histone H3, are involved in a wide range of biological processes, including the activation and repression of transcription; nevertheless, one methyl mark by itself might still have a limited biological message. As mentioned above, H3K4me is a mark that, on a genome-wide scale, is associated broadly with transcriptional activation and the epigenetic tagging of promoters and enhancers [51]. Hence, H3K4me1/3 sites correlate positively with gene expression similarly to H3K36 methylation. The methylation of histone H3 lysine 36 (H3K36) plays an important role in the partitioning of chromatin into distinctive domains, as well as in the regulation of a wide range of biological processes [57,58]. H3K36me2 regulates the distribution of H3K27me3 [57], a hallmark of heterochromatin. A study on the epigenetic silencing of inflammation-related genes demonstrated that repressive histone marks (e.g., H3K27me3) correlated with a silencing of their expression [59]. Similar to H3K27, the methylation of H3K9 was shown to be involved in heterochromatin formation and transcriptional silencing [60]. H3K9me3 is a typical mark of constitutive heterochromatin, while H3K27me3 is usually enriched in facultative heterochromatin [61]. H3K9me3 modification is associated with changes in gene transcription by alterations to the chromatin structure. Another hallmark of heterochromatin is a strong enrichment of H4K20me2/3; in fact, H3K9me3 is required for the induction of H4K20me2/3 [61]. Hence, the H4K20 histone methyl mark

is associated with gene repression [34]. Besides H3 and H4, there are only a few known methylation marks in H2A and H2B; for example, Barski et al. [51] reported that H2BK5me1 is an activation mark associated with the active promoters downstream of transcription start sites. Interestingly, no data are available on the Lys methylation of H2A, particularly of H2AK118.

In this study, we provided evidence that, in newborn rat brains, prenatal exposure to RST alters the methylation landscape in general, and the H3K4me1 and H3K4me3 histone modifications in particular. We observed that RST significantly elevated the levels of H3K4me1 and H3K4me3 compared to the controls. Furthermore, we did not find any histological structural alteration in newborn brains that could be related to RST treatment. It remains to be determined in future studies whether the changes observed in the H3K4 methylation patterns are: (1) linked to specific loci or are genome-wide, (2) reflect an adaptive or maladaptive response to RST, or (3) are the outcomes of secondary or tertiary processes in response to RST treatment. The identification of the genomic sequences involved in the control of the embryonic development of offspring whose mothers had been treated with RST remains a formidable challenge. Interestingly, statins, in general, did not directly inhibit the activity of the major epigenetic modifying enzymes, such as, "writers" or "readers" [62]. Since 50% of all pregnancies are unplanned [63], the possibility exists that a pregnant woman may be taking a statin at least for a while. The epigenetic changes elicited by rosuvastatin are not good or bad unless definitely proven either way. Although there are no such data available yet on humans, our data could provide a warning. Prenatal statin therapies, therefore, require caution and warrant further investigation until a more detailed picture of their effects on the epigenetic spectrum emerges.

4. Materials and Methods

4.1. Animal Handling and Treatment

Pregnant Sprague–Dawley rats (190–210 g) were kept under standard housing conditions and fed ad libitum with regular laboratory chow. Pregnant rats were divided into three groups: in addition to absolute controls (no supplements at all), the vehicle-treated control animals received a small amount (650 mg) of liver pâté in pellet form once a day, whereas treated rats were given daily oral doses of RST (0.25 mg/kg body weight) mixed into pellets of liver pâté. Both groups received this liver pâté supplement (with or without RST) for 10 days, beginning on the 11th day of pregnancy (or until delivery). Feeding with the liver pâté was done individually, using forceps. Five breeding runs (4–6 pregnant rats each) provided the litters (6–12 pups from each mother) from which the independent experiments were performed. On postnatal day 1, the cerebral hemispheres of the absolute control, vehicle-treated control, and RST-treated rats were removed and either homogenized for Western blot analysis or embedded in paraffin for hematoxylin and eosin (H&E) staining and fluorescent immunohistochemistry/confocal microscopy.

4.2. Antibodies

The antibodies used in this study are listed in Tables S1 and S2. Several antibodies specific for the Lys methylation sites and the states of the H2A, H2B, H3, and H4 histone proteins were selected for the Western blot analyses and the fluorescent immunohistochemistry. The antibodies for cell-specific markers were used to detect neurons, astrocytes, oligodendrocytes, and microglial cells, as well as to check for possible changes in their ratios. The anti-Ki67 antibody was used to visualize the proliferating cells [64,65].

4.3. Histology

Rat brains were dissected quickly, fixed in 0.05 M phosphate-buffered saline (PBS) containing 4% formaldehyde, and then embedded in paraffin for H&E staining and immunohistochemistry. Paraffin-embedded sections were cut (6 μm thickness) on a microtome (Leica RM2235; Leica Mikrosysteme Vertrieb GmbH, Wetzlar, Germany), mounted on glass

slides coated with (3-aminopropyl)triethoxysilane (Menzel, Darmstadt, Germany), and subsequently used for H&E staining and immunohistochemistry.

4.4. Fluorescent and Confocal Immunohistochemistry

The paraffin-embedded tissue sections were deparaffinized, rehydrated, and placed in a jar filled with 0.01 M citrate buffer (pH 6.0) containing 0.05% Tween-20, and then heated at 95 °C for 20 min. The sections were washed 3 × 10 min in 0.05 M PBS containing 0.05% Tween-20 and blocked in a 0.05 M PBS solution containing 0.05% Tween-20 and 5% normal goat serum (NGS) for 1 h at room temperature (RT). The sections were then incubated with primary antibodies in a 0.05 M PBS solution containing 0.05% Tween 20 and 5% NGS overnight at 4 °C. After washing (4 × 10 min in 0.05 M PBS containing 0.05% Tween-20), the primary antibodies were labeled with either Alexa 488- or Alexa 568–conjugated secondary antibodies (final dilution 1:1000; Invitrogen, Carlsbad, CA, USA) in a blocking solution for 3 h at RT. After 4 × 10 min washes in 0.05 M PBS containing 0.05% Tween-20, the cell nuclei were stained using a 2-[4-(aminoiminomethyl)phenyl]-1H-indole-6-carboximidamide hydrochloride (DAPI) solution (Thermo Fisher Scientific, Waltham, MA, USA). Digital images were captured on a Leica DMLB epifluorescence microscope using a Leica DFC7000 T CCD camera (Leica Microsystems CMS GmbH, Wetzlar, Germany) and the LAS X Application Suite X (Leica).

Select immuno-labeled sections were also examined with a confocal laser scanning microscope (Olympus Fluoview FV1000, Olympus Life Science Europa GmbH, Hamburg, Germany). Images (512 × 512 pixels) were captured along the Z-axis, with a distance of 0.5 μm between consecutive optical slices using the following microscope configuration: objective lens, UPLSAPO 60×; numerical aperture, 1.35; sampling speed, 4 μs/pixel; optical zoom, 2×; and scanning mode, sequential unidirectional. The excitation wavelengths were as follows: 405 nm (DAPI), 488 nm (Alexa Fluor 488), and 543 nm (Alexa Fluor 568). Z-stack images were prepared using 10–12 consecutive optical slices.

4.5. Western Blot Analyses

Brains from newborn rats were dissected, homogenized in 50 mM Tris-HCl (pH 7.5 at 4 °C) containing 150 mM NaCl, 2 μg/mL leupeptin, 1 μg/mL pepstatin, 2 mM phenylmethylsulfonyl fluoride, and 2 mM EDTA, and centrifuged at 14,000× *g* for 10 min. The supernatant was aliquoted, and the pellet was rehomogenized in 50 mM Tris-HCl (pH 7.5 at 4 °C) containing 150 mM NaCl, 0.1% Nonidet-P40, 0.1% cholic acid, 2 μg/mL leupeptin, 1 μg/mL pepstatin, 2 mM phenylmethylsulfonyl fluoride, and 2 mM EDTA. The samples were incubated on ice for 30 min and then aliquoted. The protein concentrations of these suspensions and the abovementioned supernatants were determined by the Lowry method [66]. For Western blot analyses, 15–30 μg of protein was separated on an SDS polyacrylamide gel (4–12% stacking gel/resolving gel), transferred onto a Hybond-ECL nitrocellulose membrane (Amersham Biosciences, Little Chalfont, Buckinghamshire, England), blocked for 1 h in 5% nonfat dry milk in Tris-buffered saline (TBS) containing 0.1% Tween-20, and incubated overnight with the appropriate primary antibodies as well as with those of the internal control (mouse anti-GAPDH monoclonal antibody). After five rinses in 0.1% TBS–Tween-20, the membranes were incubated for 1 h with the appropriate horseradish peroxidase-conjugated goat anti-rabbit or rat anti-mouse secondary antibodies and washed three times, as described above. The enhanced chemiluminescence method (ECL Plus Western blotting detection reagents; Amersham Biosciences) was used to reveal the immunoreactive bands, according to the manufacturer's protocol. The exposure time and film development were optimized for each antibody.

4.6. Imaging and Statistical Analyses

Grayscale digital images of the immunoblots were acquired by scanning the autoradiographic films with a desktop scanner (Epson Perfection V750 PRO; Seiko Epson Corp., Suwa, Japan). The images were scanned and processed at identical settings to allow com-

parisons of the Western blots obtained from different samples. The bands were analyzed by densitometry via ImageJ (version 1.47; developed at the U.S. National Institutes of Health (Bethedsa, MD, USA) by W. Rasband, available at https://imagej.net/Downloads; accessed on 10 July 2013) [67]. The immunoreactive densities of equally loaded lanes were quantified, the samples were normalized to the densities of internal controls (GAPDH), and, for epigenetic studies, presented as % of the absolute controls or as % of controls.

All statistical comparisons were made using SigmaPlot software (v. 12.3, Systat Software, Inc., Chicago, IL, USA), and data were analyzed with one-way analysis of variance (ANOVA) or the Mann–Whitney rank–sum test. For the Western blots, values were presented as means $\pm$ standard errors of means (SEMs) from at least five immunoblots, each representing an independent newborn. A *p*-value of < 0.05 was considered significant.

Supplementary Materials: The following are available online at https://www.mdpi.com/1422-006 7/22/7/3412/s1, Table S1: Primary and secondary antibodies used in immunohistochemistry, Table S2: Primary and secondary antibodies used in Western blots.

Author Contributions: K.G. conceived and designed the experiments. K.D., M.S., N.L., I.B. and Z.H. performed and analyzed the experiments. I.B., Z.H. and K.G. contributed reagents, materials and/or analysis tools. K.D. and K.G. wrote the manuscript. K.G. edited the manuscript. All authors have read and agreed to the published version of the manuscript.

Institutional Review Board Statement: All applicable international, national, and/or institutional guidelines for the care and use of animals were followed. Experimental procedures were carried out in strict compliance with the European Communities Council Directive (86/609/EEC) and followed Hungarian and local legislation requirements (XXVIII/1998 and 243/1998) and university guidelines regarding the care and use of laboratory animals. The experimental protocols were approved by the Institutional Animal Welfare Committee of the University of Szeged (II./1131/2018; date of approval: 30 May 2018).

Informed Consent Statement: Not applicable.

Data Availability Statement: Data are contained within the article.

Conflicts of Interest: The authors declare no conflict of interest. The funders had no role in the design of the study; in the collection, analyses, or interpretation of data; in the writing of the manuscript, or in the decision to publish the results.

Abbreviations

ANOVA	analysis of variance
CNS	central nervous system
CNPase	2′,3′-cyclic nucleotide 3′-phosphodiesterase
DAPI	2-[4-(aminoiminomethyl)phenyl]-1H-indole-6-carboximidamide hydrochloride
EAAT1	excitatory amino acid transporter 1 (also known as glutamate aspartate transporter 1 (GLAST-1))
GAPDH	glyceraldehyde 3-phosphate dehydrogenase (EC 1.2.1.12)
GFAP	glial fibrillary acidic protein
H	histone
HGM-CoA	3-hydroxy-3-methylglutaryl coenzyme A
H&E	hematoxylin and eosin

Iba1	ionized calcium-binding adaptor molecule 1
IgG	immunoglobulin G
Ki67	proliferation marker antigen identified by the monoclonal antibody Ki67
NeuN	anti-neuronal nuclei protein (hexaribonucleotide-binding protein-3)
PBS	phosphate-buffered saline
RST	rosuvastatin
RT	room temperature
SDS	sodium dodecyl sulfate
SEM	standard error of the mean
TBS	Tris-buffered saline

References

1. Taylor, F.; Huffman, M.D.; Macedo, A.F.; Moore, T.H.; Burke, M.; Davey Smith, G.; Ward, K.; Ebrahim, S. Statins for the primary prevention of cardiovascular disease. *Cochrane Database Syst. Rev.* **2013**, *2013*, CD004816. [CrossRef]
2. Burg, J.S.; Espenshade, P.J. Regulation of HMG-CoA reductase in mammals and yeast. *Progr. Lipid Res.* **2011**, *50*, 403–410. [CrossRef] [PubMed]
3. Wierzbicki, A.S.; Poston, R.; Ferro, A. The lipid and non-lipid effects of statins. *Pharmacol. Therap.* **2003**, *99*, 95–112. [CrossRef]
4. Famer, D.; Wahlund, L.O.; Crisby, M. Rosuvastatin reduces microglia in the brain of wild type and ApoE knockout mice on a high cholesterol diet; implications for prevention of stroke and AD. *Biochem. Biophys. Res. Commun.* **2010**, *402*, 367–372. [CrossRef] [PubMed]
5. Van der Most, P.J.; Dolga, A.M.; Nijholt, I.M.; Luiten, P.G.M.; Eisel, U.L. Statins: Mechanisms of neuroprotection. *Progr. Neurobiol.* **2009**, *88*, 64–75. [CrossRef]
6. Zipp, F.; Waiczies, S.; Aktas, O.; Neuhaus, O.; Hemmer, B.; Schraven, B.; Nitsch, R.; Hartung, H.P. Impact of HMG-CoA reductase inhibition on brain pathology. *Trends Pharmacol. Sci.* **2007**, *28*, 342–349. [CrossRef] [PubMed]
7. Kata, D.; Földesi, I.; Feher, L.Z.; Hackler, L., Jr.; Puskas, L.G.; Gulya, K. Rosuvastatin enhances anti-inflammatory and inhibits pro-inflammatory functions in cultured microglial cells. *Neuroscience* **2016**, *314*, 47–63. [CrossRef]
8. Kurata, T.; Miyazaki, K.; Kozuki, M.; Morimoto, N.; Ohta, Y.; Ikeda, Y.; Abe, K. Atorvastatin and pitavastatin reduce senile plaques and inflammatory responses in a mouse model of Alzheimer's disease. *Neurol. Res.* **2012**, *34*, 601–610. [CrossRef]
9. Zelcer, N.; Khanlou, N.; Clare, R.; Jiang, Q.; Reed-Geaghan, E.G.; Landreth, G.E.; Vinters, H.V.; Tontonoz, P. Attenuation of neuroinflammation and Alzheimer's disease pathology by liver x receptors. *Proc. Natl. Acad. Sci. USA* **2007**, *104*, 10601–10606. [CrossRef] [PubMed]
10. Jones, K.D.; Couldwell, W.T.; Hinton, D.R.; Su, Y.; He, S.; Anker, L.; Law, R.E. Lovastatin induces growth inhibition and apoptosis in human malignant glioma cells. *Biochem. Biophys. Res. Commun.* **1994**, *205*, 1681–1687. [CrossRef]
11. Karlic, H.; Haider, F.; Thaler, R.; Spitzer, S.; Klaushofer, K.; Varga, F. Statin and bisphosphonate induce starvation in fast-growing cancer cell lines. *Int. J. Mol. Sci.* **2017**, *18*, 1982. [CrossRef] [PubMed]
12. Afshari, A.R.; Mollazadeh, H.; Henney, N.C.; Jamialahmad, T.; Sahebkar, A. Effects of statins on brain tumors: A review. *Semin. Cancer Biol.* **2020**. [CrossRef] [PubMed]
13. Gachpazan, M.; Kashani, H.; Khazaei, M.; Hassanian, S.M.; Rezayi, M.; Asgharzadeh, F.; Ghayour-Mobarhan, M.; Ferns, G.A.; Avan, A. The impact of statin therapy on the survival of patients with gastrointestinal cancer. *Curr. Drug Targets* **2019**, *20*, 738–747. [CrossRef]
14. Kostapanos, M.S.; Milionis, H.J.; Elisaf, M.S. Rosuvastatin-associated adverse effects and drug-drug interactions in the clinical setting of dyslipidemia. *Am. J. Cardiovasc. Drugs* **2010**, *10*, 11–28. [CrossRef] [PubMed]
15. Thorogood, M.; Seed, M.; De Mott, K. Guideline Development Group. Management of fertility in women with familial hypercholesterolaemia: Summary of NICE guidance. *BJOG* **2009**, *116*, 478–479. [CrossRef] [PubMed]
16. Godfrey, L.M.; Erramouspe, J.; Cleveland, K.W. Teratogenic risk of statins in pregnancy. *Ann. Pharmacother.* **2012**, *46*, 1419–1424. [CrossRef]
17. Lecarpentier, E.; Morel, O.; Fournier, T.; Elefant, E.; Chavatte-Palmer, P.; Tsatsaris, V. Statins and pregnancy: Between supposed risks and theoretical benefits. *Drugs* **2012**, *72*, 773–788. [CrossRef]
18. Morton, S.; Thangaratinam, S. Statins in pregnancy. *Curr. Opin. Obstet. Gynecol.* **2013**, *25*, 433–440. [CrossRef]
19. Taguchi, N.; Rubin, E.T.; Hosokawa, A.; Choi, J.; Ying, A.Y.; Moretti, M.E.; Koren, G.; Ito, S. Prenatal exposure to HMG-CoA reductase inhibitors: Effects on fetal and neonatal outcomes. *Reprod. Toxicol.* **2008**, *26*, 175–177. [CrossRef]
20. Beverly, B.E.J.; Furr, J.R.; Lambright, C.S.; Wilson, V.S.; McIntyre, B.S.; Foster, P.M.D.; Travlos, G.; Earl Gray, L., Jr. In utero exposure to simvastatin reduces postnatal survival and permanently alters reproductive tract development in the Crl:CD(SD) male rat. *Toxicol. Appl. Pharmacol.* **2019**, *365*, 112–123. [CrossRef]
21. Emami, F.; Asl, B.M.; Seydi, E.; Zargar, M.; Naserzadeh, P.; Pourahmad, J. Embryotoxic effects of atorvastatin on mouse fetus. *Iran. J. Pharm. Sci.* **2013**, *9*, 13–23.
22. Henck, J.W.; Craft, W.R.; Black, A.; Colgin, J.; Anderson, J.A. Pre- and postnatal toxicity of the HMG-CoA reductase inhibitor atorvastatin in rats. *Toxicol. Sci.* **1998**, *41*, 88–99. [CrossRef] [PubMed]

23. McTaggart, F.; Buckett, L.; Davidson, R.; Holdgate, G.; McCormick, A.; Schneck, D.; Smith, G.; Warwick, M. Preclinical and clinical pharmacology of rosuvastatin, a new 3-hydroxy-3-methylglutaryl coenzyme A reductase inhibitor. *Am. J. Cardiol.* **2001**, *87*, 28B–32B. [CrossRef]

24. Asztalos, B.F.; Le Maulf, F.; Dallal, G.E.; Stein, E.; Jones, P.H.; Horvath, K.V.; McTaggart, F.; Schaefer, E.J. Comparison of the effects of high doses of rosuvastatin versus atorvastatin on the subpopulations of high-density lipoproteins. *Am. J. Cardiol.* **2007**, *99*, 681–685. [CrossRef]

25. Lwin, E.M.P.; Leggett, C.; Ritchie, U.; Gerber, C.; Song, Y.; Hague, W.; Turner, S.; Upton, R.; Garg, S. Transfer of rosuvastatin into breast milk: Liquid chromatography-mass spectrometry methodology and clinical recommendations. *Drug Des. Dev. Ther.* **2018**, *12*, 3645–3651. [CrossRef] [PubMed]

26. Luo, B.; Li, B.; Wang, W.; Liu, X.; Liu, X.; Xia, Y.; Zhang, C.; Zhang, Y.; Zhang, M.; An, F. Rosuvastatin alleviates diabetic cardiomyopathy by inhibiting NLRP3 inflammasome and MAPK pathways in a type 2 diabetes rat model. *Cardiovasc. Drugs Ther.* **2014**, *28*, 33–43. [CrossRef] [PubMed]

27. Satoh, M.; Tabuchi, T.; Itoh, T.; Nakamura, M. NLRP3 inflammasome activation in coronary artery disease: Results from prospective and randomized study of treatment with atorvastatin or rosuvastatin. *Clin. Sci. (Lond.)* **2014**, *126*, 233–241. [CrossRef]

28. Biswas, S.; Rao, C.M. Epigenetic tools (The Writers, The Readers and The Erasers) and their implications in cancer therapy. *Eur. J. Pharmacol.* **2018**, *837*, 8–24. [CrossRef] [PubMed]

29. Hyun, K.; Jeon, J.; Park, K.; Kim, J. Writing, erasing and reading histone lysine methylations. *Exp. Mol. Med.* **2017**, *49*, e324. [CrossRef]

30. Klein, B.J.; Krajewski, K.; Restrepo, S.; Lewis, P.W.; Strahl, B.D.; Kutateladze, T.G. Recognition of cancer mutations in histone H3K36 by epigenetic writers and readers. *Epigenetics* **2018**, *13*, 683–692. [CrossRef]

31. Venkatesh, S.; Workman, J. Histone exchange, chromatin structure and the regulation of transcription. *Nat. Rev. Mol. Cell. Biol.* **2015**, *16*, 178–189. [CrossRef]

32. Kouzarides, T. Chromatin modifications and their function. *Cell* **2007**, *128*, 693–705. [CrossRef] [PubMed]

33. Trojer, P.; Reinberg, D. Histone lysine demethylases and their impact on epigenetics. *Cell* **2006**, *125*, 213–217. [CrossRef] [PubMed]

34. Vermeulen, M.; Eberl, H.C.; Matarese, F.; Marks, H.; Denissov, S.; Butter, F.; Lee, K.K.; Olsen, J.V.; Hyman, A.A.; Stunnenberg, H.G.; et al. Quantitative interaction proteomics and genome-wide profiling of epigenetic histone marks and their readers. *Cell* **2010**, *142*, 967–980. [CrossRef] [PubMed]

35. Danielewicz, H.; Gurgul, A.; Dębińska, A.; Myszczyszyn, G.; Szmatoła, T.; Myszkal, A.; Jasielczuk, I.; Drabik-Chamerska, A.; Hirnle, L.; Boznański, A. Maternal atopy and offspring epigenome-wide methylation signature. *Epigenetics* **2020**, *9*, 1–13. [CrossRef]

36. Monk, D.; Mackay, D.J.G.; Eggermann, T.; Maher, E.R.; Riccio, A. Genomic imprinting disorders: Lessons on how genome, epigenome and environment interact. *Nat. Rev. Genet.* **2019**, *20*, 235–248. [CrossRef]

37. Elahi, M.M.; Cagampang, F.R.; Anthony, F.W.; Curzen, N.; Ohri, S.K.; Hanson, M.A. Statin treatment in hypercholesterolemic pregnant mice reduces cardiovascular risk factors in their offspring. *Hypertension* **2008**, *51*, 939–944. [CrossRef]

38. Smith, D.D.; Costantine, M.M. The role of statins in the prevention of preeclampsia. *Am. J. Obstet. Gynecol.* **2020**. [CrossRef]

39. Faqi, A.S.; Prohaska, D.; Lopez, R.; McIntyre, G. Developmental toxicity of the HMG-CoA reductase inhibitor (PPD10558) in rats and rabbits. *Birth Defects Res. B Dev. Reprod. Toxicol.* **2012**, *95*, 23–37. [CrossRef]

40. Morrow, T.; Song, M.R.; Ghosh, A. Sequential specification of neurons and glia by developmentally regulated extracellular factors. *Development* **2001**, *128*, 3585–3594. [PubMed]

41. Bandeira, F.; Lent, R.; Herculano-Houzel, S. Changing numbers of neuronal and non-neuronal cells underlie postnatal brain growth in the rat. *Proc. Natl. Acad. Sci. USA* **2009**, *106*, 14108–14113. [CrossRef] [PubMed]

42. Reemst, K.; Noctor, S.C.; Lucassen, P.J.; Hol, E.M. The indispensable roles of microglia and astrocytes during brain development. *Front. Hum. Neurosci.* **2016**, *10*, 566. [CrossRef] [PubMed]

43. Sauvageot, C.M.; Stiles, C.D. Molecular mechanisms controlling cortical gliogenesis. *Curr. Opin. Neurobiol.* **2002**, *12*, 244–249. [CrossRef]

44. Li, Y. Epigenetic mechanisms link maternal diets and gut microbiome to obesity in the offspring. *Front. Genet.* **2018**, *9*, 342. [CrossRef] [PubMed]

45. Johnson, I.T. The cancer risk related to meat and meat products. *Br. Med. Bull.* **2017**, *121*, 73–81. [CrossRef]

46. Khambadkone, S.G.; Cordner, Z.A.; Dickerson, F.; Severance, E.G.; Prandovszky, E.; Pletnikov, M.; Xiao, J.; Li, Y.; Boersma, G.J.; Talbot, C.C., Jr.; et al. Nitrated meat products are associated with mania in humans and altered behavior and brain gene expression in rats. *Mol. Psychiatry* **2020**, *25*, 560–571. [CrossRef]

47. Shen, E.; Shulha, H.; Weng, Z.; Akbarian, S. Regulation of histone H3K4 methylation in brain development and disease. *Philos. Trans. R. Soc. Lond. B Biol. Sci.* **2014**, *369*, 20130514. [CrossRef]

48. Batista, I.A.A.; Helguero, L.A. Biological processes and signal transduction pathways regulated by the protein methyltransferase SETD7 and their significance in cancer. *Signal Transduct. Target Ther.* **2018**, *3*, 19. [CrossRef]

49. Malik, S.; Bhaumik, S.R. Mixed lineage leukemia: Histone H3 lysine 4 methyltransferases from yeast to human. *FEBS J.* **2010**, *277*, 1805–1821. [CrossRef] [PubMed]

50. Guenther, M.G.; Jenner, R.G.; Chevalier, B.; Nakamura, T.; Croce, C.M.; Canaani, E.; Young, R.A. Global and Hox-specific roles for the MLL1 methyltransferase. *Proc. Natl. Acad. Sci. USA* **2005**, *102*, 8603–8608. [CrossRef]

51. Barski, A.; Cuddapah, S.; Cui, K.; Roh, T.Y.; Schones, D.E.; Wang, Z.; Wei, G.; Chepelev, I.; Zhao, K. High-resolution profiling of histone methylations in the human genome. *Cell* **2007**, *129*, 823–837. [CrossRef]

52. Jones, W.D.; Dafou, D.; McEntagart, M.; Woollard, W.J.; Elmslie, F.V.; Holder-Espinasse, M.; Irving, M.; Saggar, A.K.; Smithson, S.; Trembath, R.C.; et al. De novo mutations in MLL cause Wiedemann-Steiner syndrome. *Am. J. Hum. Genet.* **2012**, *91*, 358–364. [CrossRef] [PubMed]

53. Najmabadi, H.; Hu, H.; Garshasbi, M.; Zemojtel, T.; Abedini, S.S.; Chen, W.; Hosseini, M.; Behjati, F.; Haas, S.; Jamali, P.; et al. Deep sequencing reveals 50 novel genes for recessive cognitive disorders. *Nature* **2011**, *478*, 57–63. [CrossRef] [PubMed]

54. Gupta, S.; Kim, S.Y.; Artis, S.; Molfese, D.L.; Schumacher, A.; Sweatt, J.D.; Paylor, R.E.; Lubin, F.D. Histone methylation regulates memory formation. *J. Neurosci.* **2010**, *30*, 3589–3599. [CrossRef]

55. Connor, C.M.; Dincer, A.; Straubhaar, J.; Galler, J.R.; Houston, I.B.; Akbarian, S. Maternal immune activation alters behavior in adult offspring, with subtle changes in the cortical transcriptome and epigenome. *Schizophr. Res.* **2012**, *140*, 175–184. [CrossRef] [PubMed]

56. Maćkowiak, M.; Bator, E.; Latusz, J.; Mordalska, P.; Wędzony, K. Prenatal MAM administration affects histone H3 methylation in postnatal life in the rat medial prefrontal cortex. *Eur. Neuropsychopharmacol.* **2014**, *24*, 271–289. [CrossRef]

57. Jie, L.; Ahn, J.H.; Wang, G.G. Understanding histone H3 lysine 36 methylation and its deregulation in disease. *Cell. Mol. Life Sci.* **2019**, *76*, 2899–2916. [CrossRef]

58. Sun, Z.; Zhang, Y.; Jia, J.; Fang, Y.; Tang, Y.; Wu, H.; Fang, D. H3K36me3, message from chromatin to DNA damage repair. *Cell. Biosci.* **2020**, *10*, 9. [CrossRef]

59. Maleszewska, M.; Steranka, A.; Smiech, M.; Kaza, B.; Pilanc, P.; Dabrowski, M.; Kaminska, B. Sequential changes in histone modifications shape transcriptional responses underlying microglia polarization by glioma. *Glia* **2021**, *69*, 109–123. [CrossRef]

60. Bannister, A.J.; Zegerman, P.; Partridge, J.F.; Miska, E.A.; Thomas, J.O.; Allshire, R.C.; Kouzarides, T. Selective recognition of methylated lysine 9 on histone H3 by the HP1 chromo domain. *Nature* **2001**, *410*, 120–124. [CrossRef]

61. Saksouk, N.; Simboeck, E.; Déjardin, J. Constitutive heterochromatin formation and transcription in mammals. *Epigenetics Chromatin* **2015**, *8*, 3. [CrossRef] [PubMed]

62. Bridgeman, S.; Northrop, W.; Ellison, G.; Sabapathy, T.; Melton, P.E.; Newsholme, P.; Mamotte, C.D.S. Statins do not directly inhibit the activity of major epigenetic modifying enzymes. *Cancers* **2019**, *11*, 516. [CrossRef]

63. Koren, G.; Pastuszak, A.; Ito, S. Drugs in pregnancy. *N. Engl. J. Med.* **1998**, *338*, 1128–1137. [CrossRef] [PubMed]

64. Cuylen, S.; Blaukopf, C.; Politi, A.Z.; Müller-Reichert, T.; Neumann, B.; Poser, I.; Ellenberg, J.; Hyman, A.A.; Gerlich, D.W. Ki-67 acts as a biological surfactant to disperse mitotic chromosomes. *Nature* **2016**, *535*, 308–312. [CrossRef]

65. Szabo, M.; Gulya, K. Development of the microglial phenotype in culture. *Neuroscience* **2013**, *241*, 280–295. [CrossRef] [PubMed]

66. Lowry, O.H.; Rosebrough, N.J.; Farr, A.L.; Randall, R.J. Protein measurement with the Folin phenol reagent. *J. Biol. Chem.* **1951**, *193*, 265–275. [CrossRef] [PubMed]

67. Schneider, C.A.; Rasband, W.S.; Eliceiri, K.W. NIH Image to ImageJ: 25 years of image analysis. *Nat. Methods* **2012**, *9*, 671–675. [CrossRef]

II.

CERTIFICATE OF
POSTER PRESENTATION

is to certify that

Karolina Fábián-Dulka

presented a poster entitled

Prenatal exposure to rosuvastatin changes histone methylation patterns in the newborn rat brain

at the

12 FENS
Forum of Neuroscience

11-15 July 2020

FENS 2020
Virtual Forum